1974

Shallow water acoustic amplitude fluctuations at 35 and 65 kHz.

Korbet, Michael Thomas.

Monterey, California. Naval Postgraduate School

SHALLOW WATER ACOUSTIC AMPLITUDE FLUCTUATIONS AT 35 AND 65 KHz

Michael Thomas Korbet

NAVAL POSTGRADUATE SCHOOL
Monterey, California

THESIS

SHALLOW WATER ACOUSTIC AMPLITUDE
FLUCTUATIONS AT 35 AND 65 KHz

by

Michael Thomas Korbet

Thesis Advisor: W. Denner

March 1974

Shallow Water Acoustic Amplitude Fluctuations at 35 and 65 kHz

by

Michael Thomas Korbet
Lieutenant, United States Navy
B.S., United States Naval Academy, 1966

Submitted in partial fulfillment of the
requirements for the degree of

MASTER OF SCIENCE IN OCEANOGRAPHY

from the

NAVAL POSTGRADUATE SCHOOL
March 1974

ABSTRACT

An underwater acoustics experiment conducted in shallow water (70 feet) off the New Zealand east coast in 1972-1973 is described. Short acoustic pulses of 35 and 65 kHz sound were projected along near-orthogonal paths of approximately 300 yards. Environmental parameters were simultaneously observed.

Statistical and spectral analyses of pulse heights were performed on 12 selected runs using digital techniques. Coefficients of variation ranged from 2.0% to 15.5%. In almost all cases, higher variability was observed along the acoustic path oriented perpendicular to the predominant swell direction. Along this same path, periods corresponding to common surface swell periods were frequently evident in the autocorrelation functions of the fluctuations. Coherence between the fluctuations along each path was low, averaging about 0.1. Long period oscillations suggestive of modulation by internal waves were apparent in several runs. No significant dependence of variability on acoustic frequency was detected.

Microscale temperature fluctuations measured simultaneously are discussed.

TABLE OF CONTENTS

I. THE EXPERIMENT ---------- 8

A. BACKGROUND ---------- 8

B. OVERVIEW ---------- 12

C. PHYSICAL DESCRIPTION ---------- 13

D. DESCRIPTION OF SENSORS ---------- 21

1. General ---------- 21

2. Acoustic System ---------- 22

3. Temperature System ---------- 26

E. DATA ACQUISITION ---------- 27

II. DATA ANALYSIS ---------- 31

A. STRIP CHART RECORDING ---------- 31

B. DIGITIZATION ---------- 31

C. CONVERSION ---------- 35

D. PULSE HEIGHT MEASUREMENT ---------- 35

E. SELECTION OF RUNS FOR DETAILED ANALYSIS ----- 36

F. STATISTICAL ANALYSIS ---------- 39

G. SPECTRAL ANALYSIS ---------- 42

H. DISPLAY OF RESULTS ---------- 44

III. RESULTS OF ANALYSIS ---------- 45

A. TEMPERATURE FLUCTUATIONS ---------- 45

B. STATISTICAL RESULTS OF PULSE HEIGHT ANALYSIS ---------- 46

C. SPECTRAL ANALYSIS RESULTS ---------- 48

D. DISCUSSION ---------- 52

IV. CRITIQUE OF EXPERIMENT ---------- 62

A. PARAMETERS ---------- 62

B. RUN LENGTH ---------- 63

C. RECORDING OF DATA ---------- 64

D. PHASE II RUNS ---------- 65

E. RELFECTED SIGNALS ---------- 66

F. LOG KEEPING ---------- 67

V. SUMMARY, REÇOMMENDATIONS, AND CONCLUSIONS ----- 68

APPENDIX A: PULSE HEIGHT TIME SERIES AND ANALYSIS RESULTS ---------- 72

LIST OF REFERENCES ---------- 125

INITIAL DISTRIBUTION LIST ---------- 128

FORM DD 1473 ---------- 130

LIST OF TABLES

I. Basic Data on Analyzed Runs ---------- 37

II. Sea and Weather Conditions During Each Run ------ 38

III. Summary of Statistical Analysis Results --------- 47

IV. Summary of Selected Results from Spectral Analysis ---------- 49

LIST OF FIGURES

1. Map of Auckland-Leigh area in New Zealand -------- 15

2. Map of experiment site near Leigh, New Zealand --- 16

3. Schematic of acoustic propagation equipment ------ 23

4.a. Typical sample of microscale temperature fluctuations and simultaneously observed acoustic pulse heights ---------- 32

4.b. Expanded view of acoustic pulse sequence --------- 32

5. Graph of coefficient of variation versus number of bad pulses ---------- 53

6. Graph of bad pulses on Hydrophone 1 versus those on Hydrophone 2 ---------- 54

7. Histogram from Pulse Height Analyzer for pulses recorded during the 5 minute period shown on temperature record: low thermal activity ---------- 56

8. Histogram from Pulse Height Analyzer for pulses recorded during the 5 minute period shown on temperature record: high thermal activity ---------- 57

ACKNOWLEDGEMENTS

The author wishes to acknowledge the valuable guidance and encouragement of Dr. Warren W. Denner from whom, through countless hours of stimulating dialogue, I learned the value of innovative and exploratory thinking. The assistance and comments of Dr. Edward B. Thornton and Dr. Robert H. Bourke are greatfully appreciated.

Particular note is due the Department of Physics of the University of Auckland for the cooperation extended during the conduct of the experiment. Special gratitude is offered to the staff of the Naval Arctic Research Laboratory, especially Mrs. Dorothy Underwood, for the gracious hospitality and multiple resources made available during the author's work at that facility.

The experimental research discussed in this thesis was supported through contracts from the Naval Ordnance Systems Command (Code 03C).

I. THE EXPERIMENT

A. BACKGROUND

Acoustic fluctuations in the ocean first gained serious attention as a result of sonar development and acoustic experimentation during and immediately after World War II. Variability in the pressure amplitude of an acoustic signal received from a constant source was attributed to the presence of moving inhomogeneities which continuously altered the ray paths for energy to travel from the source to the receiver.

During this same time frame, the development of quick-response thermopiles enabled Urick and Searfoss (1948, 1949) to measure the micro-scale thermal structure of the ocean near Key West, Florida. Recognizing the prominent role of temperature in affecting the acoustic refractive index, they proposed that the "thermal patches" evidenced in their experiments were the cause of acoustic fluctuations.

Subsequent investigations – theoretical, laboratory, and in situ – are summarized through 1964 by Urick (1967). A more detailed theoretical development and analysis can be found in Skudryzk (1963).

Although a clearer understanding of the nature of the ocean's fine structure is available now, compared to twenty-five years ago, the equations often used to predict acoustic variability are still those developed by Bergmann (1946) and Mintzer (1953a, 1953b, 1954). Under the condition that

$$r << ka^2$$

where r = range from source to receiver,

k = acoustic wavenumber,

a = thermal microstructure scale length, i.e., the "patch size",

the acoustic variability, calculated as the coefficient of variation, V, is given by:

$$V = \left(\frac{4}{15} \pi^{\frac{1}{2}} \frac{\mu^2 r^3}{a^3} \right)^{\frac{1}{2}}$$

where μ is the RMS refractive index contrast of the inhomogeneity.

At relatively long range, such that $r >> ka^2$, the variability is given by:

$$V = \left(\frac{\pi^{\frac{1}{2}}}{2} \mu^2 k^2 a r \right)^{\frac{1}{2}}$$

These two equations were derived under the assumption of a Gaussian autocorrelation function for the temperature fluctuations. The quantities V and μ are calculated as:

$$V = \left[\frac{\langle (P - \langle P \rangle)^2 \rangle}{(\langle P \rangle)^2} \right]^{\frac{1}{2}}$$

= coefficient of variation; i.e., V is the fractional standard deviation of the pressure amplitude, P

$$\mu = \left[\overline{\left(\frac{\Delta c}{\bar{c}}\right)^2}\right]^{\frac{1}{2}} \quad \text{, where} \quad c = \text{sound speed}$$

= RMS variation of the refractive index.

The "patch size", a , is determined from the space autocorrelation function of the temperature fluctuations as measured by a sensor moving along a line through the temperature field. Invoking the hypothesis of "frozen turbulence," and allowing the temperature field to be advected past a fixed sensor, "patch size" can also be determined from the temporal autocorrelation function of the temperature fluctuations, $\phi(\tau)$, where τ is the lag time, provided the advection velocity is known.

Mintzer (1954) has shown that the autocorrelation function for the acoustic fluctuations, $R(\tau)$, should be related to the autocorrelation function for the temperature fluctuations by the equation

$$\phi(\tau) = R(\tau) \ .$$

Accepting Mintzer's hypothesis, the temporal autocorrelation function of the acoustic fluctuations should be identically equal to that of the temperature fluctuations. One recent experiment (Campanella and Favret 1969) which attempted to verify this relationship found the above expression valid under carefully controlled laboratory conditions.

Knowledge of the microstructure of the ocean has expanded significantly in the past ten years. While the classical

concepts of thermal patches — spherical, spheroidal, or lenticular — are still valid under some circumstances, they have been largely overshadowed by the discovery of a layered microstructure. Evidence of this type of structure has been observed repeatedly in widely separated areas of the oceans (Stommel and Federov 1967; Neshyba, Neal, and Denner 1971; Woods and Wiley 1972; Neal and Neshyba 1973; Gregg, Cox, and Hacker 1973, for example). However, the degree of structuring and lateral extent of the laminae have been found to vary considerably and unpredictably. Thus the tenant of local isotropy and/or homogeneity is more difficult to support than it is for the case of a patchy microstructure.

In conjunction with the investigation of a multi-layered thermal microstructure, several theories have been proposed to explain the mechanisms for the formation, maintenance, and collapse of the fine structure. Briefly these include internal waves (Garrett and Munk 1972), double diffusive processes (Stommel and Federov 1967), and billow turbulence (Woods and Wiley 1972).

In addition to the thermal microstructure, whether it be layered or patchy, other factors that cause acoustic fluctuations may be present in the ocean environment. Among these are microscopic bubble populations (Medwin 1973), micro- and macro-biologic effects, and both surface and internal wave activity (Crease 1963, Barakos 1972).

While many experiments have been performed to investigate acoustic variability, few have simultaneously monitored the

essential features of the environment. Furthermore, few, if any, measurements of acoustic variability have been made in shallow water. The experiment described in this thesis was designed to collect environmental and acoustic data which would lead to an analysis of both temperature and acoustic variability in a shallow water scenario.

B. OVERVIEW

The purpose of the experiment was to obtain simultaneous measurements of both environmental data and acoustic data in order to gain a better understanding of the nature of the environment, to determine the driving forces evoking changes in the environment, and to investigate the interaction between the environment and acoustic propagation.

The environment under study was a shallow coastal region with a mean water depth of approximately 70 feet. Several advantages were immediately gained from the selection of this site. The sensors involved could be rigidly fixed in known positions on the ocean floor, thus eliminating the problem of platform motion which is difficult to accomplish in open ocean experiments conducted from research vessels. However, the water depth was great enough to offer the opportunity to observe, as the seasons passed, both a well-mixed (and therefore homogeneous and near-isotropic) environment, and a stratified environment. The extent of either situation was determined by local wind, wave, and swell conditions. Finally, the experiment was maintained for a period of

months in the same location; this allowed the accumulation of sufficient data to form a long term time series.

During the course of the experiment, the following parameters were to be observed and recorded:

1. high frequency acoustic amplitude fluctuations in two simultaneous orthogonal directions
2. temperature microstructure data
3. mean water temperature
4. surface wave heights
5. velocity in two horizontal directions
6. vertical velocity
7. ambient noise
8. surface wind
9. stage of the tide
10. sky and cloud conditions
11. pertinent phenomena, such as sunrise, sunset, precipitation, unusual occurrences, etc.

C. PHYSICAL DESCRIPTION

The site selected for the experiment was the University of Auckland Marine Station at Leigh, New Zealand. Dr. Denner of the Naval Postgraduate School was on sabbatical leave with the Department of Physics of the University of Auckland. The Physics Department at the University had been active for several years in the area of acoustic fluctuations in the ocean. Dr. Erick Sagar had contributed several original papers in the area of sound amplitude fluctuations (Sagar 1955, Sagar 1957, Sagar 1960). Furthermore, the university had previously conducted acoustic experiments at Leigh (Brownlee 1969); hence, some of the necessary

facilities were already installed, namely, several conducting cables and underwater instrument platforms. The Marine Station provided the required logistic support including laboratory space, boats, shops, personnel, etc.

The near-shore area where the range was established was being set aside as a marine preserve and intrusions on the range by fishing and recreational boats were eliminated. The area was very biologically active, especially in plankton, nekton, and algae populations (Morton and Chapman 1968, Taylor 1972).

Geographically, the Leigh Marine Laboratory is located on the mainland across from Goat Island in the vicinity of Leigh, approximately 40 miles north of Auckland on the east coast of New Zealand (Figure 1). The range was located off-shore from the laboratory between the mainland and Goat Island (Figure 2).

The laboratory had served as a center of marine research for a number of years and some of the environmental characteristics of the area were known. In this regard, local climatology was an important factor because the experiment was planned to span a period of one year. Statistically, the diurnal air temperature range was about 6°C in all seasons of the year; this range was only slightly less than the mean annual temperature change of about 10°C. The warmest month was February with an average daily temperature range of 20 to 24°C; the coldest month was August with a mean daily range of 10 to 15°C. Sea surface temperatures historically

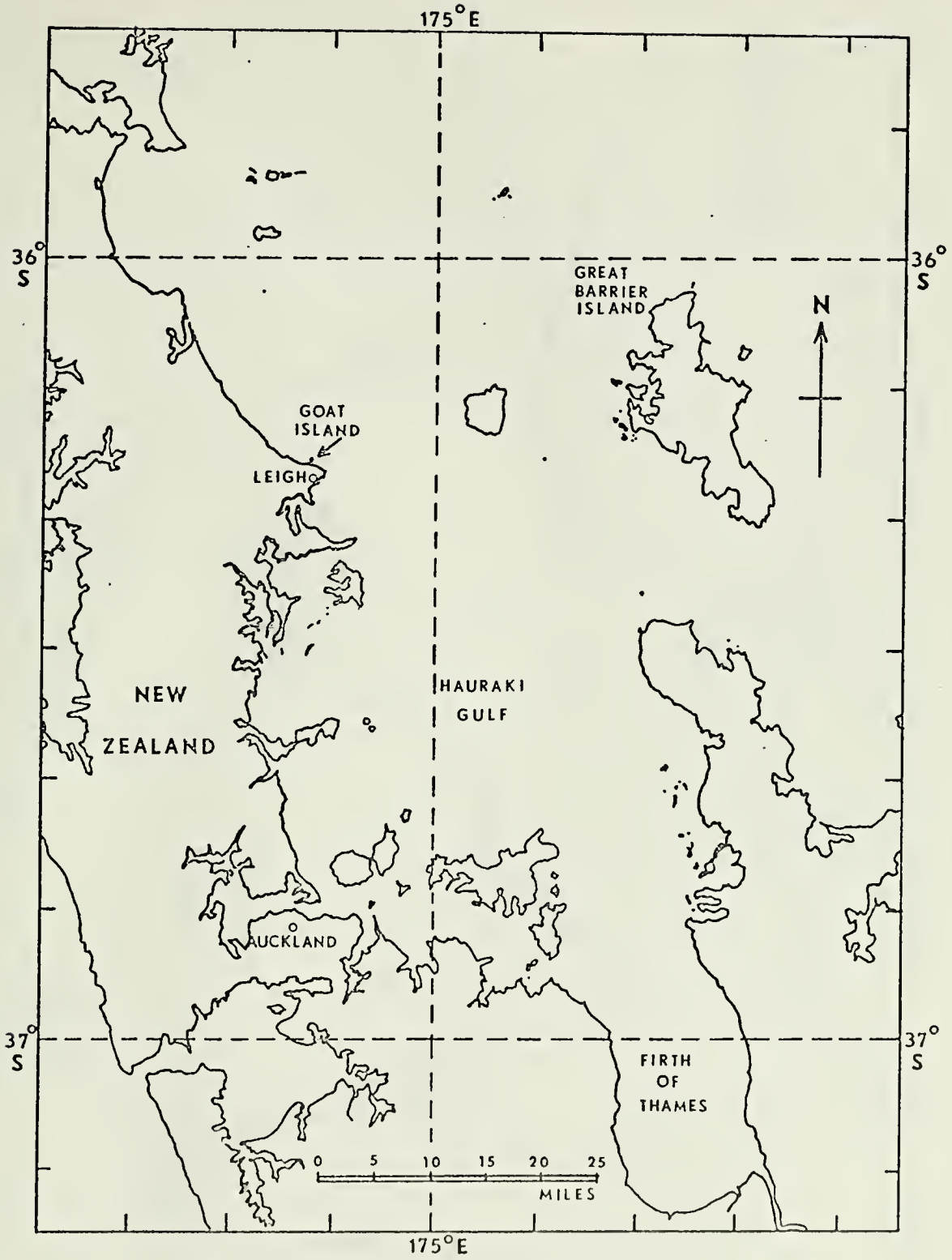

Figure 1. Map of Auckland-Leigh area in New Zealand.

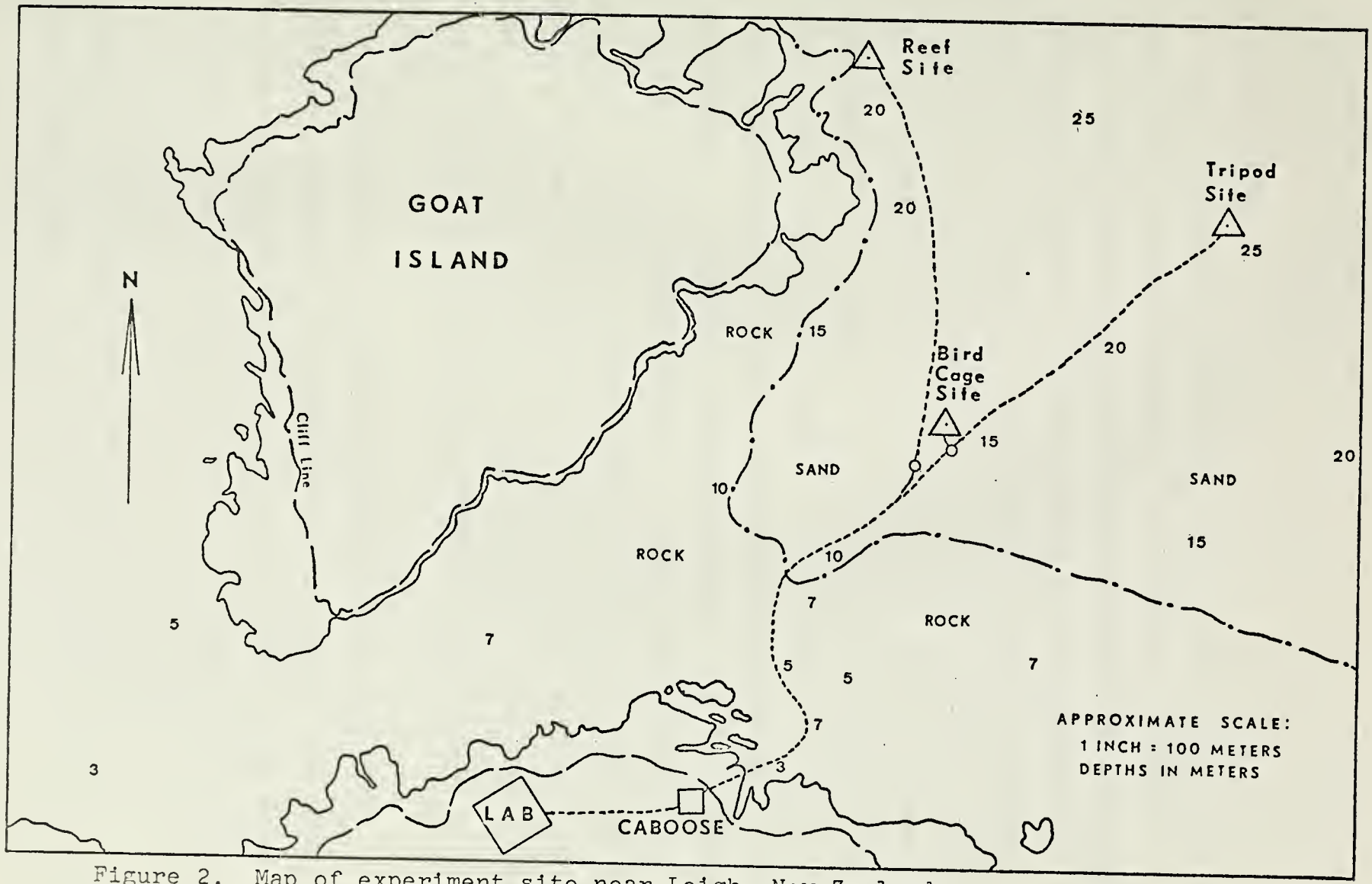

Figure 2. Map of experiment site near Leigh, New Zealand.

varied from a low of about 13.5°C in August to a high of about 20.4°C in February. In the winter the water column was isothermal to the bottom. Warming of the water column as summer approached resulted in slight thermal stratification which reached a maximum in late October or November. Due to the shallow depth at the range, temperature difference between the surface and bottom waters was not expected to exceed 2°C. No permanent thermocline existed and seasonal thermoclines, if present at all, were weak. Surface salinity values ranged from 34.20 to 35.86‰ with a slight increase with depth on the order of 0.1 to 0.2‰ between the surface and 70 feet. Salinities tended to be slightly higher in the winter and spring months, although this trend was not well-established. Light to moderate winds were to be anticipated for the majority of the time with speeds seldom exceeding 18 knots. Currents in the immediate vicinity of the experiment site were irregular in direction and speed, the primary contribution arising from tidal influence. Mean tidal range varied from 5 feet during neap tides to 8 feet during spring tides.

Geologically, the coasts currounding the site were primarily greywacke and sedimentary type rocks. The rugged coastal topography extended approximately 100 to 150 yards offshore where it changed abruptly to a fairly level sandy bottom upon which the instruments were situated. The bottom sediment was friable fine sand of mixed siliceous and calcareous origin. High surface wave activity had the effect

of agitating the bottom sediments and distributing fine particulate matter throughout the water column in a short period of time.

The laboratory was the location of the majority of the shore-based equipment. Twenty-one conducting cables from the laboratory terminated at a secondary shelter, referred to as the "Caboose," where they were joined to three seven-conductor armored cables. The three armored cables were laid over the coastal cliff and out to approximately 250 yards offshore where a set of underwater junctions was located. This site became known as the Bird Cage Site, an identity referring to the metal protective cages in which the armored cables were each joined to a four-conductor cable. Cables of the latter type comprised the remainder of the range wiring. One of the two hydrophones used in the acoustic propagation portion of the experiment was placed at this site atop a 20 foot mast; water depth was about 40 feet.

About 312 yards seaward from the Bird Cage Site was the Tripod Site. A 20 foot high metal tripod had been erected at this site as an instrument platform for a previous experiment. The tripod became the main sensor platform for this experiment. It was situated in approximately 80 feet of water with an initial height of 20 feet above the bottom. A 20 foot extension of PVC (Poly Vinyl Chloride) pipe was added to the tripod to elevate the sensors to the center of the water column. On the tripod mast were mounted the acoustic projector, temperature and temperature microstructure

sensors, and ambient noise hydrophone. Approximately 100 feet seaward of the tripod, one Aanderaa current meter was moored 20 feet above the sea floor.

In additon to the hydrophone placed at the Bird Cage, a second receiving site was established at the base of an underwater reef extending northeast from Goat Island (Figure 2). Water depth at this location – the Reef Site – was approximately 65 feet; the hydrophone was mounted atop a 40 foot mast secured to the sea floor.

By positioning the hydrophones in the manner described, two near-orthogonal acoustic paths of approximately the same length (actual path difference, determined acoustically, was 30 meters) were established. The Tripod-to-Bird Cage path was oriented in the same direction as the predominant swell, i.e., from the northeast to the southwest. Thus, the effects of simultaneous acoustic propagation across-swell and along-swell could be observed. Additionally, if the water were stratified, the effect of internal waves could also be observed if present.

A second Aanderaa current meter was moored 20 feet above the bottom at a location approximately 100 feet east of the Reef Site. The wave and tide sensor was situated in an exposed area about 110 feet south of the Tripod Site.

All of the equipment and cables had to be installed by divers operating from a 12 foot skiff. In addition to the pre-existing cabling mentioned above, new cables had to be installed from the Bird Cage Site to the Tripod, to the Reef

Site, and to the wave and tide sensor. These feeder cables were terminated in either smaller, lighter cables that could easily be brought to the surface for sensor connection, or in underwater housings in which the instrument connection was made.

Several significant problems were encountered in establishing the range. The small boat available required that all of the equipment be relatively light. The use of divers to install the equipment further dictated that size and weight be limited to manageable dimensions. Virtually calm weather was mandatory to insure a satisfactory installation. Many of the sensors, particularly the thermistors, were very fragile and required extreme care in handling.

Fouling and corrosion proved to be constant problems. Experience showed that only a few days' data could be obtained from the thermistors before they had to be cleaned by a diver. Biological fouling grew at a rate of several millimeters per week on exposed unprotected areas. Stainless steel bolts available in New Zealand corroded through in only a few weeks.

The occurrence of large waves, either locally generated or swell from a distant storm, occasionally resulted in damage to the underwater equipment. Such damage mainly consisted of cable displacement and consequent stress or failure of the junction terminals, thus necessitating inspection and repair by divers.

D. DESCRIPTION OF SENSORS

1. General

At the commencement of the experiment in September 1972, the following sensors had been installed:

Tripod Site:

1. mean temperature thermistor
2. temperature microstructure thermistor array
3. acoustic projector
4. ambient noise hydrophone
5. three components of ducted current meters
6. Aanderaa current meter moored about 100 feet northeast of tripod
7. pressure sensitive wave and tide sensor located about 110 feet south of the tripod

Reef Site:

1. hydrophone
2. Aanderaa current meter moored about 100 feet east of the hydrophone mast

Bird Cage Site:

1. hydrophone

The horizontal components of the ducted current meters failed within the first few days of operation. The remaining vertical component operated successfully for the duration of the experiment.

All sensors, with the exception of the Aanderaa current meters, were hard-wired to the shore station for data recording. The Aanderaa meters, which were Savonius rotor type meters, digitally recorded current speed and direction internally on magnetic tape for later retrieval.

In addition to the underwater measurements, meteorological observations were made by personnel at the Marine Laboratory under a program separate from this experiment. Standard atmospheric parameters, including air temperature, dew point temperature, barometric pressure, wind velocity, precipitation, and insolation, were monitored.

Two unique aspects of the sensor suite were the acoustic and temperature components. Early in the preparation for the experiment, two special problems were recognized. The first was the requirement to measure temperature fluctuations to an accuracy of at least $\pm$ 0.01°C; the second was the recording for analysis purposes of short ultrasonic pulses received at two sites. Temperature was a problem because of the sensitivity required over a large temperature range. The acoustic pulses were a problem for two reasons: 1) the tape recorder could not record directly the high frequencies used without excessive tape usage, and 2) direct recording of the received pulses would require an extremely fast digitizing system if the data were to be analyzed on a digital computer.

Systems were designed to cope with these problems and are described in the following sections.

2. Acoustic System

A block diagram of the equipment involved in the acoustic propagation portion of the experiment is shown in Figure 3. Two Wavetek oscillators were used to initiate an acoustic pulse at the desired frequency. The first oscillator, which established the pulse repetition rate, triggered the

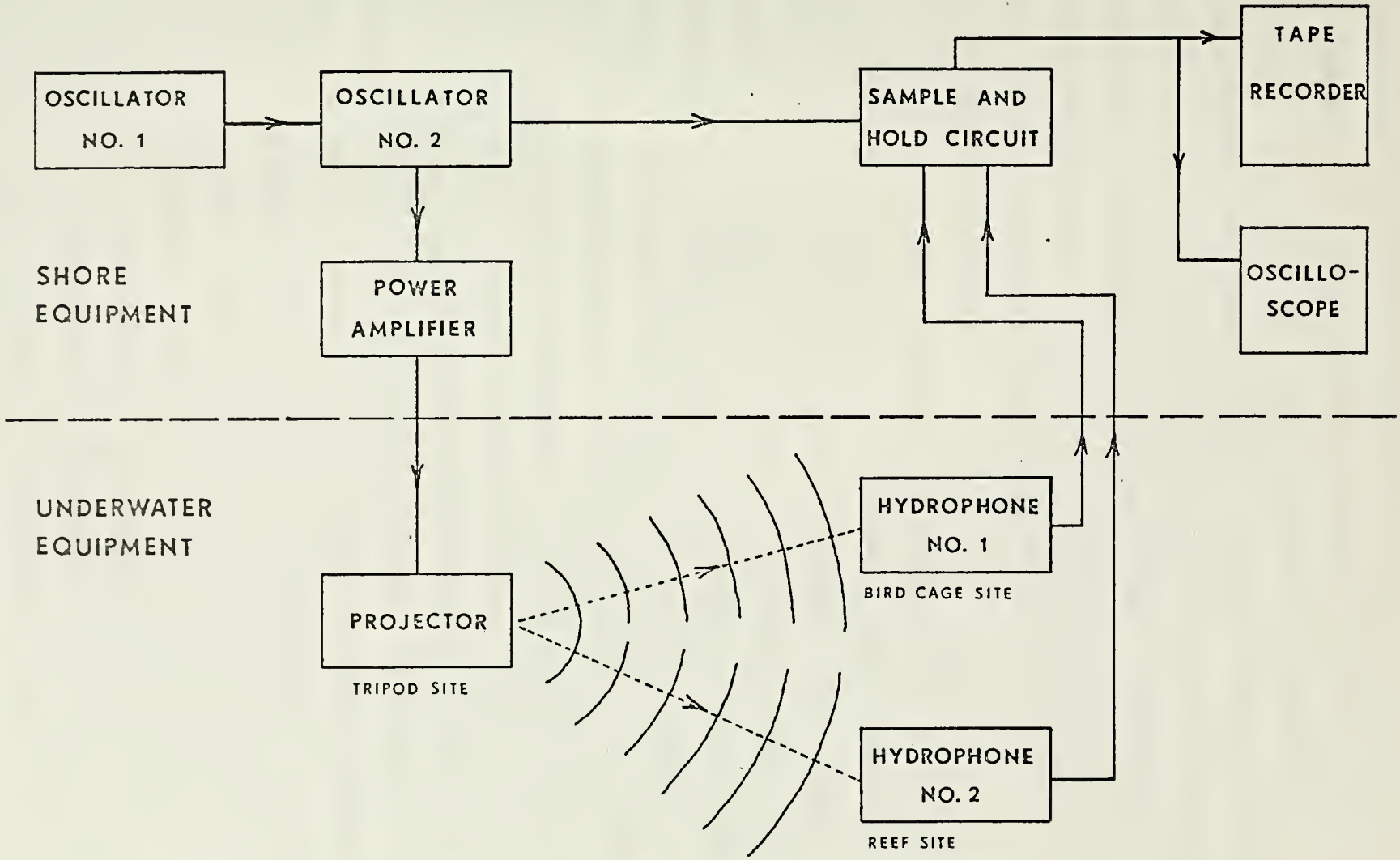

Figure 3. Schematic of acoustic propagation equipment.

second oscillator which produced the pulse. The second oscillator, in turn, triggered the power amplifier and simultaneously input the trigger signal to a specially designed sample and hold circuit. The power amplifier drove a horizontally omnidirectional projector at one of the two experimental frequencies, 35 kHz or 65 kHz. The signals from the hydrophones were passed via cabling back to the shore station where they were input to the dual channel sample and hold circuit.

This circuit, designed and constructed by personnel of the Physics Department at the University of Auckland in New Zealand (Ash 1972) operated as follows. The trigger signal from the second oscillator initiated a sample inhibit instruction in the sample and hold circuit to prevent the circuit from being falsely triggered while the acoustic pulse was traveling down range. The pulse output from the hydrophone preamplifier, approximately 2 volts peak-to-peak, was amplified in the circuit to approximately 8 volts peak-to-peak. By the time the pulse arrived at the circuit, the sample inhibit signal had been cancelled. The first cycle from the arriving pulse that exceeded a pre-set comparator level enabled a 200 msec sample hold component. At this point the peak-to-peak voltage value of the pulse cycle was held for 200 msec. The 200 msec output signal was then applied to a tape recorder. Approximately five cycles of the pulse were required to initiate the sample and hold process. After a pulse was identified, the sampling circuit

was disabled by a logic sub-circuit to avoid triggering of the system by noise or reflections between direct path pulse arrivals.

Pulse durations of 1.0, 1.5, and 2.0 msec were used in various phases of the experiment. However, this did not affect the operation of the sample and hold circuit since pulse height was determined in the first five cycles of the pulse train and later arrivals were ignored.

Pulse repetition rate as determined by the first oscillator also varied, with nominal rates of 1 and 3 pulses per second in use at different times. Problems associated with the higher rate will be discussed in Chapter IV.

The three transducers used in the experiment were basically identical. Each transducer was comprised of a low frequency and high frequency section, resonant to 35 kHz and 65 kHz respectively. The transducers were Model ITC601D manufactured by the International Transducer Corporation of Goleta, California.

Peripheral equipment consisted of an oscilloscope which was used to monitor the performance of the sample and hold circuit and to observe the degree of fluctuation occurring during a run. In the latter stages of the experiment, a pulse height analyzer was also placed in line to obtain immediate analysis of height distributions.

Range geometry and water depths were such that surface-reflected and bottom-reflected signals arrived at the hydrophones sufficiently late enough to insure that only

direct path measurements were made. During the initial phase of the experiment, however, occasional interference from surface-reflected arrivals did occur at the Bird Cage Site under conditions of low tide and an acoustic frequency of 35 kHz. A satisfactory solution to this problem was obtained by lowering the mast at the site by 5 feet prior to the commencement of later phases.

3. Temperature System

Glass encapsulated, fast response thermistors were used for measurement of gross temperature and temperature microstructure. For the gross temperature thermistor, the Wheatstone bridge components were chosen so that the bridge balanced at 14.5°C, the center of the anticipated temperature range of 12°C to 17°C. A temperature range of this magnitude was expected due to the long period of time planned for the conduct of the experiment.

With the high resolution required for the microstructure measurements, a small change in gross temperature would have quickly moved the microstructure bridge off balance if a conventional Wheatstone bridge arrangement were used. Thus, high resolution would have been available only over a very limited temperature range. This problem was overcome by using two equal resistors in the ratio arms of the bridge and two matched thermistors in the opposite arms. Thermal inertia added to one of the thermistors ensured that only slow temperature changes were sensed. The other thermistor in the adjacent arm sensed both gross temperature and

temperature microstructure. Thus, the bridge output was proportional to microscale temperature fluctuations but had the ability to stay balanced over a wide range of gross temperature. The stock of thermistors available was calibrated in a bath from 11°C to 25°C and proved to be very well matched and therefore suitable for this type of arrangement.

For the microstructure measurements, a temperature change of 0.1°C was set equivalent to a 1.0 volt change in the bridge output; the microstructure thermistors were essentially linear over a range of ± 0.1°C from the zero point. The gross temperature range of 12°C to 17°C was equivalent to a voltage output range of -2.0 volts to +2.0 volts with 0.0 volts registered at 14.5°C.

To make efficient use of the limited conducting cables available, temperature data signals were frequency multiplexed in the underwater equipment and then transmitted to the shore equipment in the laboratory where the signal was demultiplexed by filters. The carrier frequencies for the two signals were spaced sufficiently far apart to insure that rejection of the unwanted signal by the filters was effective.

E. DATA ACQUISITION

Preparation for the experiment began during the summer of 1971. This included renovation of the Tripod Site and underwater surveys to determine the best locations for

additional instrument masts and optimum routing to bring the armored cables ashore. Placement of cables, masts, and instruments was executed at various times through the summer of 1972.

Phase I of the experiment with all sensors operating was conducted during the period 26 September to 19 October 1972. Following a six week break when alterations to the mast at the Bird Cage Site were made, Phase II was executed in the first two weeks of December 1972. Phase III of the experiment took place during the first week of July 1973. The runs analyzed in this thesis were all made during Phase I.

In order to establish a comprehensive data base, it was planned to take measurements on an hourly basis and whenever significant phenomena were observed. During Phase I, this schedule was put into effect. However, data storage requirements dictated that the original schedule be modified to acquisition of acoustic and environmental data four times daily and during unusual occurrences (e.g., high swell, high winds, abnormally calm sea, etc.). The four periods specified were sunrise, midday, sunset, and midnight. This schedule was maintained during the latter stages of Phase I and during Phase II. The schedule for Phase III was further modified to provide for as near-continuous data collection as possible during the two days that spanned this phase.

Because of the expansive data accumulation anticipated, run length during Phases I and II was planned to be nominally 10 minutes. It was calculated that a run of this relatively

short length would be long enough to satisfy the requirements for statistical and spectral analysis of the fluctuations in the temperature and acoustic data. On occasions when extreme variability was observed, run length was extended to twenty minutes. During Phase III, run length was arbitrary, with the shortest run being 27 minutes and the longest 77 minutes.

In order to investigate the frequency dependence of the acoustic fluctuations, runs were generally conducted in series of two, alternating the high and low frequencies in each series. Due to the mechanical manipulations required to change frequency, the two runs in a series were separated by a period of about 8 to 20 minutes.

Two magnetic tape recorders were in use during Phases I and II of the experiment. One was a four channel Hewlett-Packard Model 3960, with a tape capacity of 1800 feet of 1.5 mil tape; the second was a seven channel Ampex FR1300 model with a capacity of 2500 feet of 1.5 mil tape. On the Ampex tapes mean temperature, temperature microstructure, pulse heights from both hydrophones, and the current data from the three ducted current meters were recorded. Wave height data, turbulent velocity data from the vertical component ducted current meter, multiplexed temperature data, and pulse height data on a time-sharing basis were recorded on the Hewlett-Packard recorder. The first half of a run was dedicated to Hydrophone 1 at the Bird Cage Site, and the second half to Hydrophone 2 at the Reef Site.

Aanderaa current meter tapes were processed after retrieval by displaying the data on a calibrated strip chart. Except for a few runs in Phase II, ambient noise was not recorded, but was monitored during each run. Also in use was a four channel strip chart recorder which displayed wave and tide information, gross temperature, and temperature microstructure data on a real time basis.

Log-keeping involved recording of dates, times, tape recorder channel allocations, significant wave height ($H_{1/3}$), stage of the tide, and a summary of weather conditions. Wave height and tide information were determined to the nearest 0.1 foot from the strip chart.

Because the experiment was a joint venture between personnel from the University of Auckland and from the Naval Postgraduate School, copying of data tapes was required after each phase to make the data available to both parties. Selected tapes from the Ampex and Hewlett-Packard recordings were transcribed onto one inch, fourteen track magnetic tapes with the use of a Sangamo 3562 tape recorder. Additionally, copies of the experiment logs and of some of the current and wave strip charts were returned to the United States for analysis.

During Phase III, the Sangamo recorder was used for initial data acquisition and dubbed tapes were provided to the University of Auckland.

II. DATA ANALYSIS

A. STRIP CHART RECORDING

The first step in the analysis procedure was to survey the transcribed data to determine qualitatively the nature of the experimental runs available. Initially, this was attempted by viewing the data on a dual-trace oscilloscope. However, only two channels could be viewed simultaneously and no permanent visible record was produced.

The magnetic data tapes were then played back on the Sangamo tape recorder with the output displayed on an eight channel Brush strip-chart recorder. The two tape channels containing hydrophone information were input directly to the Brush recorder. Each channel containing temperature data was first low pass filtered through a Krohn-Hite Model 3340 filter at 20 Hz to eliminate high frequency noise that may have contaminated the signal. The filtered data were then displayed on the Brush recorder chart.

A typical section of pulse height data and temperature microstructure data is shown in Figure 4(a). Figure 4(b) shows an expanded view of a typical pulse sequence.

B. DIGITIZATION

After screening the data for noise and run length, thirty-five runs made during the period 30 September through 13 October 1972, and five runs from the period 2 through 3 July 1973 were selected to be digitized. None of the runs from

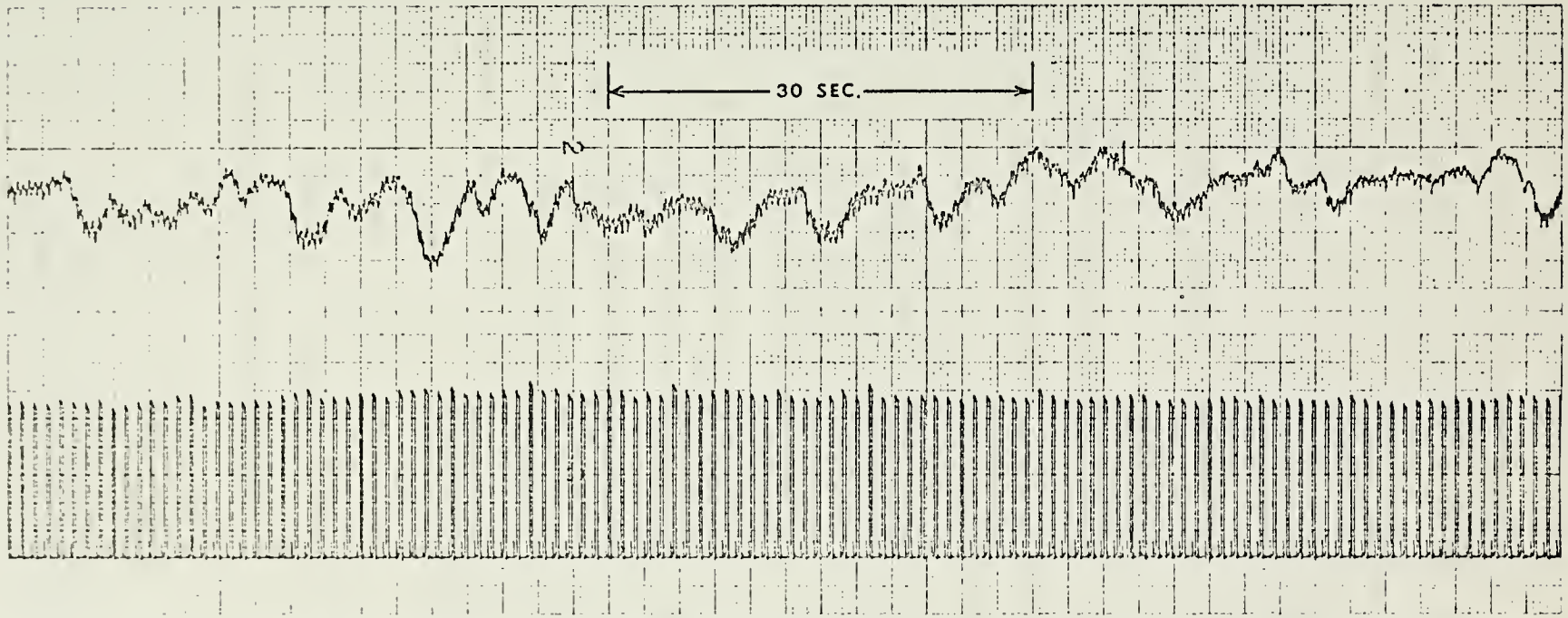

Figure 4.a. Typical sample of microscale temperature fluctuations and simultaneously observed acoustic pulse heights.

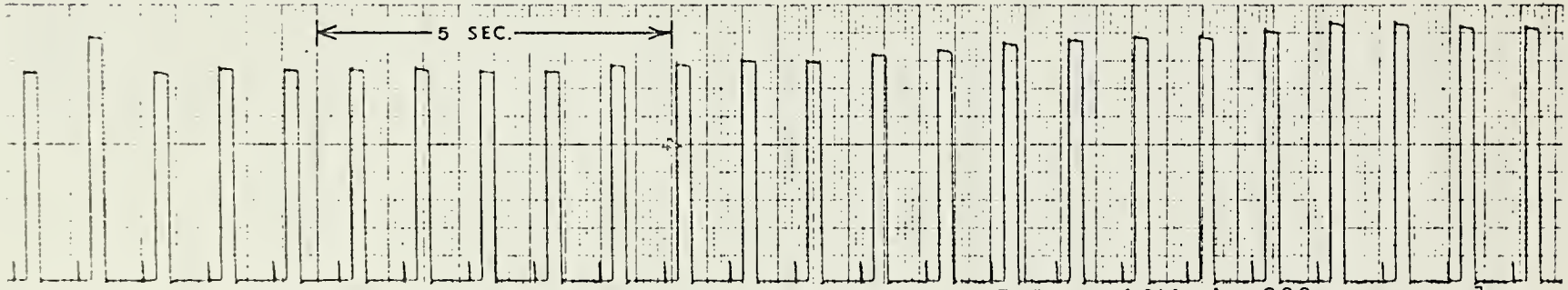

Figure 4.b. Expanded view of acoustic pulse sequence. Pulse width is 200 msec; pulse repetition rate is slightly greater than 1 Hz. Small spike prior to each pulse is the trigger pulse.

Phase II of the experiment were chosen. Four channels of acoustic and temperature data were digitized. Digitization was accomplished through the use of a COMCOR 5000 analog computer, a Scientific Data Systems XDS 9300 digital computer, and a Naval Postgraduate School analog-to-digital conversion program. All of the above were available in the Electrical Engineering Computer Laboratory of the Naval Postgraduate School.

In the digitization process, the most critical factor to be specified was the sampling rate. Based on a requirement to accurately define the pulse height on the digitized record, a sampling rate equivalent to 256 samples per channel per digital record was selected. This rate translated to a sampling time increment of 0.04 seconds between samples. Since the length of a pulse was 200 msec (0.2 seconds), the sampling rate insured a minimum of five samples on a normal pulse height and a maximum of six samples if the first sample on the pulse happened to occur exactly at the leading edge. Each hydrophone channel was input directly from the Sangamo tape recorder to the analog patchboard where the signal was amplified 25 times.

The Nyquist frequency associated with the sampling rate was given by the equation,

$$f_c = \frac{1}{2\Delta t}$$

where Δt = sampling time increment.

For the increment chosen, 0.04 sec, the Nyquist frequency was 12.5 Hz. This frequency was above the highest frequency of significant fluctuations expected in the temperature microstructure data and was high enough to minimize aliasing.

Temperature data were played into the input of the analog patchboard where a plus 10 gain was applied. The amplified signal was then low pass filtered at 50 Hz to eliminate locally generated 60 Hz noise that was apparent in initial trial runs. Because tape playback during digitization was conducted at 16 times real time, the actual temperature data was, in effect, filtered at 3.125 Hz. The filtered signal was then input to the patchboard where a second plus 10 gain was applied. Total amplification of the temperature data was 100 times. Of several methods evaluated for filtering and amplifying the temperature data, the above method appeared to be the most practical and efficient in eliminating the locally introduced 60 Hz signal.

In addition to the above procedures, biasing of the amplified signal was required to keep the signal voltage within the ± 100 volt range of the analog computer. The COMCOR 5000 provided bias adjust on each channel.

Each analog run was converted to a digital file of discrete samples. These samples were written on seven track magnetic tape in octal base notation. Each file contained all four channels of digitized data applicable to that run. Data in a file were written in blocks of 1024 samples called digital records; each record spanned 10.24 seconds of real time data.

C. CONVERSION

Continued analysis was to be performed on the IBM 360/67 digital computer at the Naval Postgraduate School. However, it was first necesary to make the digitized data compatible with the IBM 360 system. The conversion process involved changing the notation from octal base to hexadecimal base, and rewriting the data on a nine track magnetic tape. The conversion was made using programs available at the Naval Postgraduate School computer center and described in a current technical note (Raney 1973).

D. PULSE HEIGHT EXTRACTION

Of the 256 samples per channel in one digital record which represented 10.24 seconds of data, only about 50 of the acoustic channel samples actually fell on a pulse height peak. Furthermore, these 50 samples accounted for only 10 pulses. In order to conserve core storage, it was necessary to compute and store only the pulse height value, rather than read into memory an entire file, consisting of an average 58 digital records.

A program was written to read from the tape only the two channels containing pulse data. When one digital record had been read in, the pulse heights for each acoustic data channel were computed and stored. Upon completion, the next succeeding record was read from the tape and processed. This sequence was continued until the entire file had been analyzed.

Programming precautions were taken to insure that no pulse heights were missed on either channel and that only actual pulse heights were retained; i.e., spurious noise spikes were omitted.

E. SELECTION OF RUNS FOR DETAILED ANALYSIS

Of the 35 runs in Phase I that were digitized, three were unacceptable due to excessive random noise that was apparently acquired during digitizing. From the remaining 32 runs, twelve were selected for detailed analysis. The selection criteria were to form a suite of runs that were representative of all typical environmental conditions, and to choose runs that for one reason or another (e.g., frequency, time of day, time sequence) were suitable for comparison with each other.

No runs from Phase III were considered due to low apparent variability and difficulty with the data resulting from unexplained interchannel feedback somewhere in the data acquisition stage.

Pertinent details of the twelve analysis files are shown in Table I. Because of digitizing requirements, the file length was always slightly shorter than the actual experiment run length. Table II summarizes the environmental conditions present during each run. The comments section of Table II was synopsized from the original logs kept during the experiment.

Run Number	Date (1972)	Local Time Period	Frequency (kHz)	Pulse Rep. Time Increment Δt (sec)	File Length (min,sec)	Number of Pulses
45	30 Sep	1200-1210	35	0.90033	9m 11.90s	614
46	30 Sep	1220-1230	65	0.90046	9m 11.98s	614
48	30 Sep	1518-1528	35	0.90170	9m 11.84s	613
49	30 Sep	1636-1646	65	0.96068	9m 52.74s	618
56	1 Oct	0542-0552	35	0.96068	9m 51.78s	617
58	1 Oct	0616-0626	65	0.96029	10m 3.06s	629
60	1 Oct	0900-0910	35	0.96071	9m 52.76s	618
61	1 Oct	0919-0929	65	0.96065	9m 52.72s	618
72	2 Oct	1810-1820	65	0.92079	9m 21.68s	611
73	2 Oct	2016-2036	65	0.92138	19m 5.28s	1244
116	13 Oct	1823-1833	35	1.02768	10m 2.22s	587
117	13 Oct	1851-1901	65	1.01082	9m 52.34s	587

Table I. Basic Data on Analyzed Runs. Runs 45 and 46, 56 and 58, 60 and 61, and 116 and 117 constitute the set of runs conducted in pairs, as referred to in subsequent discussion.

Run Number	Tide (ft)	Wave Height $H_{1/3}$ (ft)	Weather and Comments
45	+3.5	0.6	2/10 cloud cover, mostly sunny, very light wind.
46	+3.8	0.6	3/10 cloud cover, sun obscured by cloud at start of run, sun back out again at 1223.
48	+1.8	0.6	Partly cloudy, but sun unobscured; very light wind from the south.
49	0.0	0.6	Sky clear, bright sun, very light easterly wind, sea near tripod is calm.
56	-1.7	0.9	Sky clear, no wind.
58	-2.0	0.8	No wind, no clouds, sun just coming up; killer whale heard on ambient noise hydrophone. [During succeeding run (0637-0647), two whales were observed diving at the tripod.]
60	-2.3	0.7	1/10 cloud cover, wind very light, sea state 1, southerly swell.
61	-1.8	0.6	2/10 cloud cover, wind very light from south, sea calm.
72	+1.0	0.5	Sun just going down (at 1800), very light wind from west.
73	-2.0	0.6	Dark, very light wind.
116	-2.0	1.8	Overcast, nearly dark, moderate to fresh wind from west, squally rain.
117	-1.6	1.8	Overcast, fresh wind.

Author's note: Sky had been overcast for 48 hours preceding runs 116 and 117. Winds were varying from "calm" to "fresh" mainly from west to northwest. No precipitation was recorded prior to run 116. On 13 October, the date of runs 116 and 117, there had been no sun all day, and winds had been continually increasing from "calm" reported at 0500.

Table II. Sea and Weather Conditions During Each Run

F. STATISTICAL ANALYSIS

In order to perform the planned spectral analysis, an accurate determination of the pulse repetition period was required. To obtain this, the average time increment, Δt, between pulses (Table I) was computed. This increment was the measure of the frequency with which an acoustic pulse "sampled" the medium.

The time increment, Δt, was found by computing the total time elapsed between the first sample on the first pulse in a run, and the first sample on the last pulse in the same run. This elapsed time, referred to as file length in Table I, was then divided by one less than the total number of pulse heights.

The analog-to-digital sampling period of 0.04 seconds was the maximum error possible between the actual analog file length and the digital file length as computed above. Thus, for a file having a nominal 601 pulses (see Table I), the maximum possible error in the computed average pulse time increment, Δt, was on the order of:

$$(\Delta t)_{\substack{\text{max} \\ \text{error}}} = \pm \frac{.04 \text{ sec}}{600} \cong \pm 6.7 \times 10^{-5} \text{ seconds}$$

An error of this magnitude was considered acceptable for the precision required to perform a valid spectral analysis of the pulse heights.

Computation of certain statistical parameters was the next step in the analysis scheme. A pre-compiled subroutine available in the Naval Postgraduate School IBM 360 library was used to compute the coefficient of variation, the minimum and maximum values and the range of the distribution. The pulse height histogram was also computed and plotted.

It was immediately apparent from the histograms that a small percentage of pulses had either extremely high values or low values. However, this result was expected from the Brush recordings which showed a random occurrence of "drop-outs" and "spikes". The origin of these anomalies was not exactly known, but it was apparent that they did not represent real acoustic fluctuations. To eliminate these a program was written to filter the pulse heights through a gate whose width could be varied. The acceptable gate width was determined by a trial and error process. The method employed in this smoothing process was to compare a pulse height with a running mean computed from the previous ten pulses. The first ten pulses in a file were tested against the mean of the first twenty heights to initiate the process. The gate was centered around the mean. A bad value was eliminated by substituting an artificial pulse whose height was determined from a linear interpolation between the preceding good pulse and the next succeeding good pulse. Pulse heights filtered in each computer run were compared with the Brush chart to determine if any good data had been filtered or if any anomalies had been missed. This method

did not eliminate all bad pulses and on some runs one or two erroneous pulses escaped correction. Since these few represented a very small percentage of the total sample — less than 0.5% — no further attempts were made to smooth them. Thus the temporal fluctuations in the smoothed distribution were, with rare exception, the result of actual acoustic variability.

The smoothed data were then re-analyzed as discussed above. Of all the basic statistics computed, the coefficient of variation was the most pertinent. Skewness and kurtosis, which were computed along with other statistics, would have been valuable for comparison of histograms but were invalidated for this purpose because the class interval varied among distributions. In computing the histograms, the constant factor was the number of class intervals rather than the width of the class interval; this feature was a set characteristic of the subroutine.

To facilitate comparison of results among runs, the pulse heights of each run were normalized to the mean for that run. Each pulse height sequence, then, had a mean of 1.0, and each pulse value was expressed as a percentage of the mean. This process had no mathematical effect on the coefficient of variation. Conversion of pulse heights to standard variables was also done so that distribution in terms of standard deviations was available.

G. SPECTRAL ANALYSIS

Following procedures detailed in Bendat and Piersol (1966), preparation of the pulse height time series for spectral analysis started with removal of the mean and of any linear trend present in the series.

An estimate of the autocorrelation function, $R(\tau)$, for each time series was computed using the formula:

$$R(\tau) = \frac{1}{N} \sum_{n=1}^{N-m} (X_n)(X_{n+m})$$

where N = the number of time samples, i.e., the number of pulses in each run

m = the lag number

τ = the lag time = $m(\Delta t)$

X = the individual pulse height value

The values for τ were incremented from $\tau=0$ to a maximum lag value of approximately one-tenth of the file length. The increment used was the Δt determined by the method in Section II.F.

A Parzen lag weighting function was then applied to the autocorrelation function in order to insure a better estimate of the spectral energy density values.

The autocorrelation function was Fourier transformed to arrive at an estimate for the spectral energy density function, $G(f)$. The digital programming was derived from the integral expression:

$$G(f) = 4 \int_0^\infty R(\tau) \cos 2\pi f\tau \, d\tau$$

where $R(\tau)$ = the autocorrelation function

f = frequency

τ = lag time

Estimates were computed for narrow frequency bands over the range from D.C. to f_c where f_c is the Nyquist frequency applicable to each run.

The cross correlation function $R_{xy}(\tau)$ between Hydrophone 1 and Hydrophone 2 was computed next, using the equation:

$$R_{xy}(\tau) = \frac{1}{N-m} \sum_{n=1}^{N-m} X_n Y_{n+m}$$

where X = pulse height value for Hydrophone 1

Y = pulse height value for Hydrophone 2

and N, m, and τ were as previously defined.

As with the autocorrelation functions, a Parzen window was used to smooth the cross correlation function prior to computation of the cross-spectral energy density function. The co-spectral density and quadrature spectral density functions were used to obtain the coherence, γ_{xy}^2, and phase, θ_{xy}, functions for the pulse height time series:

$$\gamma_{xy}^2(f) = \frac{C_{xy}^2(f) + Q_{xy}^2(f)}{G_x(f)\, G_y(f)}$$

$$\theta_{xy}(f) = \tan^{-1} \frac{Q_{xy}(f)}{C_{xy}(f)}$$

where $\gamma_{xy}^2(f)$ = coherence between Hydrophone 1 and Hydrophone 2 as a function of frequency

$\theta_{xy}(f)$ = phase between Hydrophone 1 and Hydrophone 2

$C_{xy}(f)$ = co-spectral energy density function

$Q_{xy}(f)$ = quadrature spectral energy density function

$G_x(f)$ = spectral energy density function for Hydrophone 1

$G_y(f)$ = spectral energy density function for Hydrophone 2.

H. DISPLAY OF RESULTS

The following computer generated plots were made on the CALCOMP plotter:

1. relative pulse height time series for each hydrophone
2. autocorrelation functions for each hydrophone
3. auto-spectral energy density of the acoustic fluctuations for each hydrophone
4. phase and coherence between Hydrophone 1 and 2.

Except for one instance (Run 73) where the file length was longer than usual, all runs were plotted using identical scaling factors.

III. RESULTS OF ANALYSIS

A. TEMPERATURE FLUCTUATIONS

Detailed analysis of the temperature microstructure data was not performed in the course of this thesis. However, the Brush chart recordings previously described afforded an opportunity for a qualitative evaluation of the microstructure activity present during each run. Of the twelve runs under discussion, four showed temperature fluctuations that were considerably more active than the others. The remainder of the runs occurred under temperature conditions varying from negligible to moderate activity. The most active runs were numbers 72, 73, 116, and 117. Representative samples of the twelve temperature records are shown in Appendix A.

The temperature microstructure fluctuations were evaluated using the thermistor calibration factors, tape recorder gains, and the gain and chart speed settings for the Brush recorder. An arbitrary classification scheme was employed to assign qualitative descriptors:

Temperature Fluctuation	Classification
< 0.05°C	Negligible
.05°C to 0.2°C	Moderate
> 0.2°C	High

B. STATISTICAL RESULTS OF PULSE HEIGHT ANALYSIS

Table III summarizes the statistical results obtained from the analysis. Reference to Tables I and II supplies information relating the acoustic frequency, time of day, and environmental conditions to these results.

The coefficients of variation ranged from a low of 2.03% (Run 56) to a high of 15.53% (Run 116). The five highest coefficients occurred in runs of relatively high thermal activity. In general, the variation observed on Hydrophone 2 was slightly higher than that on Hydrophone 1, the exceptions being Runs 45, 46, and 72. However, in only four runs (60, 73, 116, 117) was the difference between the two hydrophones greater than 2%; three of these four runs were also classified as having higher microstructure content than the others.

Significant differences between the high frequency runs and low frequency runs were more difficult to determine. For runs that were conducted in high and low frequency pairs (see Table I), the coefficients of variation for both Hydrophone 1 and 2 during the high frequency run were generally slightly higher than during the low frequency run. However, since the two runs in a pair were conducted 8 to 24 minutes apart (Table I), the difference may not have been due to frequency change alone.

Table III also has two sections pertaining to the range of the distributions of pulse heights. The first of these sections lists the extremes of the distribution in terms of standard deviation. The second shows the range in terms

Run #, Freq.	Hydro-phone	# of Bad Pulses	Coeff of Variation(%)	Distribution in Terms of σ Minimum	Maximum	Range	Distribution in % Relative to Mean Minimum	Maximum	Range
45	1	2	2.77	-3.38	3.54	6.92	90.64	109.81	19.17
LO	2	2	2.16	-3.21	3.68	6.89	93.07	107.94	14.87
46	1	11	4.28	-2.35	3.04	5.39	89.94	113.02	23.08
HI	2	19	2.83	-4.98	4.93	9.91	85.91	113.95	28.04
48	1	1	3.34	-3.93	3.34	7.27	86.86	111.17	24.31
LO	2	1	4.07	-2.52	2.64	5.16	89.75	110.73	20.98
49	1	6	4.08	-2.22	3.74	5.96	90.97	115.23	24.26
HI	2	15	5.34	-3.97	3.26	7.23	78.78*	117.43	38.65*
56	1	0	2.03	-3.63	4.21	7.84	92.64	108.55	15.91
LO	2	1	4.22	-3.06	2.56	5.62	87.06	110.81	23.75
58	1	17	3.87	-2.79	3.37	6.16	89.19	113.03	23.84
HI	2	53	5.54	-3.68	3.93	7.61	79.62	121.76	42.14
60	1	0	3.17	-3.15	3.73	6.88	90.02	111.83	21.81
LO	2	0	7.00	-2.90	2.83	5.73	79.73	119.80	40.07
61	1	10	3.65	-3.18	3.14	6.32	88.40	111.45	23.05
HI	2	31	5.52	-2.68	3.17	5.85	85.20	117.52	32.32
72	1	6	9.61	-2.25	2.93	5.18	78.40	128.13	49.73
HI	2	13	8.96	-3.30	2.13	5.43	70.44	119.08	48.64
73	1	35	5.78	-3.17	5.51	8.68	81.71	131.84	50.13
HI	2	98	9.50	-3.52	3.80	7.32	66.59	136.07	66.48
116	1	5	5.69	-3.91	2.88	6.79	77.78	116.40	38.62
LO	2	23	15.53	-2.52	3.23	5.75	60.81	150.08	89.27
117	1	8	7.63	-4.10	2.35	6.45	68.73	117.90	49.17
HI	2	29	15.32	-2.22	3.25	5.47	66.05	149.77	83.72

*Due to a "drop-out" pulse that escaped correction, actual minimum should be 87.06% with resultant range of 30.37%.

Table III. Summary of Statistical Analysis Results

of percentage deviation from the mean. Information about the shape of the distribution can be inferred from these statistics. A relatively large σ range coupled with a relatively small percentage deviation indicates that the distribution is closely packed about the mean; this is reflected in a low coefficient of variation. The converse situation implies a relatively flat, dispersed distribution with a consequently higher coefficient of variation. The coefficient of variation can be obtained by computing the ratio of relative percentage range to standard deviation range. However, the defining equation given in Chapter I was used to calculate the coefficients given in Table III.

C. SPECTRAL ANALYSIS RESULTS

Computer generated plots for the twelve analyzed runs are presented in Appendix A. Each series of four plots for each run contains the time series of pulse heights plotted relative to the mean, the autocorrelation functions for each time series, the auto-spectral energy density functions, and the coherence and phase functions determined from the cross-spectral analysis between Hydrophones 1 and 2.

Table IV summarizes the lag times determined for three values of the autocorrelation function (0.5, e^{-1}, and 0.0), approximate values of strong periodicities observed in the autocorrelation functions, and the maximum value of coherence attained between the two hydrophones.

Run Number	Hydrophone	Autocorrelation Lag Times (sec) $\tau_{0.5}$	$\tau_{1/e}$	$\tau_{0.0}$	Apparent Periodicity	Maximum Coherence
45	1	5.5	8.1	17.1	None	0.21
	2	2.0	2.5	33.3	None	
46	1	7.4	9.8	28.8	None	0.34
	2	1.2	2.0	19.8	8 sec	
48	1	1.1	4.0	19.3	None	0.20
	2	11.1	17.6	-	None	
49	1	13.9	17.3	28.8	None	0.28
	2	5.3	11.1	29.8	None	
56	1	0.8	1.8	11.1	None	0.23
	2	1.2	1.6	3.2	8 sec	
58	1	0.9	1.9	19.2	None	0.21
	2	1.7	2.1	11.0	None	
60	1	4.8	16.3	-	None	0.21
	2	1.1	7.7	-	7 sec	
61	1	0.8	1.7	20.1	6 sec	0.19
	2	1.1	1.8	3.5	6 sec	
72	1	-	-	-	None	0.18
	2	12.6	15.5	26.7	None	
73	1	3.1	6.5	31.3	None	0.43
	2	10.9	17.6	-	None	
116	1	1.3	1.7	24.2	4 sec	0.29
	2	2.7	25.2	-	7.5 sec	
117	1	1.5	1.9	40.4	7.7 sec	0.22
	2	2.8	41.9	-	6.5 sec	

Table IV. Summary of Selected Results From Spectral Analysis

The autocorrelation functions exhibited a wide variety of characteristics which were related to the acoustic fluctuations, and consequently to the state of the medium at the time the run was conducted. In a run when the temperature microstructure activity was low to moderate, evidenced by the figures in Appendix A, and the wave activity was low (Table II), the two autocorrelation functions were roughly comparable. For runs that occurred in pairs (Table I), no reliable trend was detected to indicate significant difference due to a change in acoustic frequency. When periodicities were apparent in the autocorrelation functions, they were stronger on Hydrophone 2 than on Hydrophone 1. Runs 72 and 73, conducted two hours apart during periods of relatively high thermal activity, did not evidence any strong periodicity, unlike Runs 116 and 117, conducted under apparently similar thermal conditions. Significant wave heights for these two sets of runs were 0.6 feet and 1.8 feet, respectively. For runs where the autocorrelation function showed a marked periodicity, a distinct peak in the spectral energy density was evident. However, many of the peaks in the energy spectrum were not manifested in readily definable periodicities in the autocorrelation function.

All but two autocorrelation functions exhibited a definite trend towards zero with increasing lag time. Hydrophone 1 for Run 72 was decaying very slowly, but had not reached

a value of 0.5 at the maximum time lag of 55 seconds. In Run 49, Hydrophone 1 decayed continuously from $\tau = 0$, crossing the zero axis at 30 seconds and continued to decay until it exceeded the scale capability of the plot at a value of -0.34 and $\tau = 43.2$ seconds. However, the computer printout showed that the autocorrelation function reached a minimum of -0.38 at 51 seconds and was increasing towards zero at the maximum lag time of 58 seconds.

For all runs, the coherence between Hydrophones 1 and 2 was very low with an average value on the order of 0.1. The maximum coherence listed in Table III occurred on a coherence peak that was not representative of the entire run. A maximum coherence of 1.0 would have indicated a linear relationship between the fluctuations on Hydrophone 1 and those on Hydrophone 2; conversely, a coherence function of 0.0 would have meant that the fluctuations were unrelated. For intermediate values, three possible situations could have existed [Bendat and Piersol 1966]:

1. extraneous noise was present in the measurements
2. the relationship between the fluctuations on each hydrophone was non-linear
3. the fluctuations on one hydrophone were not driven entirely by the same mechanisms as the fluctuations on the other hydrophone

With consideration of the experimental parameters, a non-linear relationship between the fluctuations was the most plausible reason for the low coherence.

The phase function for all runs is very erratic, a further indication that a simple linear relationship did not exist between the two hydrophones.

D. DISCUSSION

The success of the analysis of the acoustic data was predicated on the reliability of the sample-and-hold circuit described in Section I.D.2. Therefore, due scrutiny was given to the number of bad pulse heights that were detected by the smoothing process outline in Section II.F. If the number of bad pulses were proportional to the acoustic variability, the probability that such pulses may have been actual acoustic fluctuations is increased. Plotting the coefficient of variation versus the number of bad pulses, Figure 5, did not support a relationship between the two parameters. Data for Figure 5 were taken from Table III and all points were plotted except those for Run 73 which was twice as long as any other run.

The number of bad pulses, however, did seem to be related to frequency. There were significantly more rejected pulses at 65 kHz than at 35 kHz. This suggested that the sample and hold circuit was encountering trouble in "following" the 65 kHz wave form. However, Hydrophone 2 showed 2 to 3 times more bad pulses than Hydrophone 1. A plot of the number of bad pulses that occurred on Hydrophone 1 against the number on Hydrophone 2 for both frequencies, Figure 6, indicated a strong relationship between the two parameters.

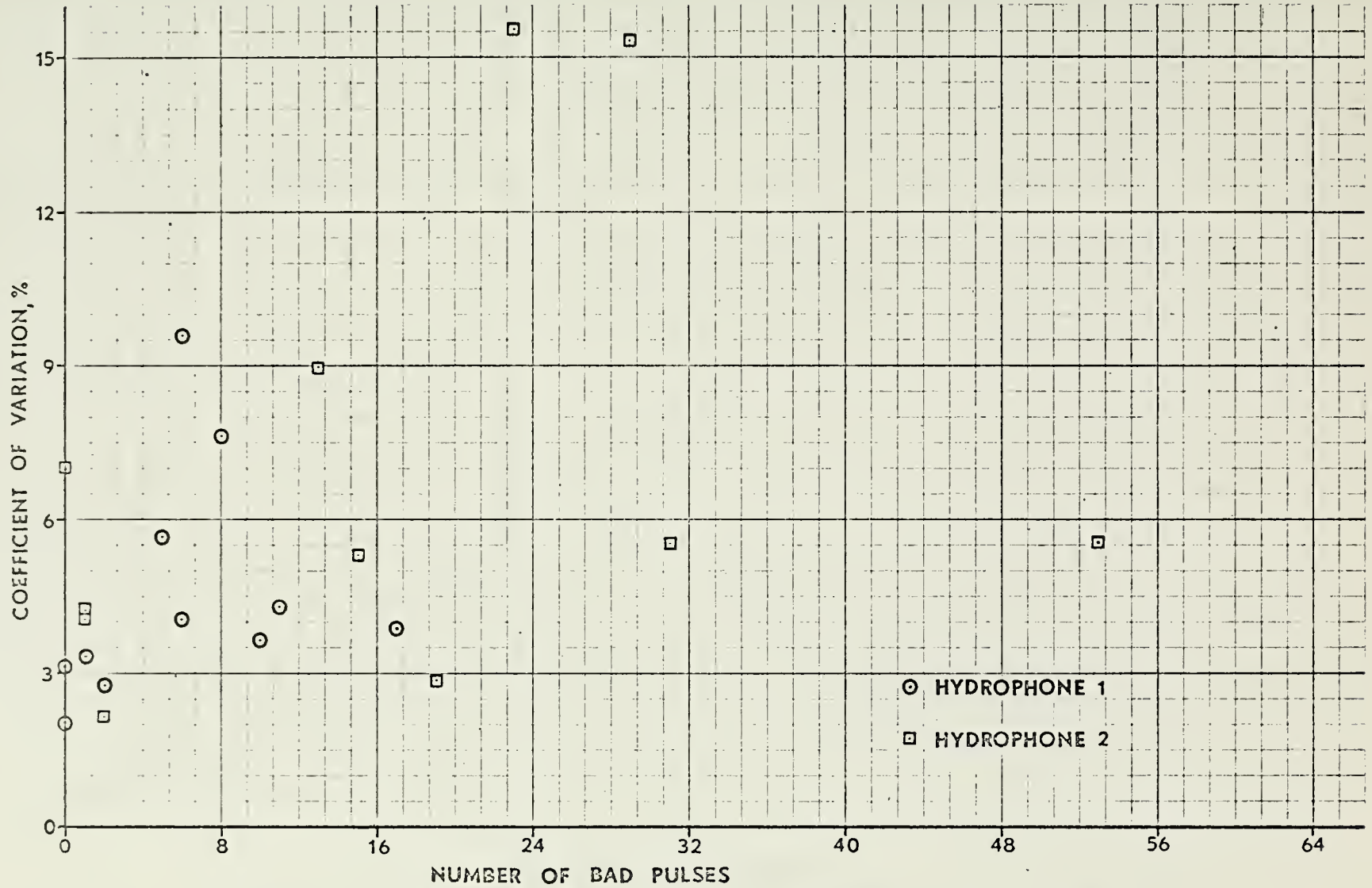

Figure 5. Graph of coefficient of variation vs. number of bad pulses.

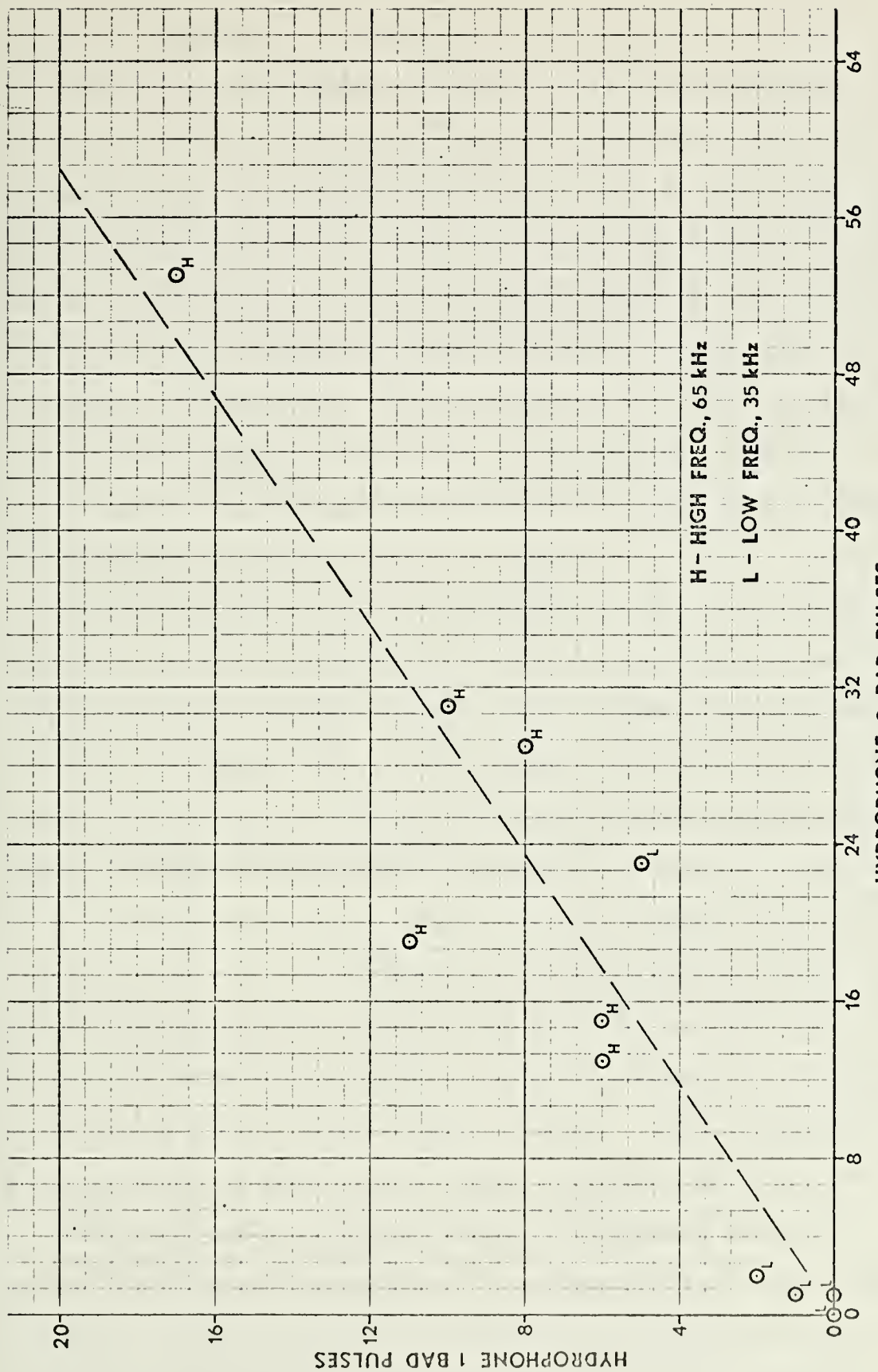

Figure 6. Graph of bad pulses on Hydrophone 1 vs. those on Hydrophone 2. Frequency dependence is indicated by subscripts.

Since the hydrophones were identical and operated well throughout the experiment, the bad pulses could only have been generated in the two channels of the sample and hold apparatus. The critical question was: Did the malfunction nullify the experiment? Evidence to the contrary was explicit in the pulse height histograms which clearly showed the bad pulses separated from either side of the main grouping. Furthermore, the Brush chart time series supported the conclusion that, except for the random occurrence of a bad pulse, the sample and hold circuit performed reliably on all other pulses.

During Phase II of the experiment, an on-line Pulse Height Analyzer was installed to obtain a real-time analog display of pulse height distributions. Sample histograms from two runs made under conditions of low and high microstructure activity are shown in Figures 7 and 8. The Pulse Height Analyzer was storage limited to the number of pulses in a five minute segment of the run. The corresponding five minute portion of the temperature microstructure record is shown for comparison. The histograms obtained by digital methods in this thesis were comparable to the distributions accumulated by the Pulse Height Analyzer. This promoted additional confidence in the sample and hold electronics.

As noted previously, the degree of thermal activity varied considerably during the runs from Phase I that were analyzed. Runs 72, 73, 116, and 117, all conducted under conditions of similar temperature fluctuations, exhibited

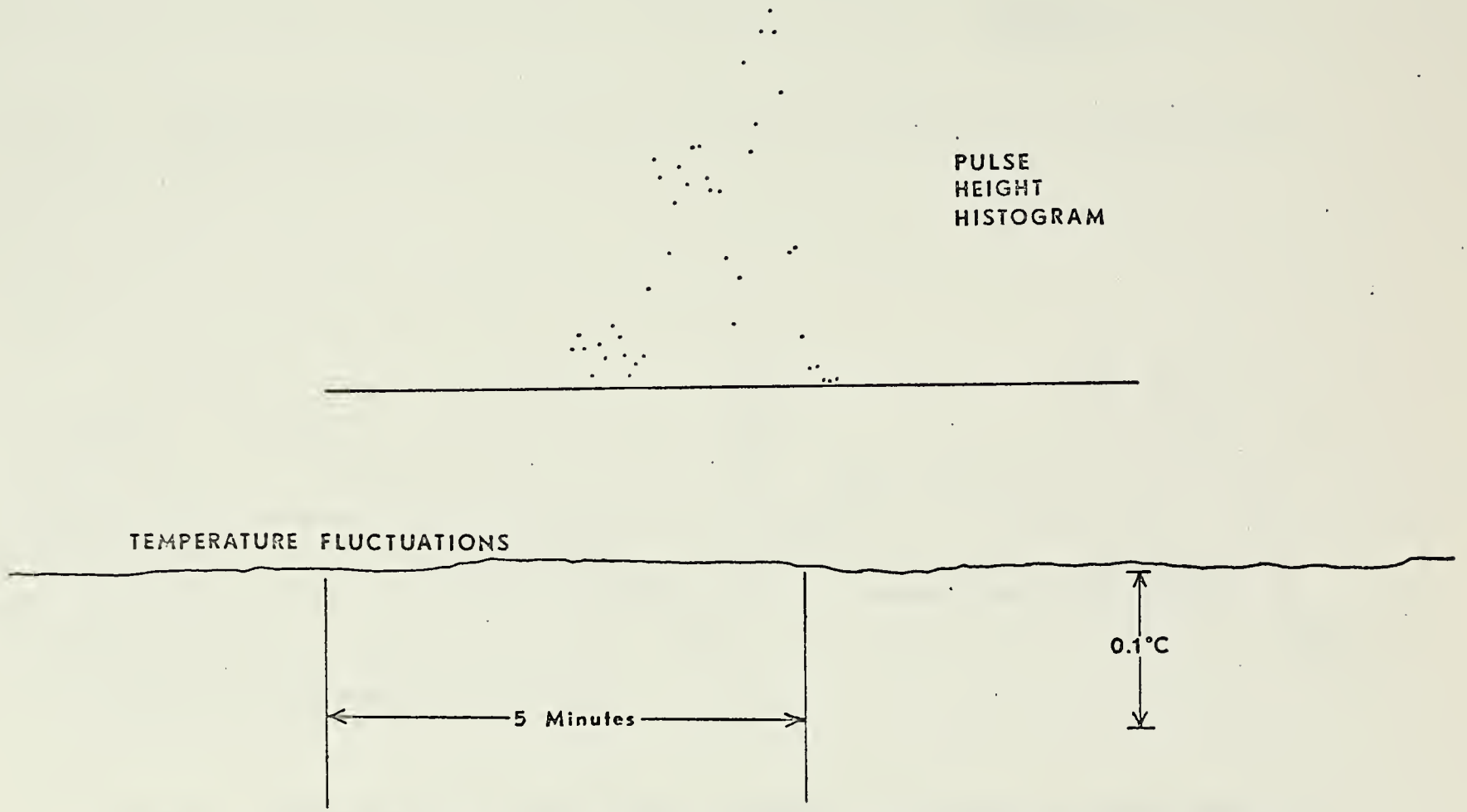

Figure 7. Histogram from Pulse Height Analyzer for pulses recorded during the 5 minute period shown on temperature record: negligible thermal activity.

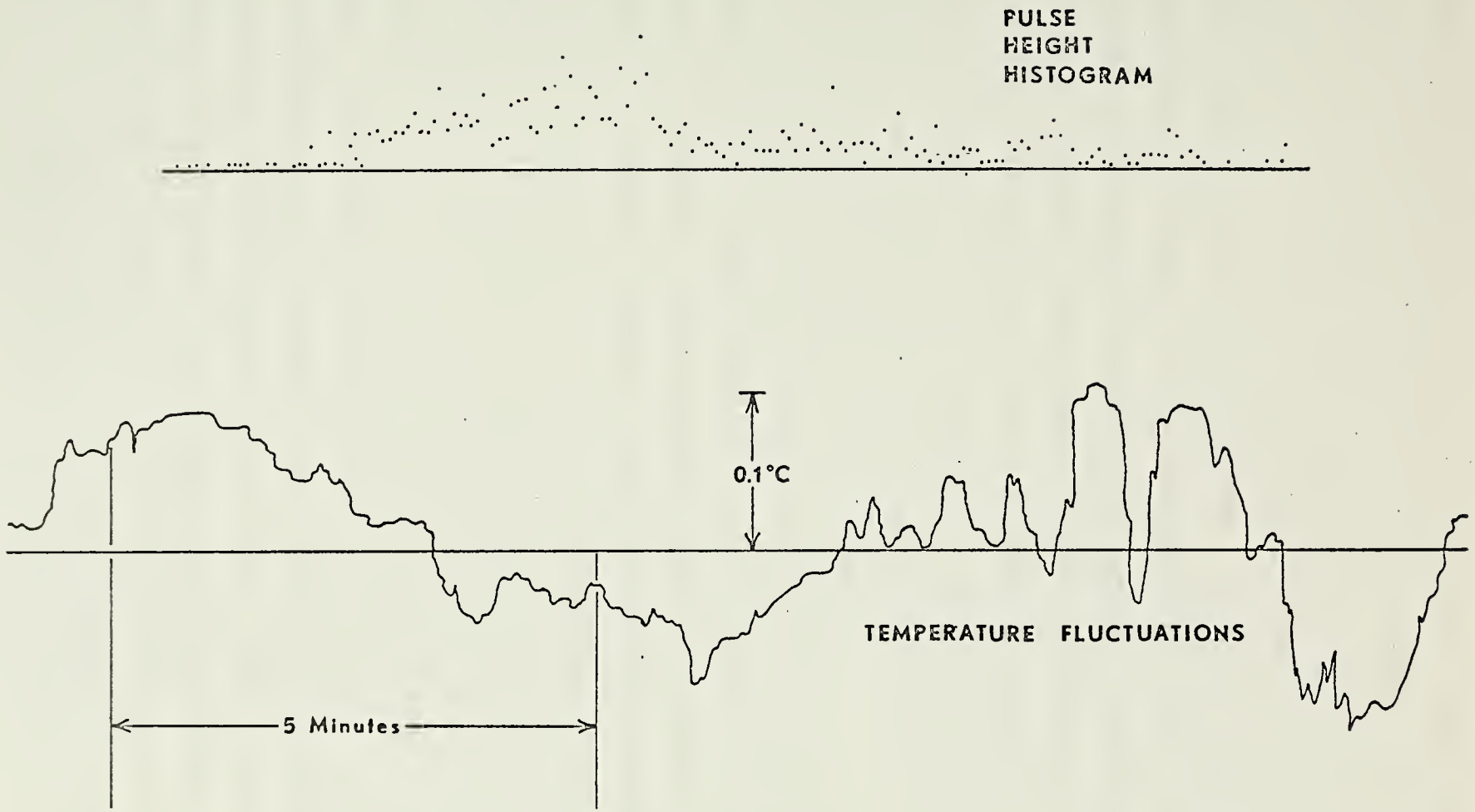

Figure 8. Histogram from Pulse Height Analyzer for pulses recorded during the 5 minute period shown on temperature record: high thermal activity.

notable differences in acoustic variability. Referring to Tables I and II, Runs 72 and 73 were made under conditions of very light wind and a virtually calm sea surface over the acoustic range. The runs conducted the previous day (Runs 56-61) also experienced calm weather. From the logs, the conditions on 2 October prior to Run 72 were similar with calm winds and sea and a high, thin broken to overcast sky. The large acoustic fluctuations observed during Runs 72 and 73 were indicative of the microstructure activity. No strong periodicities were apparent in the autocorrelation functions and the spectral energy density functions for both hydrophones during each run were similar.

In contrast, the weather and sea conditions (Table II) were different during Runs 116 and 117. The acoustic, as well as temperature, fluctuations were large, similar to the runs on 2 October. However, the autocorrelation functions exhibited marked periodicities and the spectral energy density functions had a distinct peak at about 0.14 Hz.

Although the comparison is made between two sets of runs conducted eleven days apart, one conclusion appears reasonable. The acoustic fluctuations were induced by at least two mechanisms in the medium, the temperature inhomogeneities and the effect of surface wave activity. This situation has been observed in other experiments as well [Alexander 1972, for example]. Confirmation of the effect of surface waves would require an analysis of the wave spectrum, the data for which were not available for this study. However, the periods

seen in the autocorrelation function (Table IV) are readily observed in a surface wave spectrum. A sample calculation of the water particle velocity at a depth of 20 feet indicated that the velocity effects should have been small for the wave heights present. However, the presence of waves can affect the transmitted acoustic energy in the wave spectrum if inhomogeneities are present, viz., temperature and salinity contrasts, bubbles, biologics. Then the wave induced particle motion would serve to move these inhomogeneities in and out of the propagation path in a periodic manner.

The pulse height time series for Runs 116 and 117 also presented evidence of long period fluctuations upon which the higher frequency excursions were imposed. The oscillation was distinct on the records for Hydrophone 2, but barely discernible on Hydrophone 1. Run length was too short to define this fluctuation in the spectral analysis, although its effect was evident in the autocorrelation functions for Hydrophone 2. The high coefficients of variation for Hydrophone 2 in Runs 116 and 117 were caused by the non-stationarity of the mean associated with this fluctuation. If the coefficients for these two runs are discounted, the variation for the set of 12 runs analyzed then ranged from 2% to 10%. The apparent period, greater than five minutes, and its occurrence in two runs conducted eighteen minutes apart indicated the possibility of the presence of internal waves. Climatology, discussed in Section I.C., showed a trend for thermal stratification to

occur in October as the summer months approach, thus providing the requisite density interface for internal waves. Other runs, particularly 60, 72 and 73, showed indications of long period fluctuations, but not as distinctly as Runs 116 and 117. Analysis of the temperature microstructure data would not be conclusive in evaluating the internal wave hypothesis because of the short run length compared to the period of fluctuation. A similar situation was reported by Shoemaker (1971) in the Arctic.

The definite appearance of this "wave" on Hydrophone 2 and its simultaneous absence from Hydrophone 1 were supportive of the anisotropy of the range. Further evidence of a direction dependence was apparent in the time series plots of pulse heights and in differences in the autocorrelation functions for other runs, notably those runs where a marked periodicity occurred (Table IV). In those cases, Hydrophone 2 always exhibited a stronger periodicity than Hydrophone 1. In all but three runs (45, 46, 48), the total spectral energy, derived from computing the area under the spectral energy density curves, was greater for Hydrophone 2. The apparent cause of the difference in acoustic fluctuations along the two orthogonal paths was the influence of surface waves.

In addition to the possible causes discussed above - temperature inhomogeneities, internal waves, and turbulent water particle velocity - other factors that may have influenced the acoustic propagation were bubbles, sediment

particulate stirred into the water column, and biological activity, not the least of which were the whales observed during Run 58.

IV. CRITIQUE OF EXPERIMENT

A. PARAMETERS

Data on several additional parameters would have aided in the analysis of the acoustic data. The first of these was vertical temperature profile information. No profiles were available to determine the presence or confirm the absence of seasonal or diurnal thermoclines during the runs. Such information could only be weakly inferred from climatology and current and past weather data pertinent to each run. A temperature profiling system was designed and built but technical problems and lack of conductors precluded its operation. The requirement for a remotely controlled system which would operate reliably from a known, fixed location under a variety of sea state and temperature regimes was not attainable in the time frame of the experiment. The other alternative was to take bathythermographs from a vessel stationed on the range during each run, but the instrumentation was not available.

Turbulent velocities measured by the ducted current meters were limited to the vertical direction after the failure of the horizontal components in the initial stage of the experiment. Although the remaining component was recorded, it was not recoverable from the magnetic tape. The reason for this malfunction was the failure of the microswitches, which could not be replaced during the

experiment. Availability of the vertical velocity data would have enabled a cross-correlation investigation of the effects of particle velocity on the acoustic fluctuations, although time for this analysis may not have been available.

The current records from the Aanderaa current meters are being analyzed in New Zealand and the data corresponding to the runs analyzed herein were not available during this effort. Hence no information concerning advective processes affecting the range could be determined.

Surface wave data were restricted to significant wave height as recorded on the logs. Data on wave periods present during a run would have aided the analysis of periodicities in the autocorrelation functions.

As detailed in Section I.B., the purpose of the experiment was to investigate both the acoustic fluctuations and the microscale features of the medium. It is felt that the parameters listed above would have been useful in an analysis of the temperature microstructure as well as of the acoustic propagation. With regard to temperature analysis, a measure of insolation more quantitative than logged comments about sky conditions would have been advantageous.

B. RUN LENGTH

In Phase I, run length was nominally ten minutes. By using a maximum time-lag of one-tenth the run length, periods ranging from D.C. to about 55 seconds were able to be detected with reasonable definition in the autocorrelation and

spectral energy density functions. Better resolution could have been obtained with the same number of lags by decreasing the maximum lag time or increasing the run length. Decreasing the maximum lag time has the effect of shortening the longest resolvable period with the same number of lags. Thus, maximum lag was selected as large as possible to take advantage of the entire run length as a fixed parameter.

During Phase II, run length was increased to twenty minutes to enable the detection of longer periods of fluctuation - up to two minutes if a maximum lag of one tenth the run length criterion were used.

The long period oscillation apparent in Runs 116 and 117 was not detected in the analysis because of the short length of the run compared to the period of oscillation. However, the use of run lengths long enough to ensure analysis of such long periods would have been prohibitive in terms of data storage requirements and, later, computer analysis requirements. Since no information was available beforehand to suggest the presence of long periods, run lengths of 20 minutes were best suited to the purposes of the experiment.

C. RECORDING OF DATA

Two tape recorders were used to record separate parameters of simultaneous time series, a system not beneficial to analysis due to the problem of tape synchronization during reconstruction. Had a fourteen track tape recorder been

available, all of the data could have been recorded simultaneously on one machine. As it was, the surface wave data was recorded on a different tape from the one used to record the pulse height and temperature data.

In preparation for digitization of the data, it was discovered that on at least one of the dubbed tapes, the pulse height data had exceeded the ±40% deviation from the carrier center frequency for the FM recording band and tape speed used during the dubbing process. Attempts to reproduce the data on a tape recorder other than the Sangamo were unsuccessful due to the bandwidth limitation. Careful testing of the Sangamo tape recorder, which was used to dub the tapes, revealed that this machine was capable of handling signals that exceeded the standard ±40% deviation; in fact, the discriminators proved to be linear out to at least ±60% deviation from the center frequency. Had this tape recorder not been designed to such broad specifications, much, and perhaps all, of the pulse height data would have been irretrievable due to an apparent operator oversight in recording the data out of band.

D. PHASE II RUNS

The temperature microstructure activity during the runs conducted in Phase II was generally higher than during the Phase I runs. However, the acoustic pulse repetition rate employed in Phase II precluded an analysis of the pulse height time series by the digital methods used during this

thesis investigation. With a repetition rate of 3 Hz, a pulse was transmitted every 333 milliseconds. Nominal travel time from the projector to the hydrophones was 195 msec, after which a pulse height was held by the sample and hold circuit for 200 msec. Thus, the trigger signal that initiated a pulse sequence arrived at the sample and hold circuit while the previous pulse height was still being held. The result was a distorted, two-step, pulse shape with the actual pulse height not readily distinguishable from the effect of the trigger arrival. A minimum pulse repetition interval not less than the sum of the hold time (200 msec) and maximum travel time would have precluded this problem.

E. REFLECTED SIGNALS

Calculated reflected path arrival times varied from 0.2 to 0.8 msec after the direct path arrival for the various reflected paths. For the smallest time difference, 0.2 msec, only 7 cycles of the 35kHz direct path pulse would have arrived before the reflected signal reached the hydrophone. Due to these considerations, the sample and hold circuit was designed to require only five cycles to sense and hold the signal. Thus, with the circuit operating properly, no interference from reflected signals should have occurred. However, surface reflected signals were observed on Hydrophone 1 under certain circumstances (low tide and 35 kHz frequency). This problem was alleviated by a reduction in mast height.

F. LOG KEEPING

Reconstruction of an experiment that was conducted one year prior to analysis depended heavily on the comments recorded in the logs. Scrupulous attention to detail in original log-keeping made this effort relatively successful. However, certain omissions occurred. These included lack of weather data for a run, no notation of the acoustic frequency used during a run, and inadvertent omission of one run when transferring data from the rough log to smooth log. This is the human factor in experimental work and only constant care and cross-checking can minimize errors such as these.

V. SUMMARY, RECOMMENDATIONS, CONCLUSIONS

The experiment conducted was unique for several reasons:

1) It involved simultaneous transmission along near-orthogonal paths to investigate the degree of isotropy in acoustic propagation.

2) Two acoustic frequencies were employed to investigate the frequency dependence of the acoustic fluctuations.

3) A unique sample-and-hold device was designed and constructed to measure acoustic pulse heights without the need for envelope detectors or recording of the pulse train.

4) A unique micro-scale temperature sensor system was also designed and constructed to measure thermal microstructure.

5) The sensors were fixed to stable platforms, and were remotely operated and monitored.

6) Multiple sensors were employed to investigate all important aspects of the ocean environment.

7) Because of the fixed locations, experimental runs were able to be conducted at various times of the year at the same site.

The part of the experiment analyzed in this thesis represented only the initial stages of a project that has since expanded and is still in operation. The fact that the project was still in its embryonic development when these runs were conducted resulted in several shortcomings which have

already been commented upon. However, it is felt that useful information about the environment and its relation to the acoustic propagation results presented herein can be gained from implementation of the following recommendations:

1. Conduct an analysis of the temperature microstructure data for the same runs as analyzed here. Comparison of the results of spectral analysis may indicate the degree of influence of surface wave activity on the microstructure.

2. Obtain the magnetic tape records for the surface wave spectrum for similar analysis and comparison to the results of acoustic and temperature analysis. Because of previously noted problems with tape synchronization, this effort would probably not prove conclusive.

For future experiments with purposes similar to this one, it is suggested that:

1. Every effort be made to measure turbulent velocity, temperature microstructure, surface waves, and acoustic fluctuations simultaneously. It is imperative that all sensors be maintained to accurately define the environmental interactions.

2. All data be recorded on the same magnetic tape simultaneously to avoid problems with synchronization.

3. Vertical and horizontal thermistor arrays be employed vice a single thermistor.

4. The geometry of the acoustic range be carefully investigated with regard to the effect of reflected path signals.

5. Equipment operating characteristics be well understood to avoid difficulties such as those experienced in this experiment with tape recording technique.

6. Vertical temperature profiles be included as a data requirement.

7. Run length be modified as necessary to fully observe the longest period fluctuations suspected to be present.

Conclusions from this analysis of the acoustic variability are listed below:

1. The acoustic fluctuations were caused by variations in the refractive index along with each propagation path. These variations were most likely caused by the temperature microstructure and by turbulent water particle velocity resulting from surface waves. Whether the turbulent velocity served solely as a mechanism for temperature distribution and modification, or whether it also caused changes in the refractive index by advecting other inhomogeneities, such as bubbles or sediment particulate, could not be determined from this analysis.

2. The fluctuations exhibited various degrees of anisotropy with the propagation along the acoustic path oriented perpendicular to the predominant swell direction generally subject to greater variability.

3. No reliable trend was observed to indicate a significant difference in variability due solely to the acoustic frequencies used.

4. The possible influence of internal wave activity was indicated by a long period fluctuation of the mean in at least two runs.

APPENDIX A

Pulse Height Time Series and Analysis Results

This appendix contains two sections of figures. The first section presents representative samples of the temperature microstructure activity present during each run. On each sample, time increases to the right. Appropriate scales and the qualitative classification are noted for each figure.

The second section presents four plots for each of the twelve runs analyzed. With two exceptions, the X and Y scales for the same plot from different runs are identical to aid comparison among runs. The first exception is for Run 73 which was twice as long as any other; for this run the X-scale of the time series and autocorrelation plots has been modified and is defined on the plots. The other exception applies to the Y-scale of the spectral energy density plots. This scale varies slightly among the plots due to the varying degree of fluctuations. The density function values are acceptable for comparison among runs.

Reference to Tables I - IV is helpful in obtaining a meaningful comparison among runs.

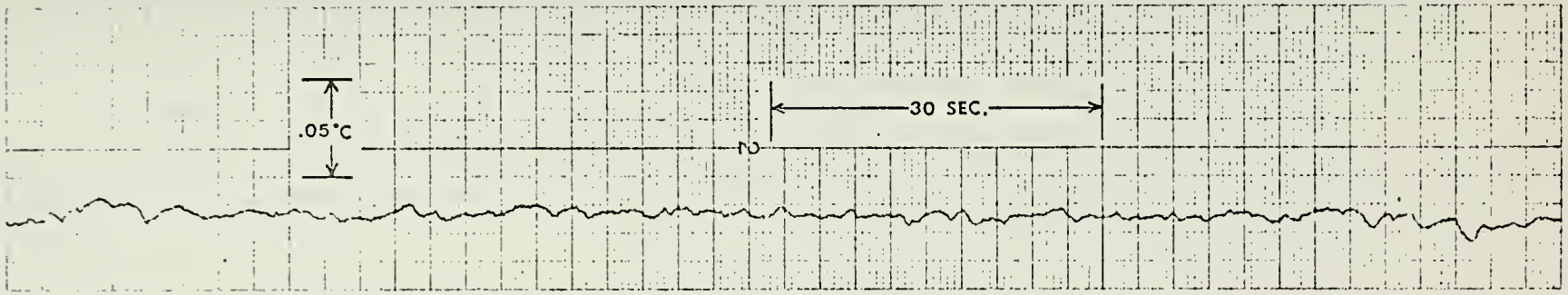

Run 45. Temperature fluctuations: negligible activity.

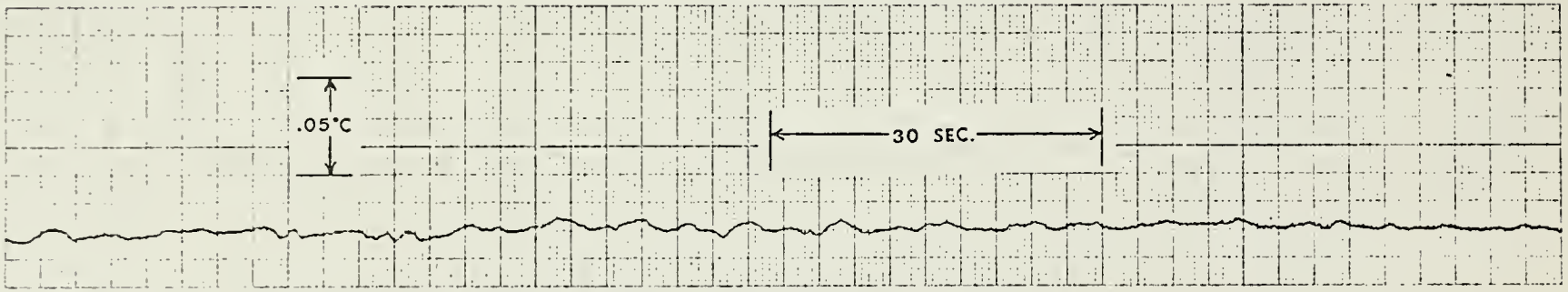

Run 46. Temperature fluctuations: negligible activity.

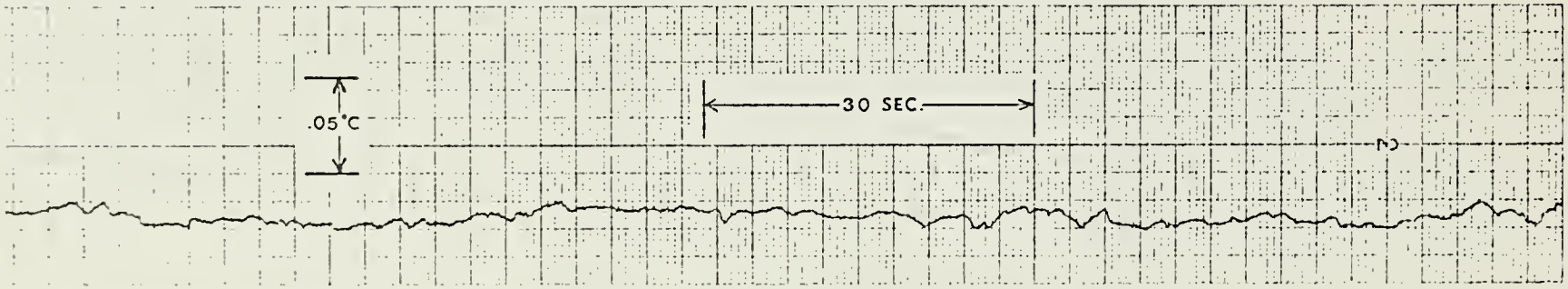

Run 48. Temperature fluctuations: negligible activity.

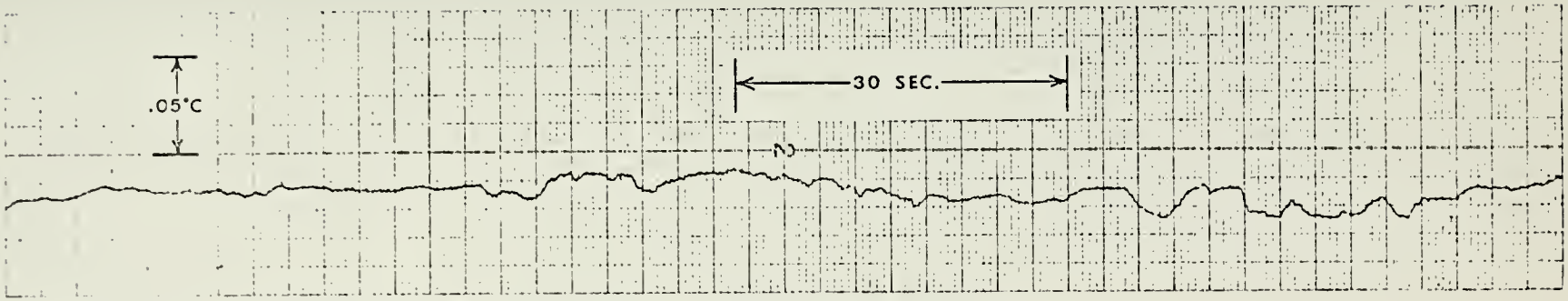

Run 49. Temperature fluctuations: negligible activity.

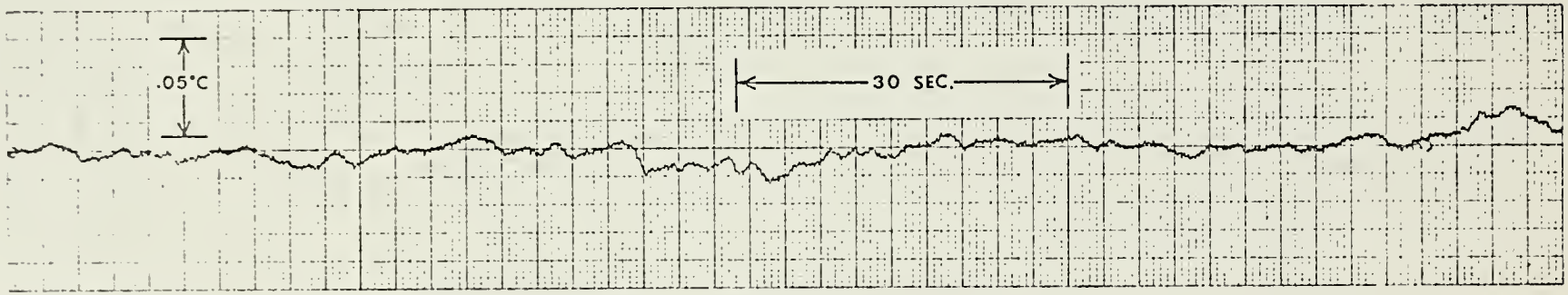

Run 56. Temperature fluctuations: negligible activity.

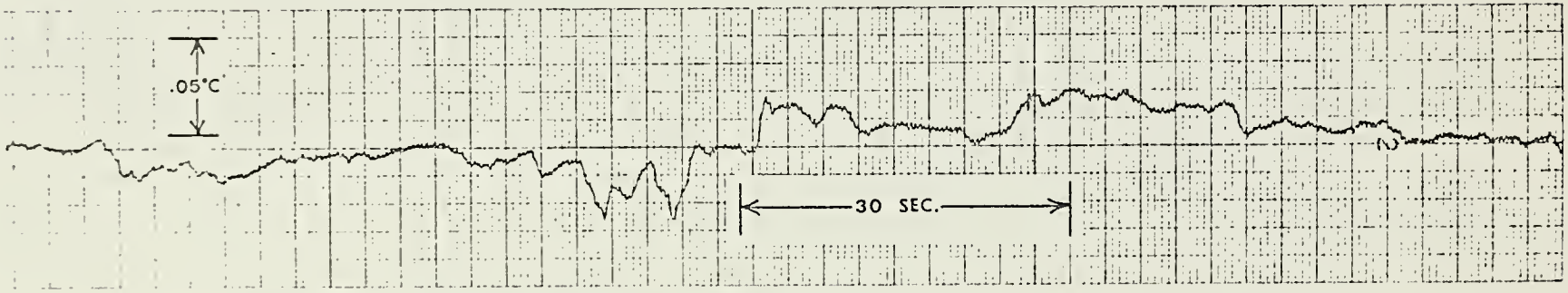

Run 58. Temperature fluctuations: moderate activity.

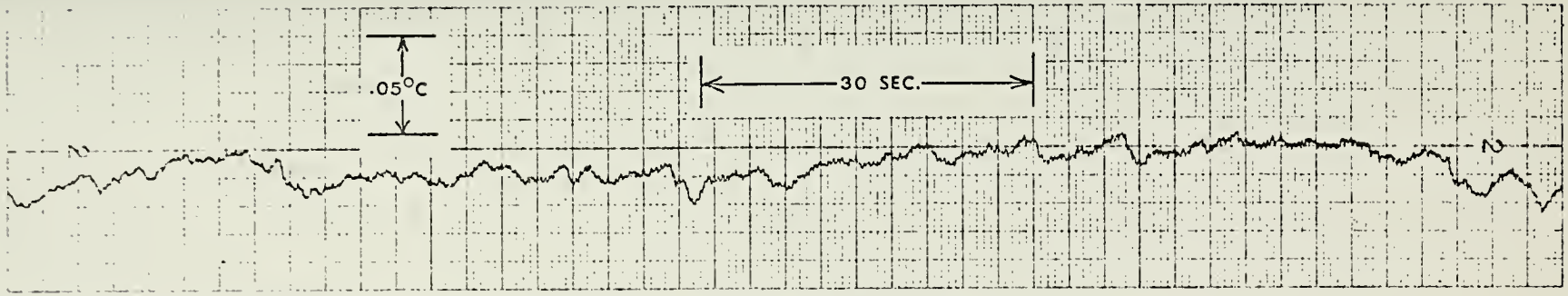

Run 60. Temperature fluctuations: moderate activity.

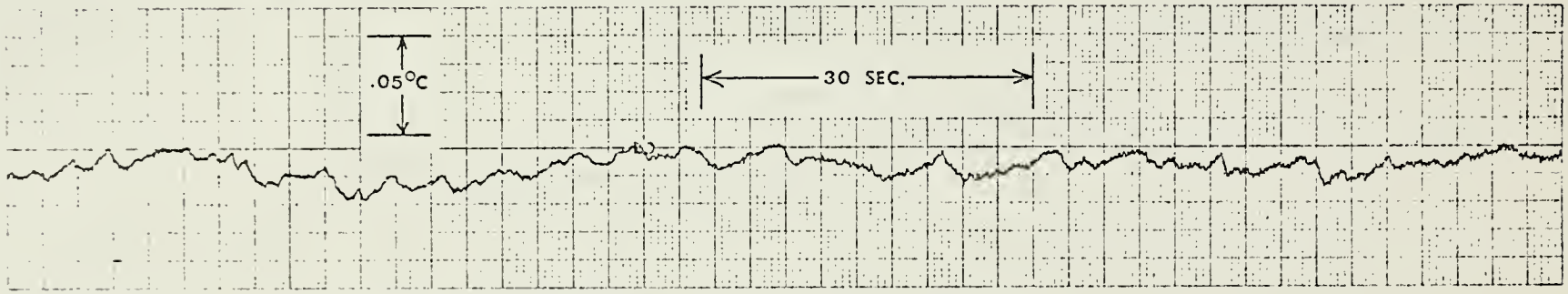

Run 61. Temperature fluctuations: negligible activity.

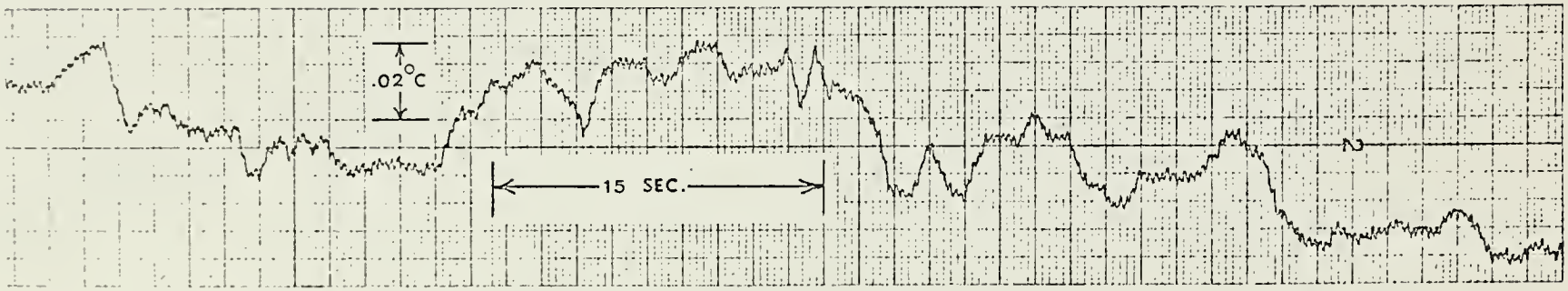

Run 72. Temperature fluctuations: moderate activity.

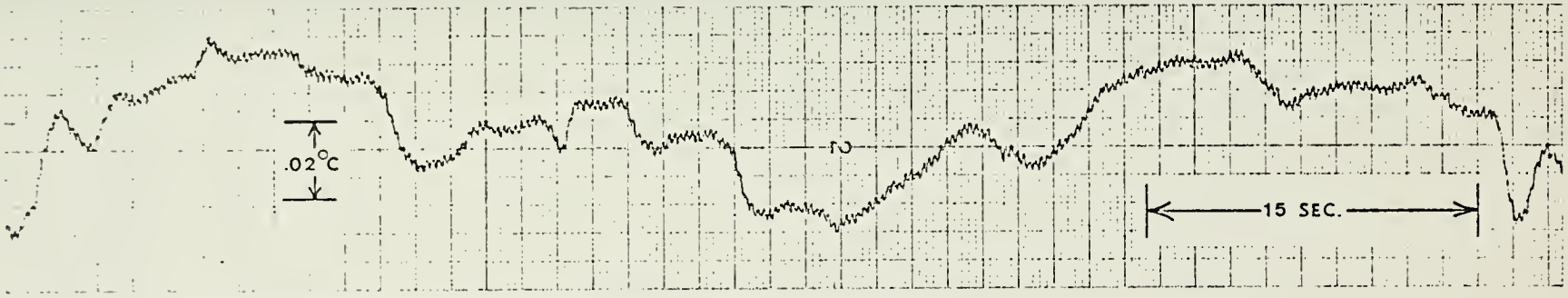

Run 73. Temperature fluctuations: high activity.

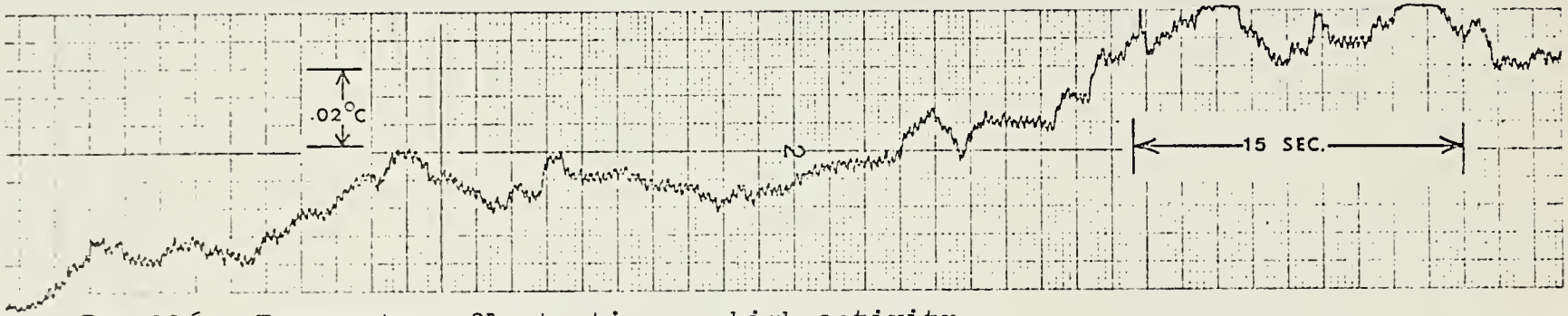

Run 116. Temperature fluctuations: high activity.

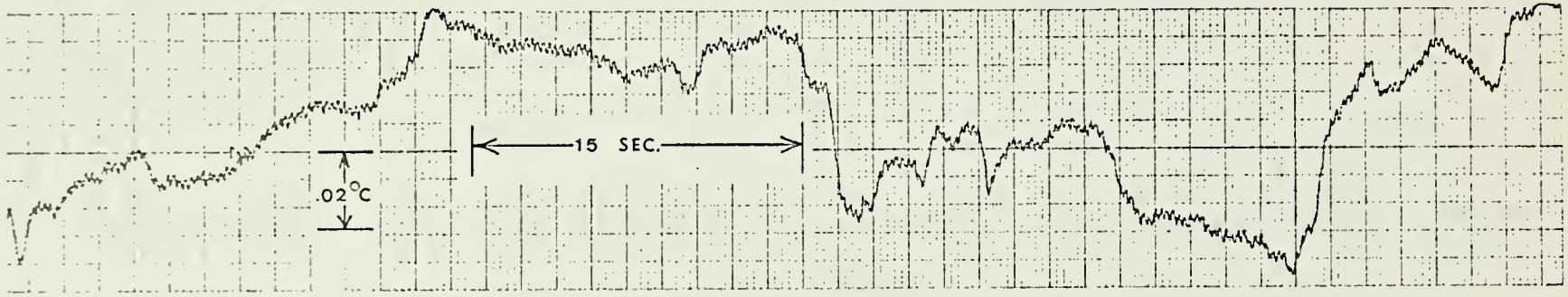

Run 117. Temperature fluctuations: moderate activity.

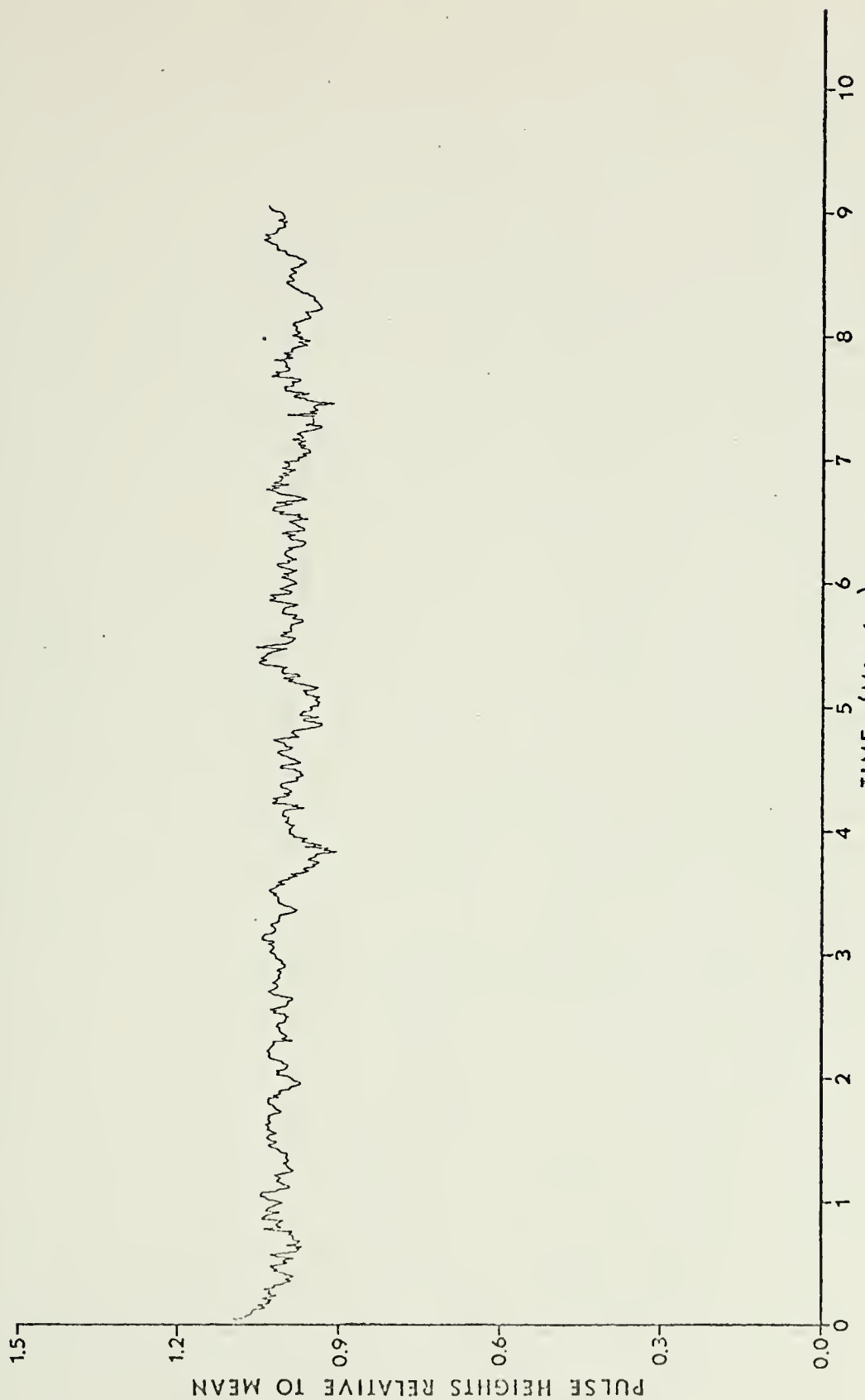

Run 45. Hydrophone 1 Pulse Heights.

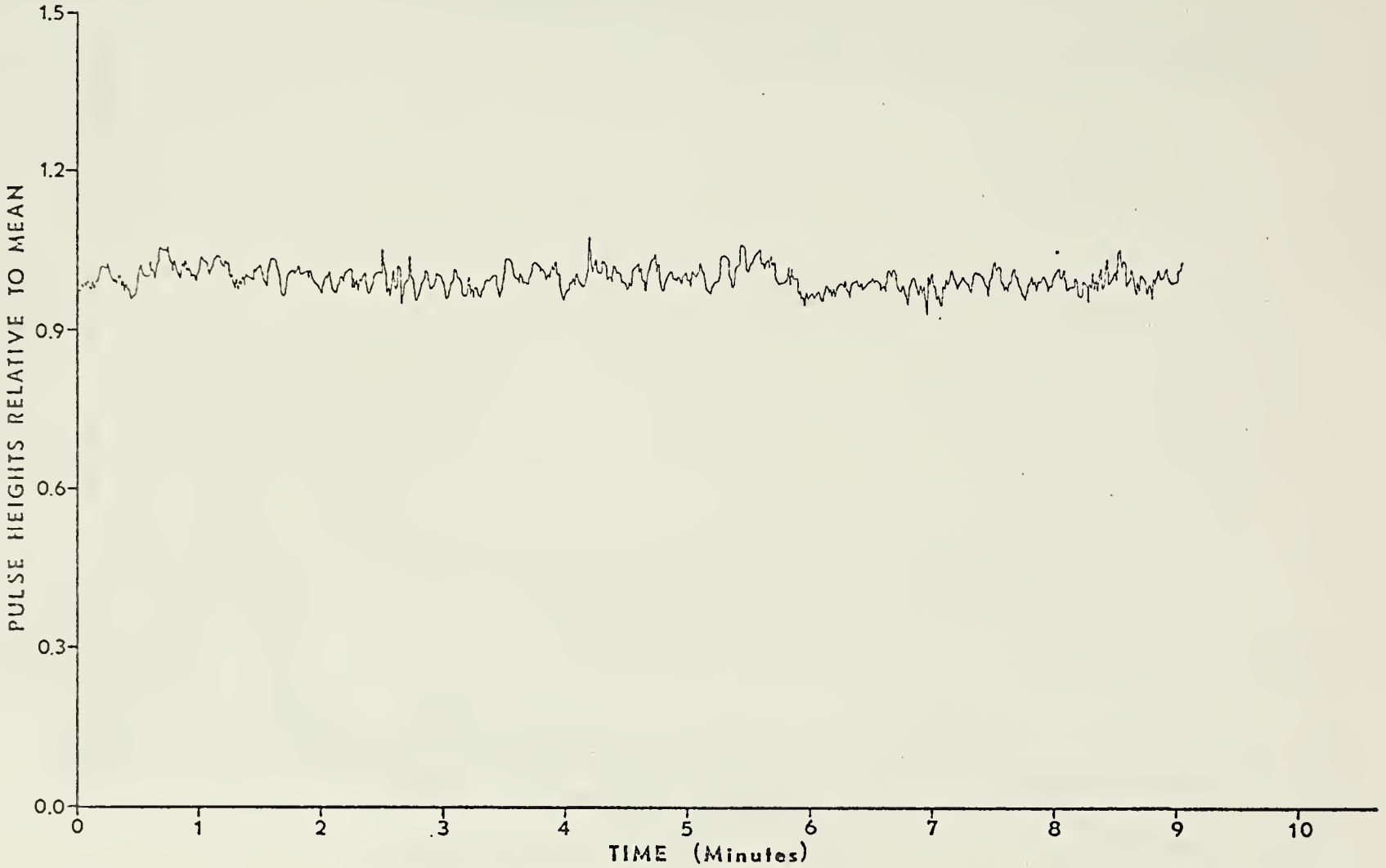

Run 45. Hydrophone 2 Pulse Heights.

Run 45. Autocorrelation Functions

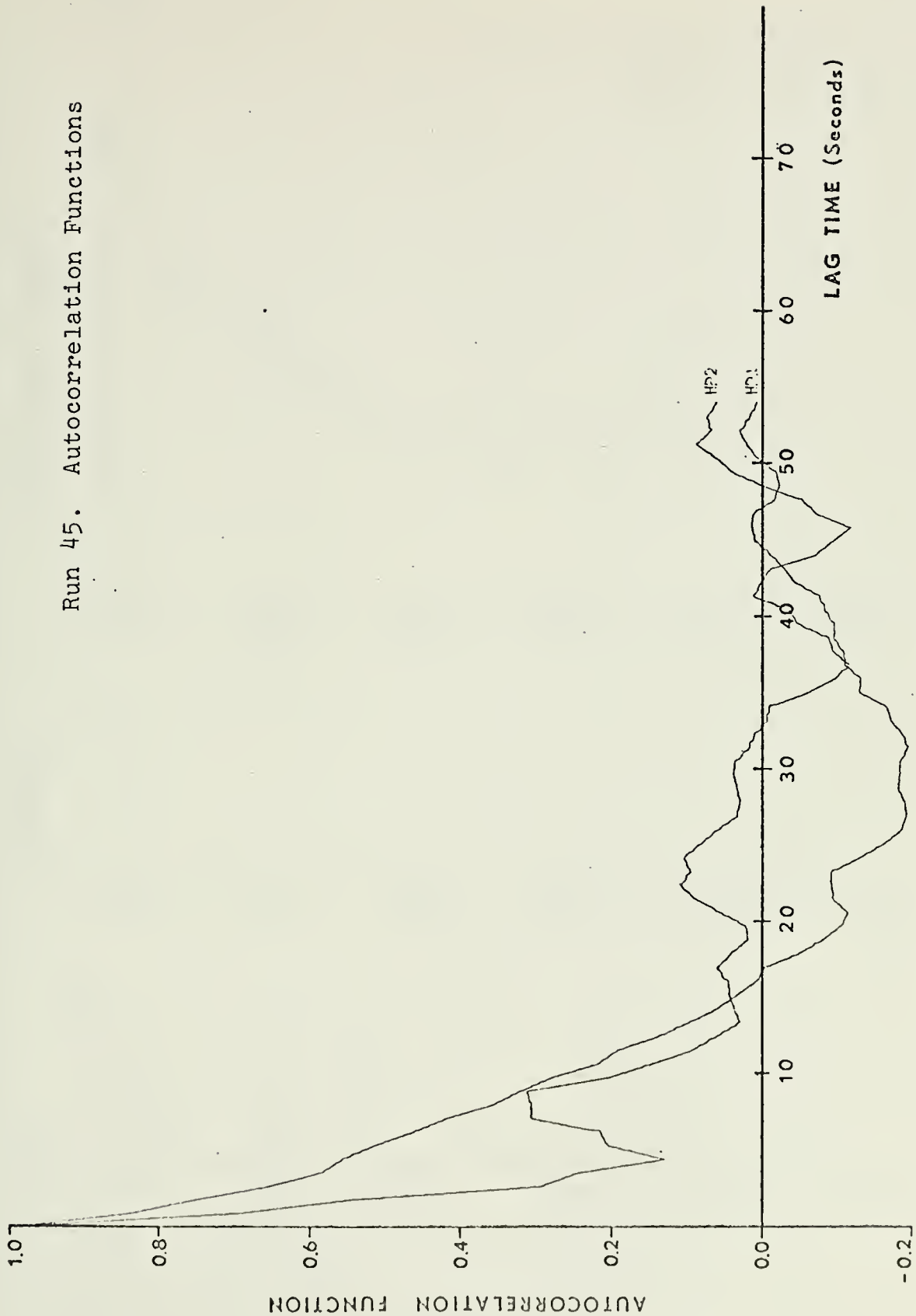

Run 45. Spectral Density, Coherence, and Phase.

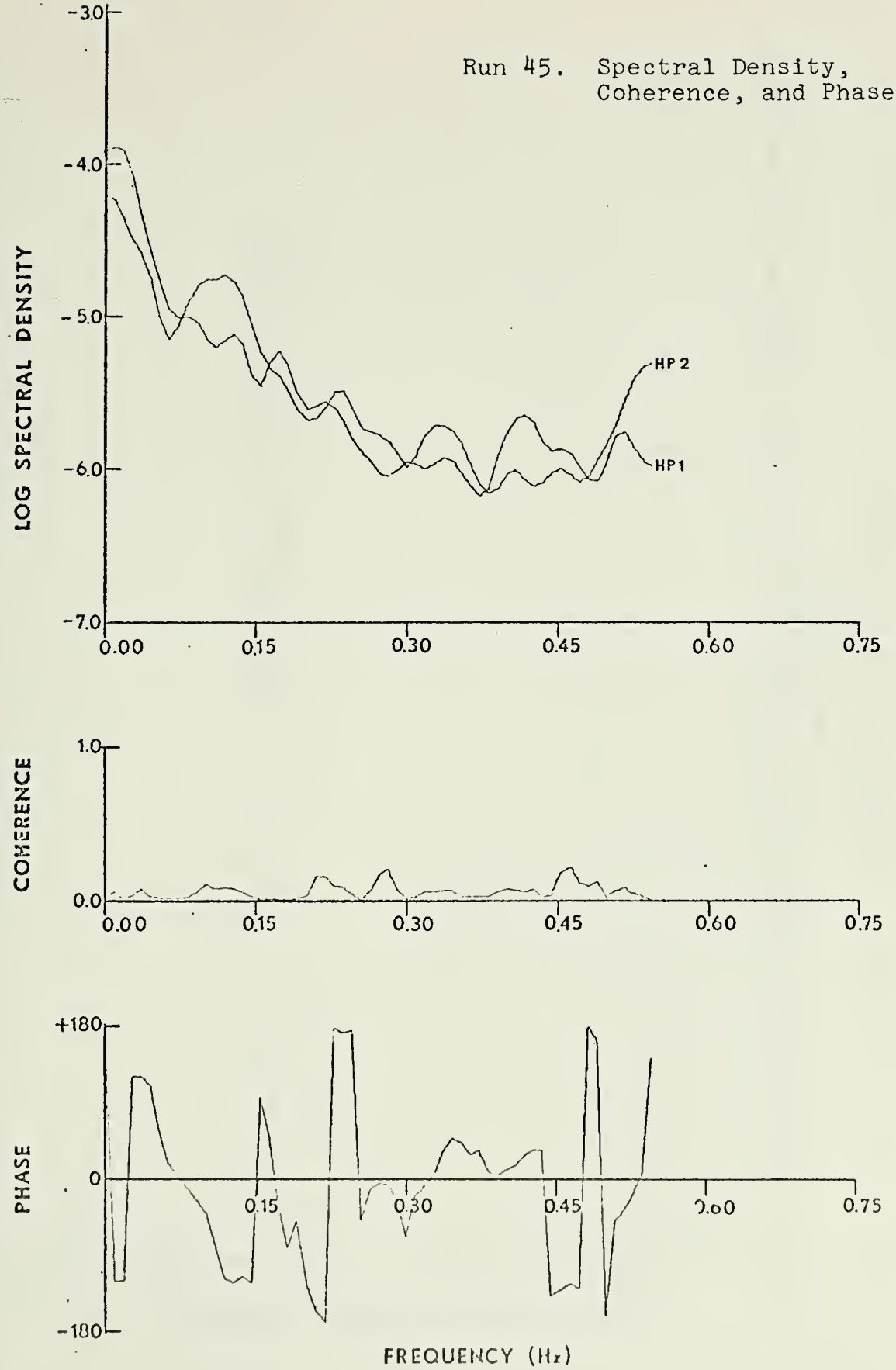

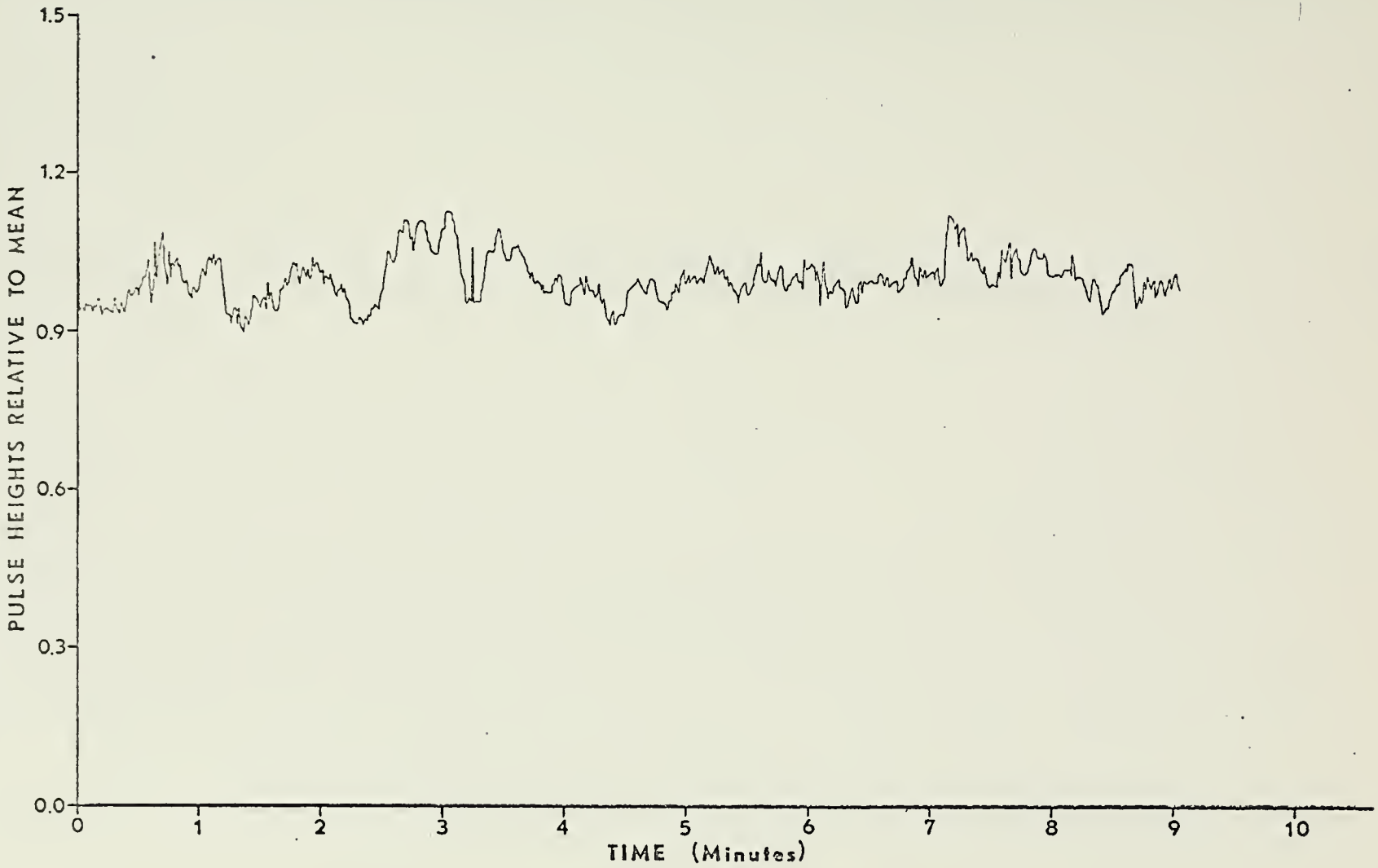

Run 46. Hydrophone 1 Pulse Heights.

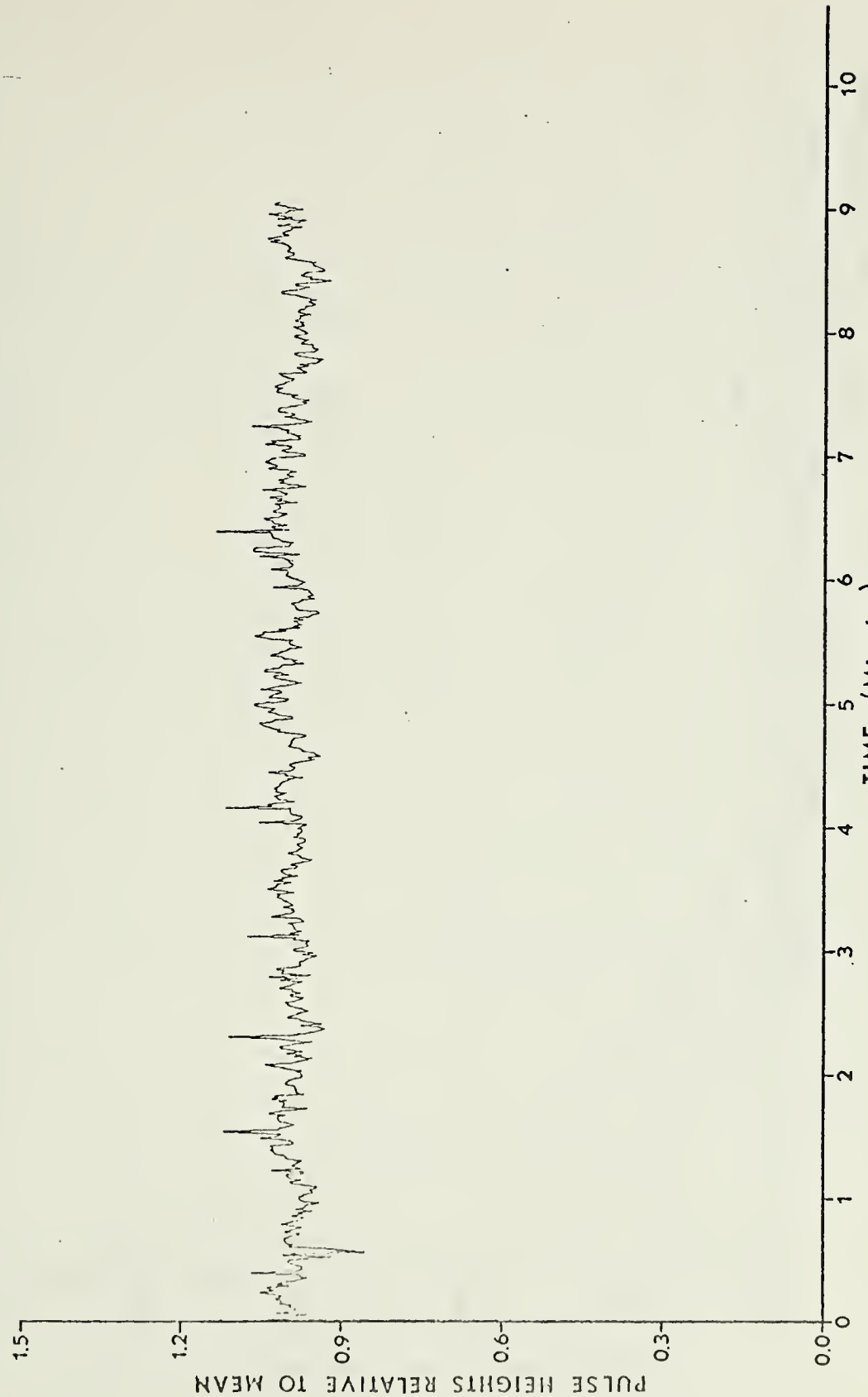

Run 46. Hydrophone 2 Pulse Heights.

Run 46. Autocorrelation Functions

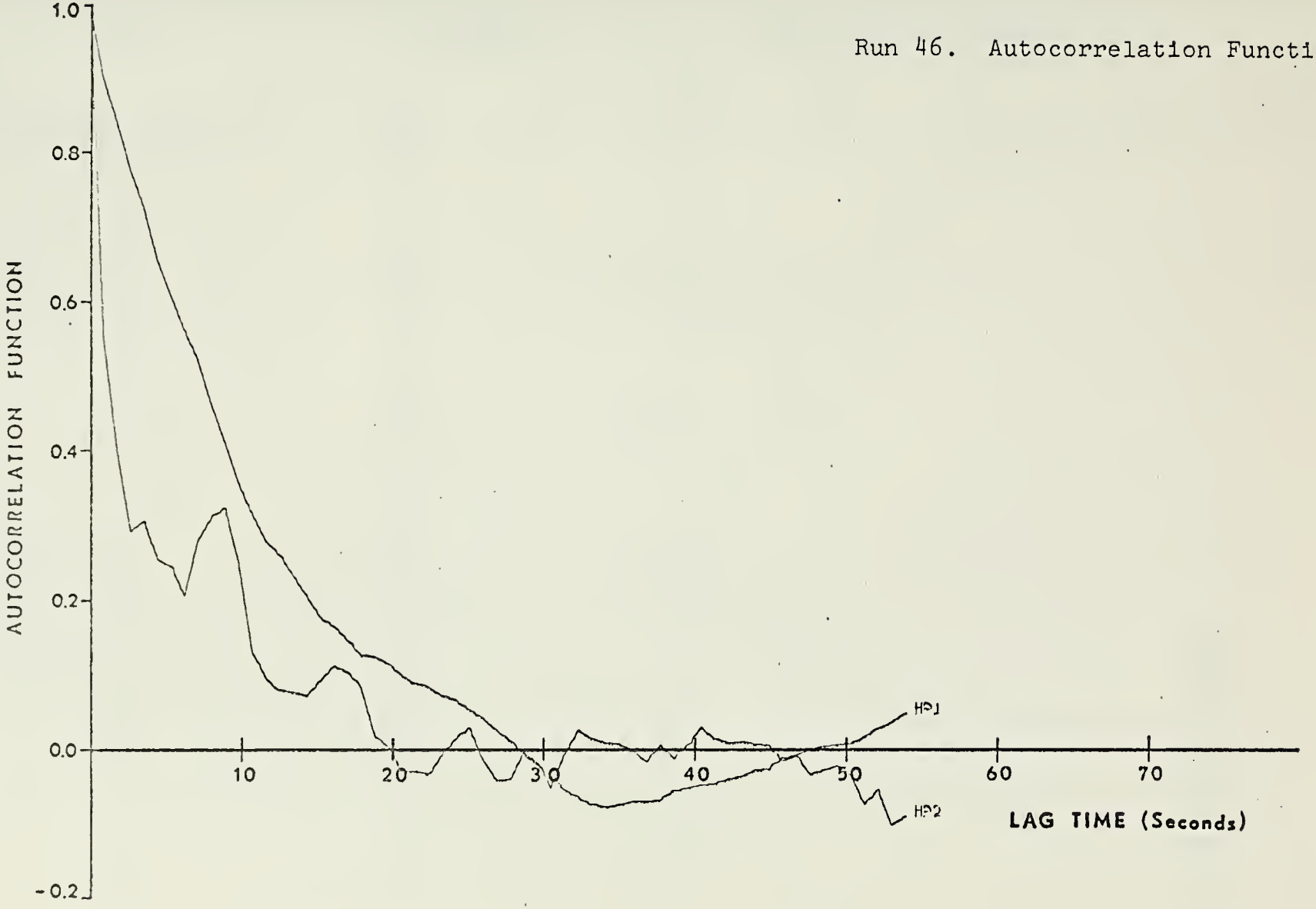

Run 46. Spectral Density, Coherence, and Phase.

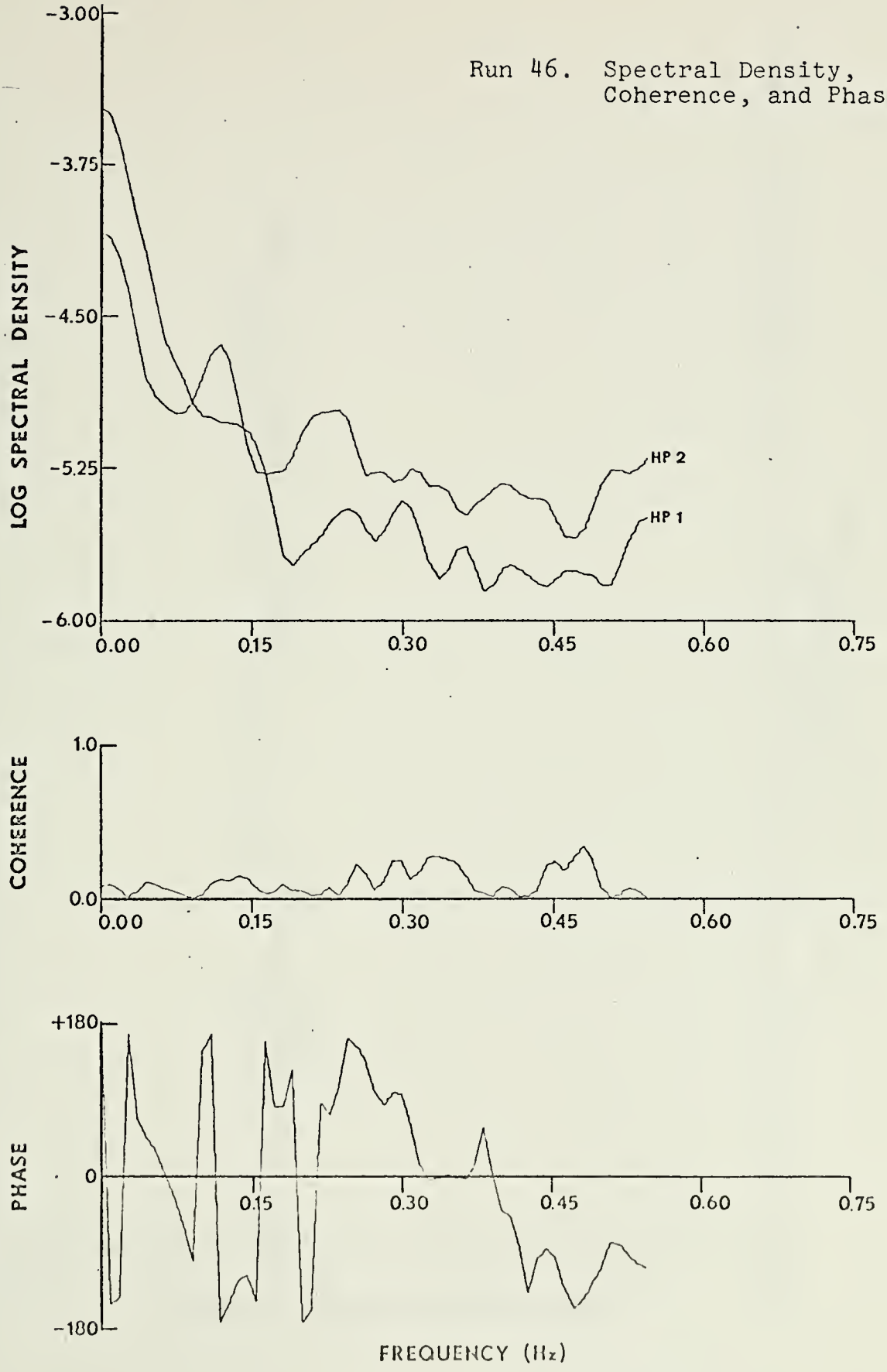

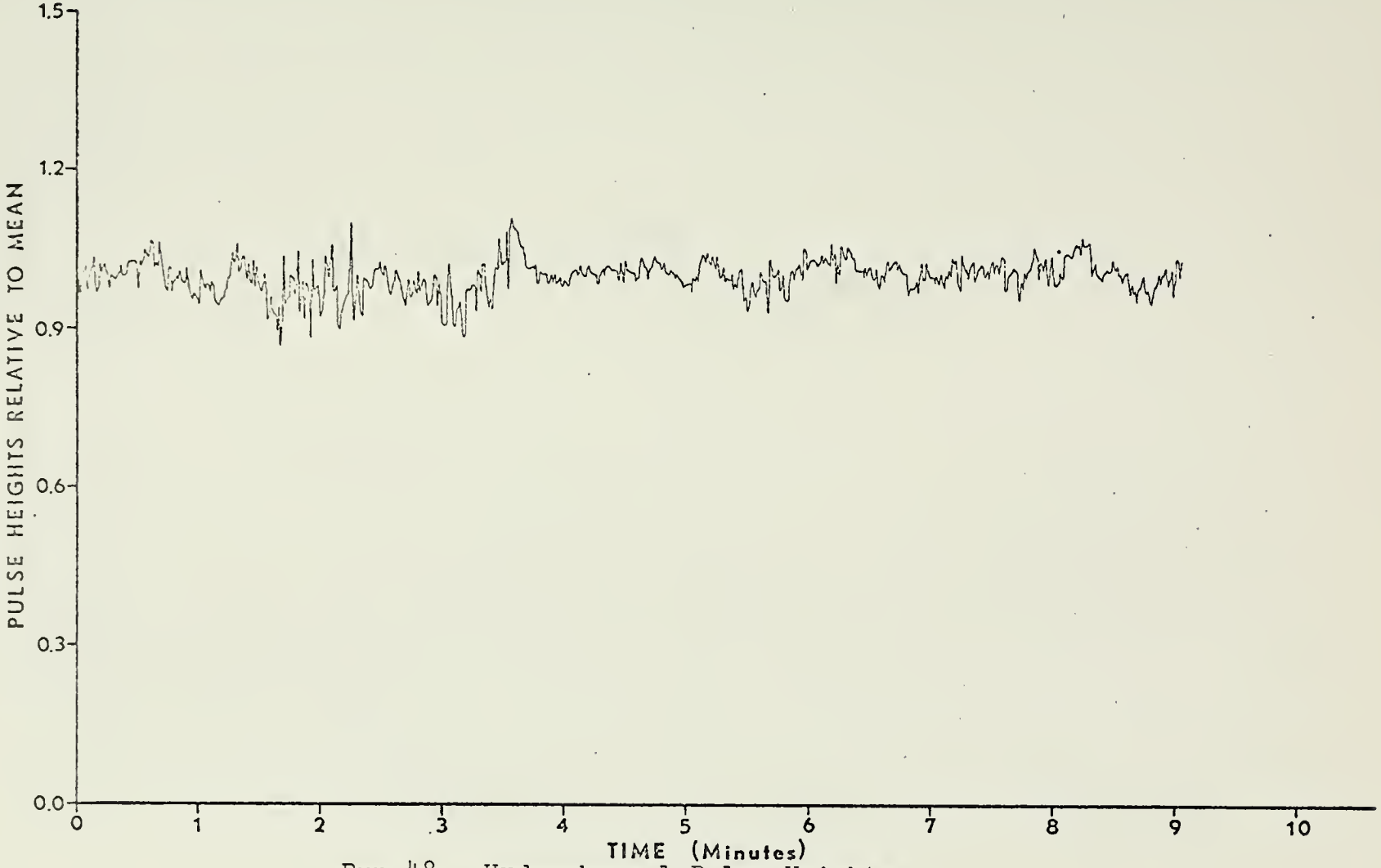

Run 48. Hydrophone 1 Pulse Heights.

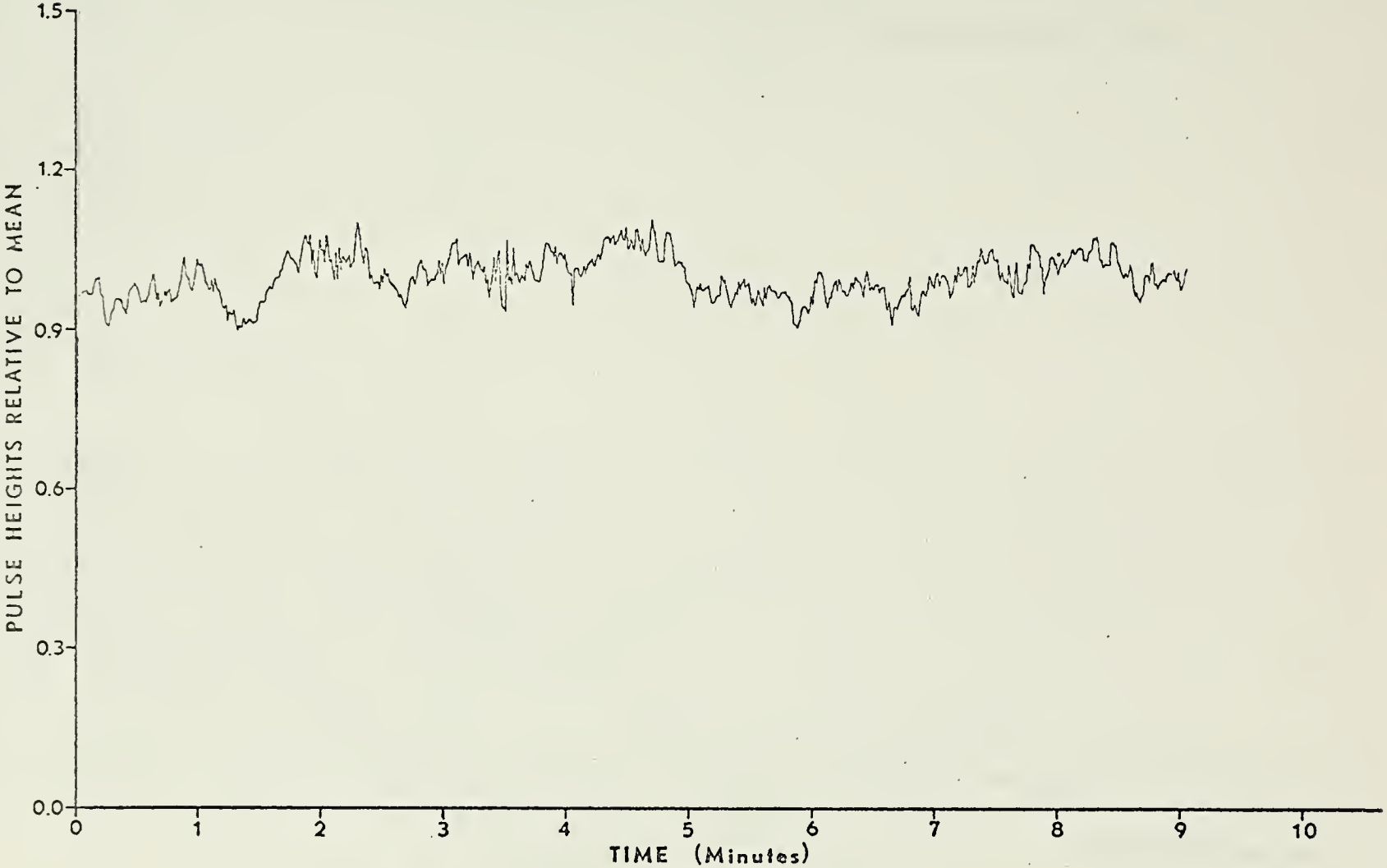

Run 48. Hydrophone 2 Pulse Heights.

Run 48. Autocorrelation Functions.

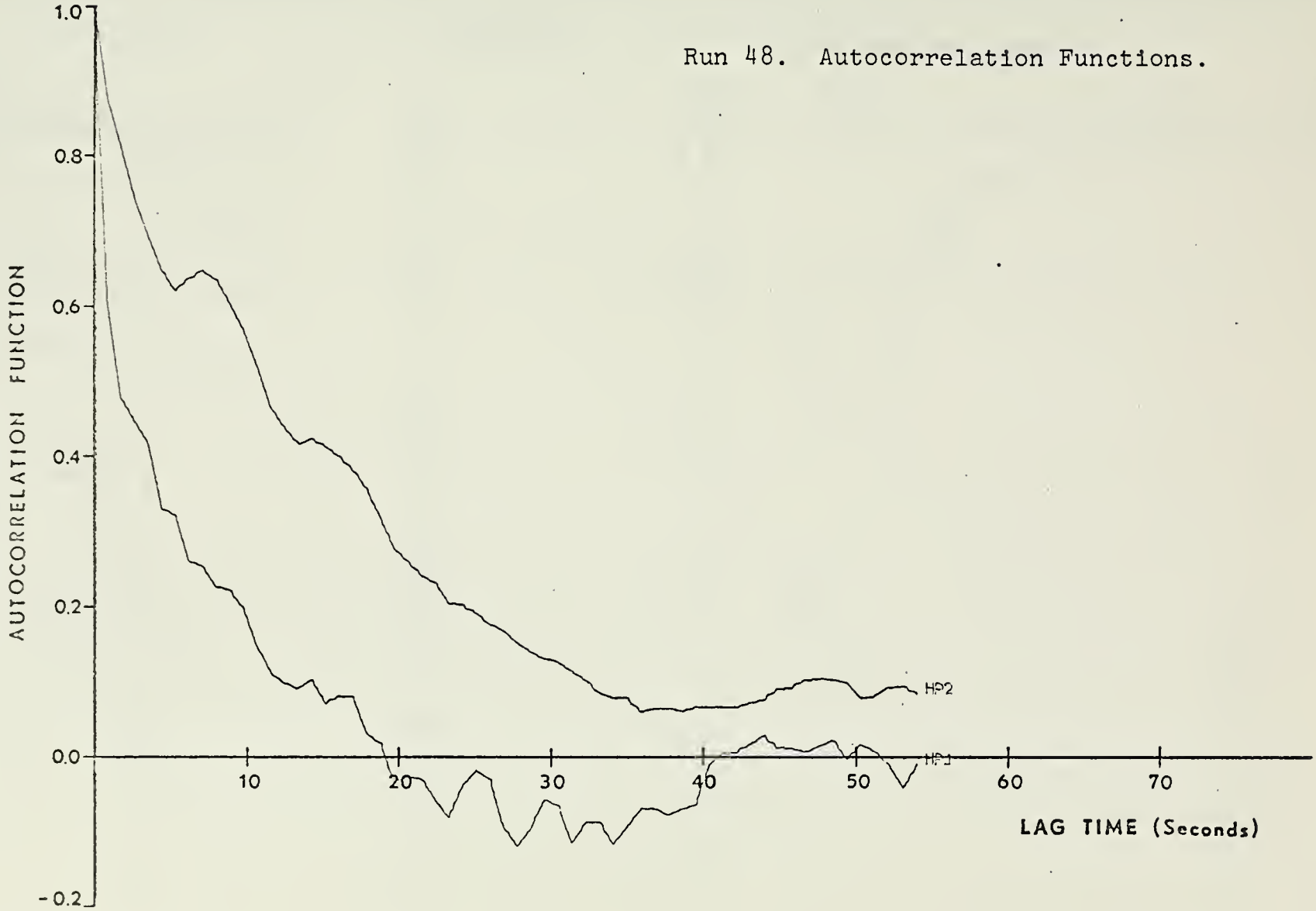

Run 48. Spectral Density, Coherence, and Phase.

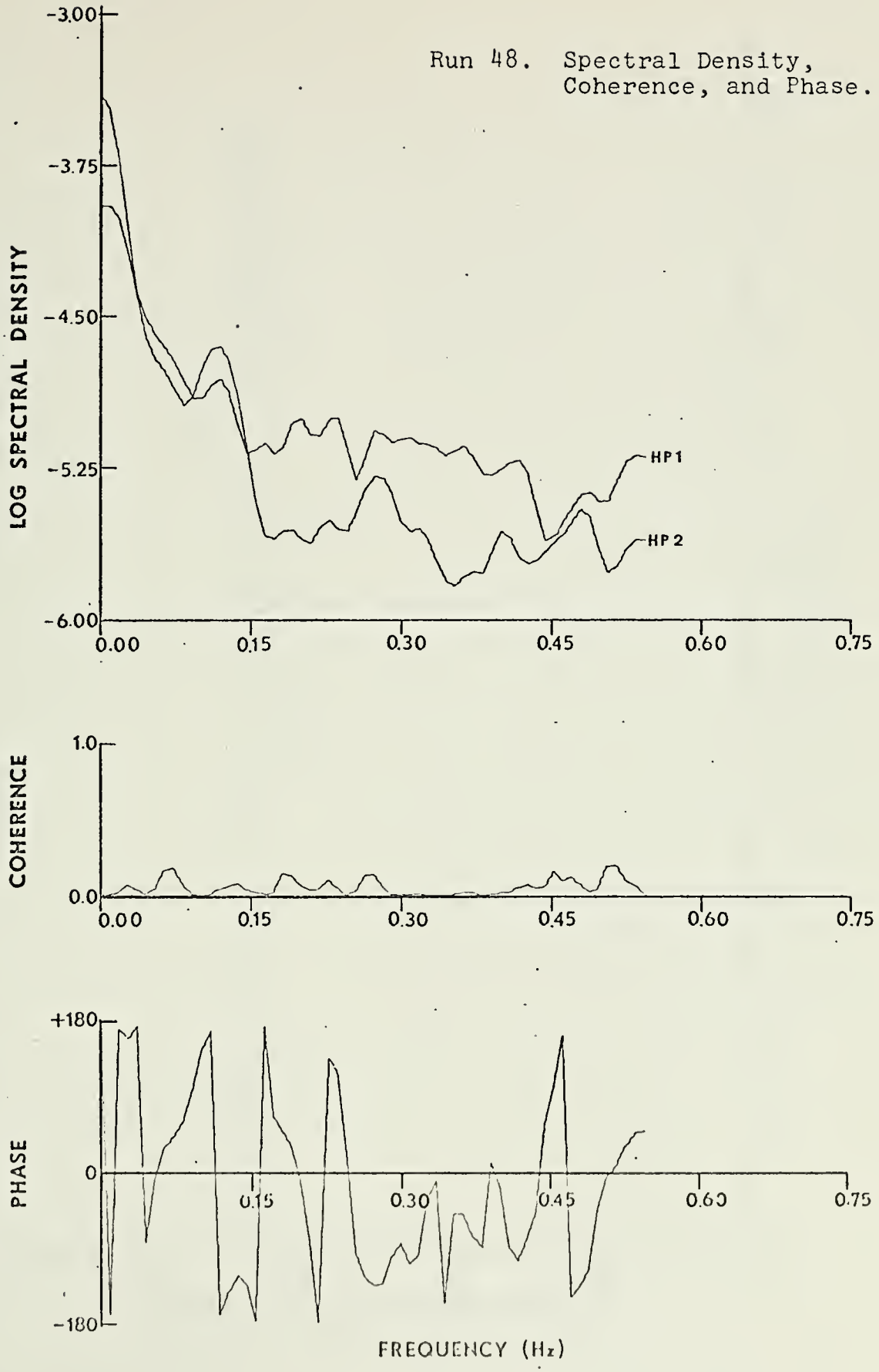

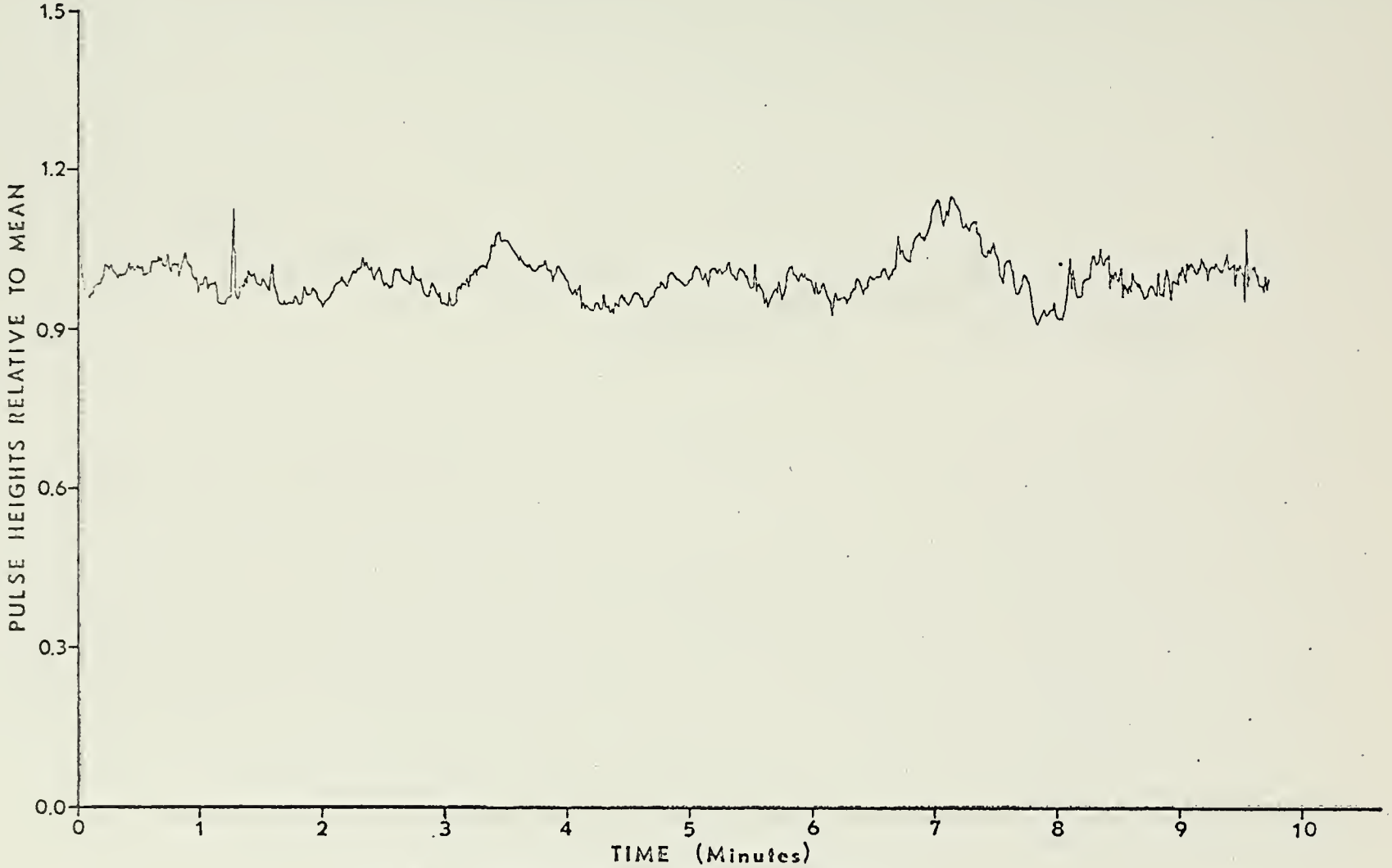

Run 49. Hydrophone 1 Pulse Heights.

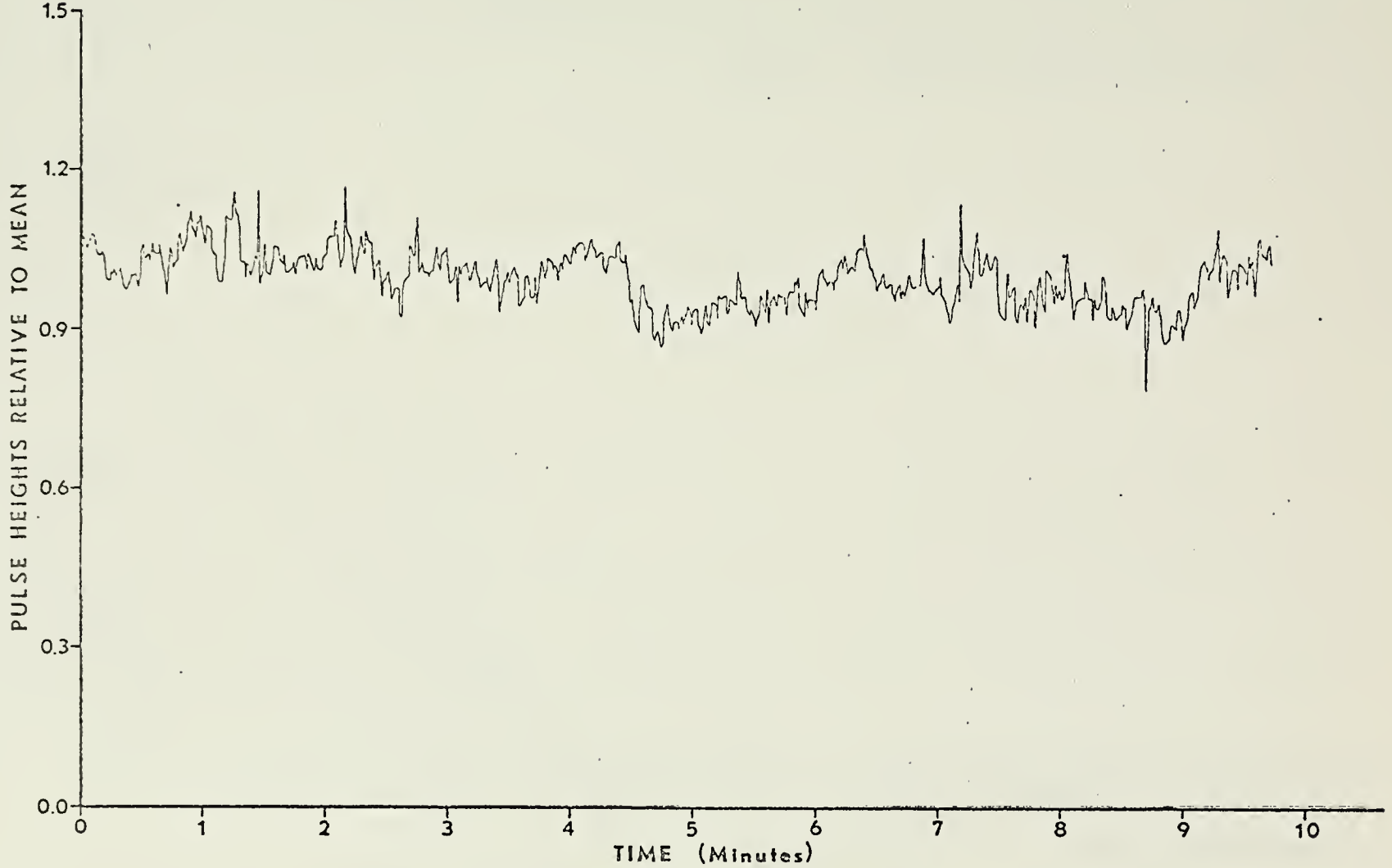

Run 49. Hydrophone 2 Pulse Heights.

Run 49. Autocorrelation Functions.

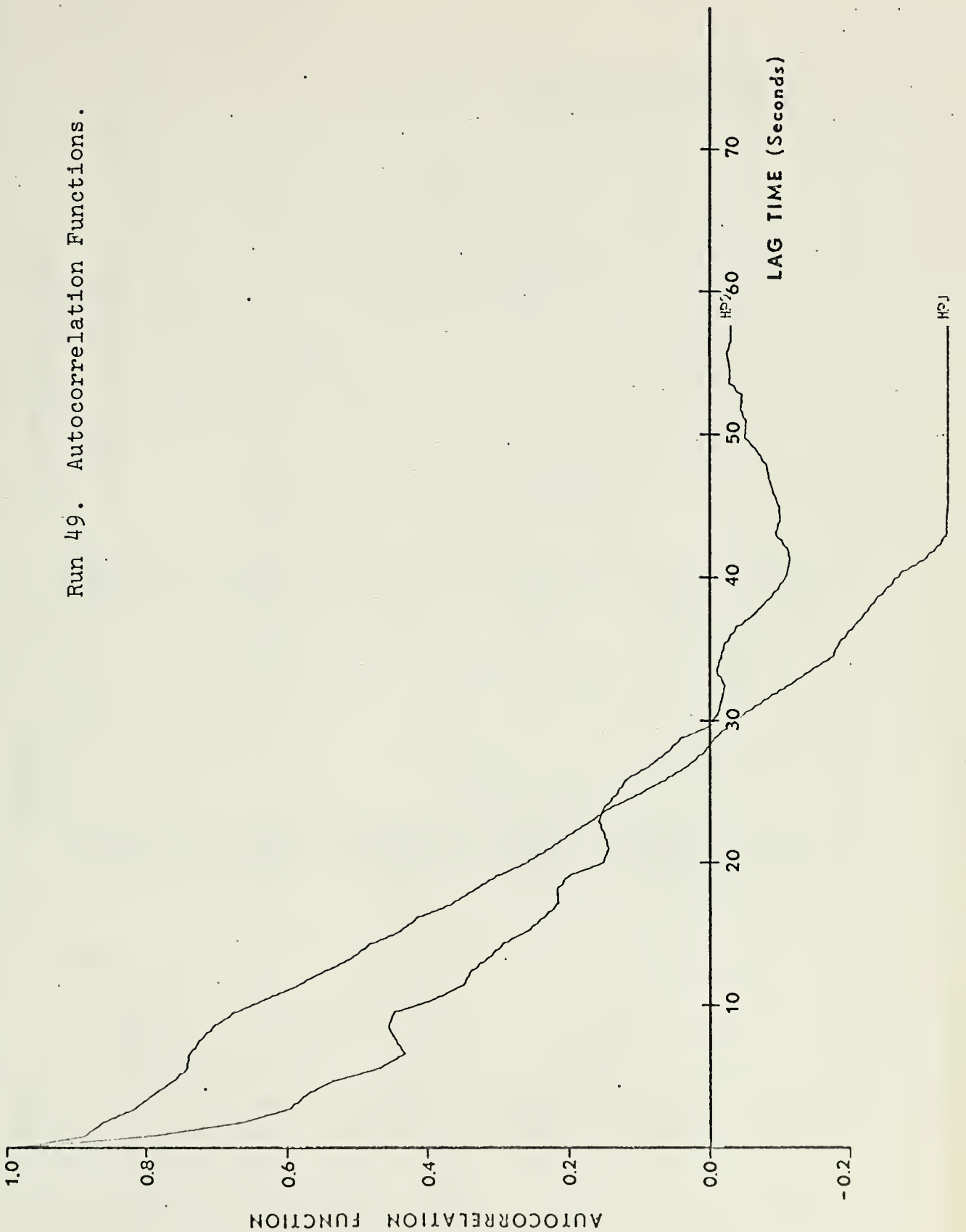

Run 49. Spectral Density, Coherence, and Phase.

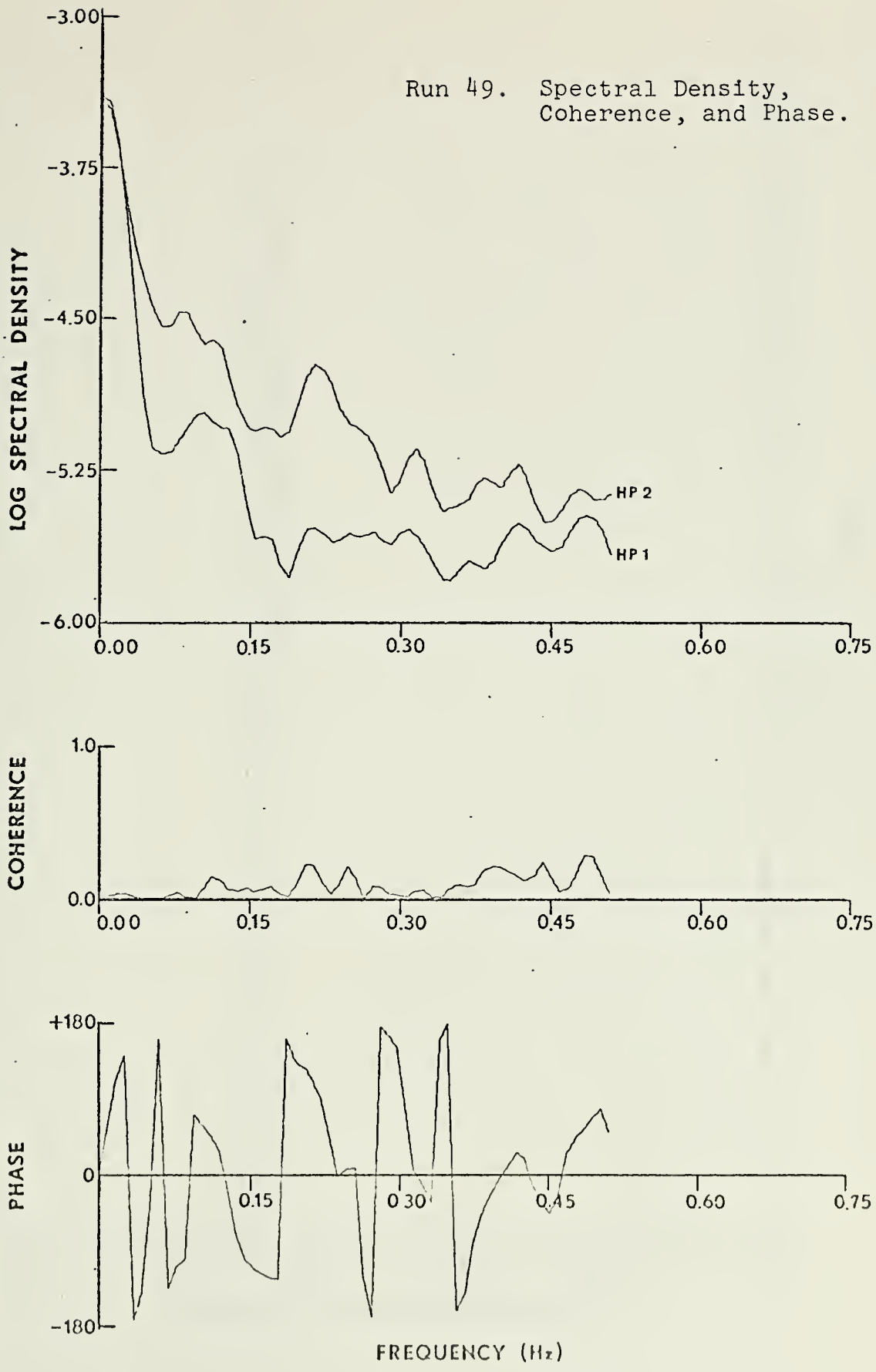

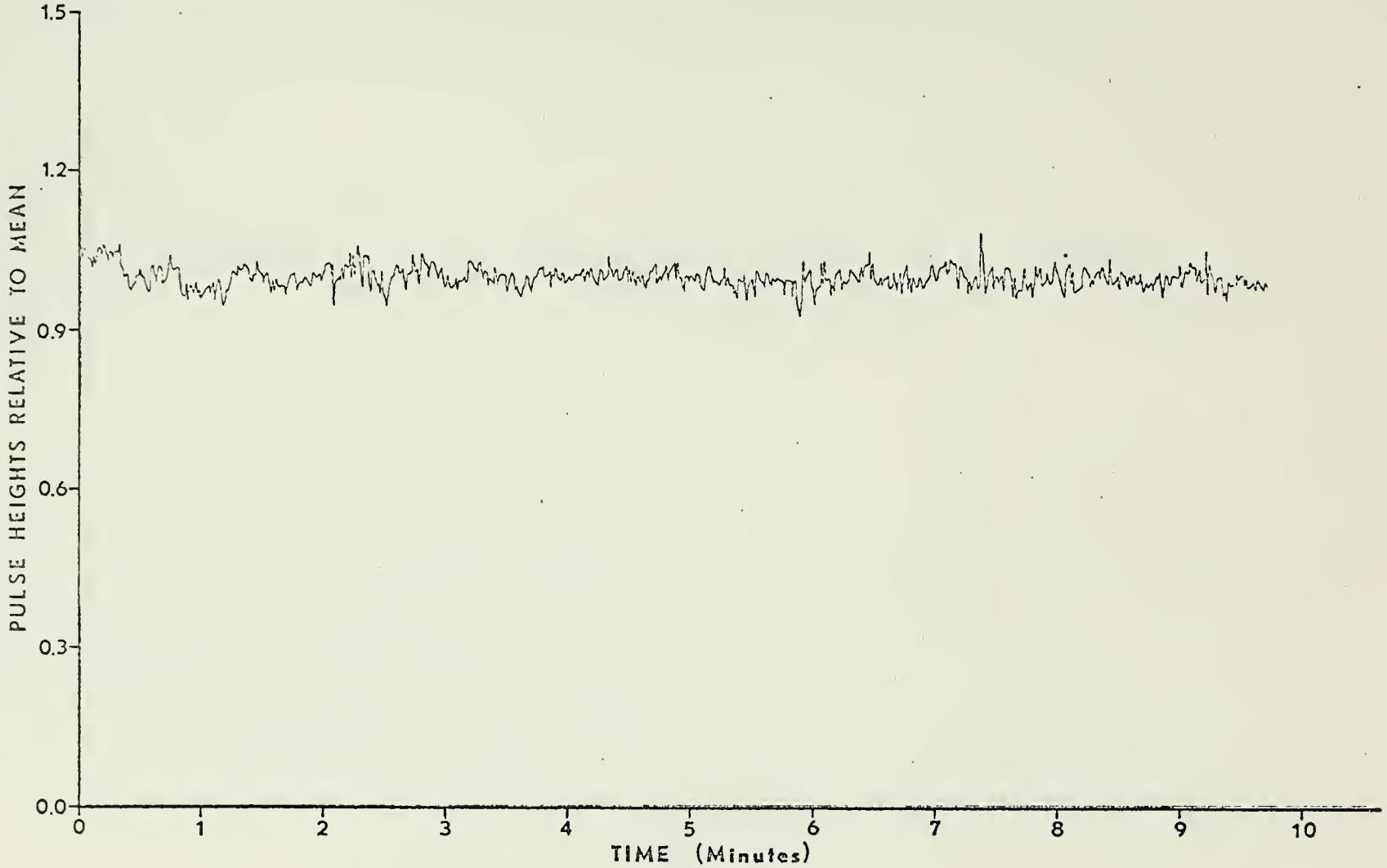

Run 56. Hydrophone 1 Pulse Heights.

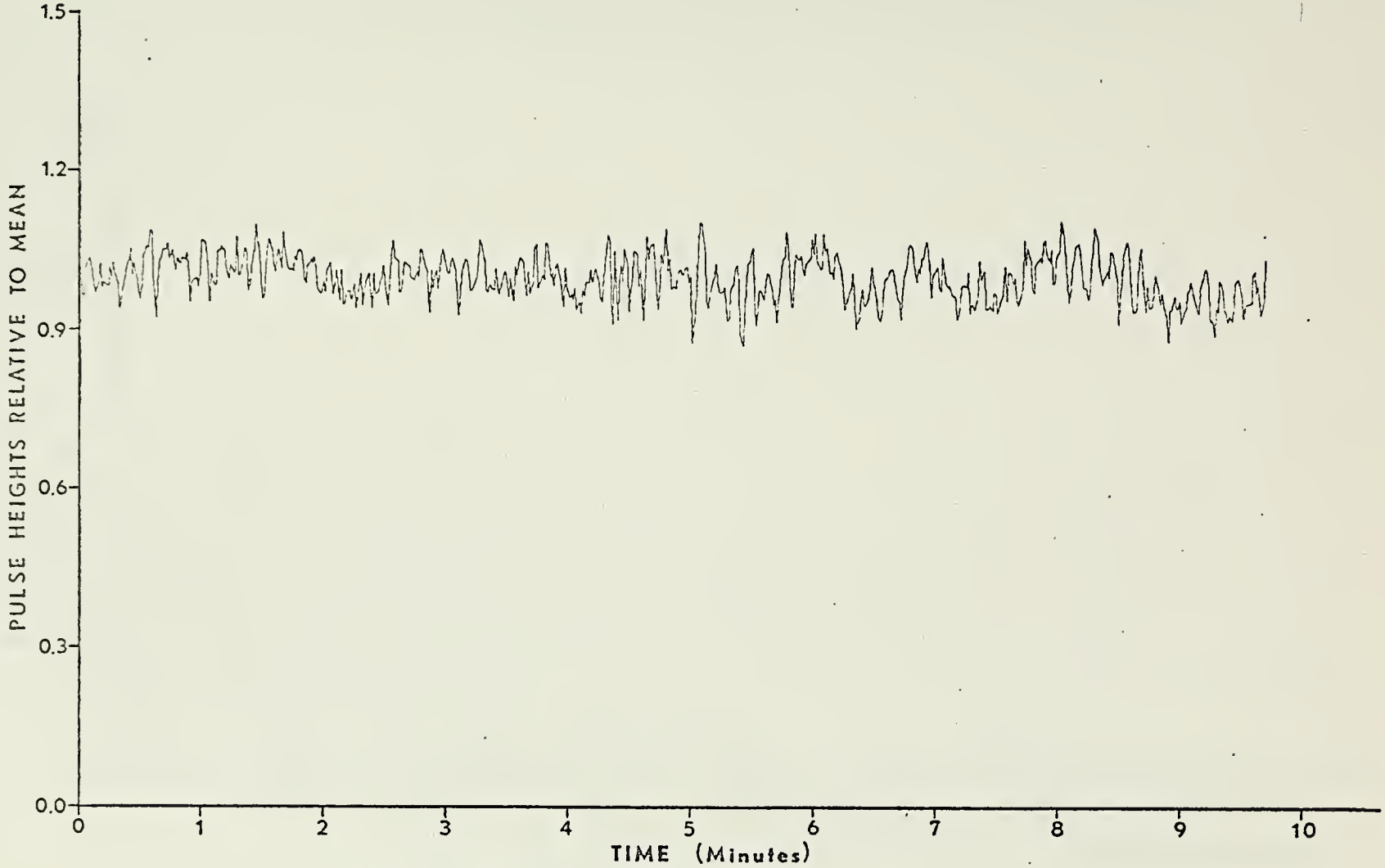

Run 56. Hydrophone 2 Pulse Heights.

Run 56. Autocorrelation Functions.

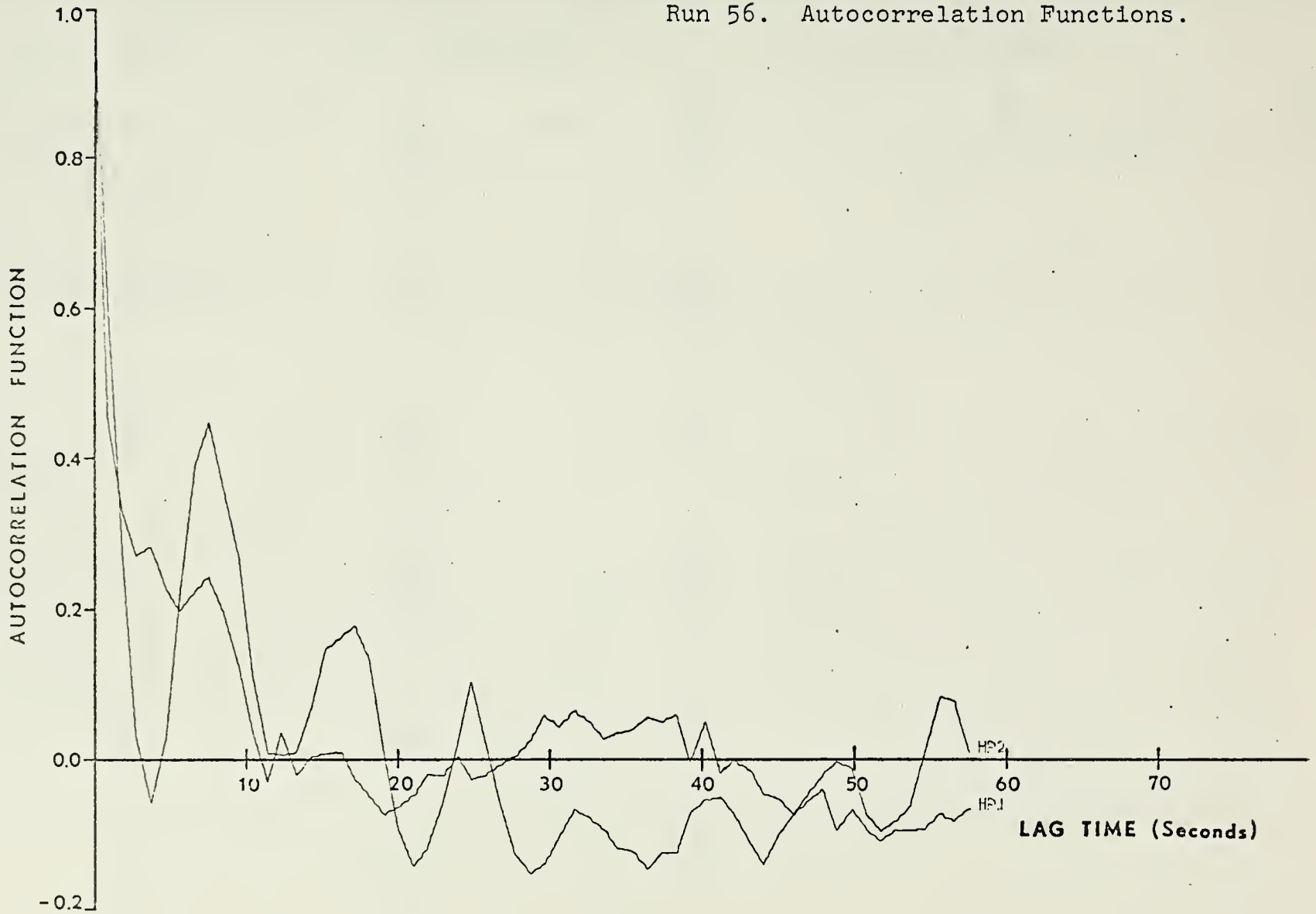

Run 56. Spectral Density, Coherence, and Phase.

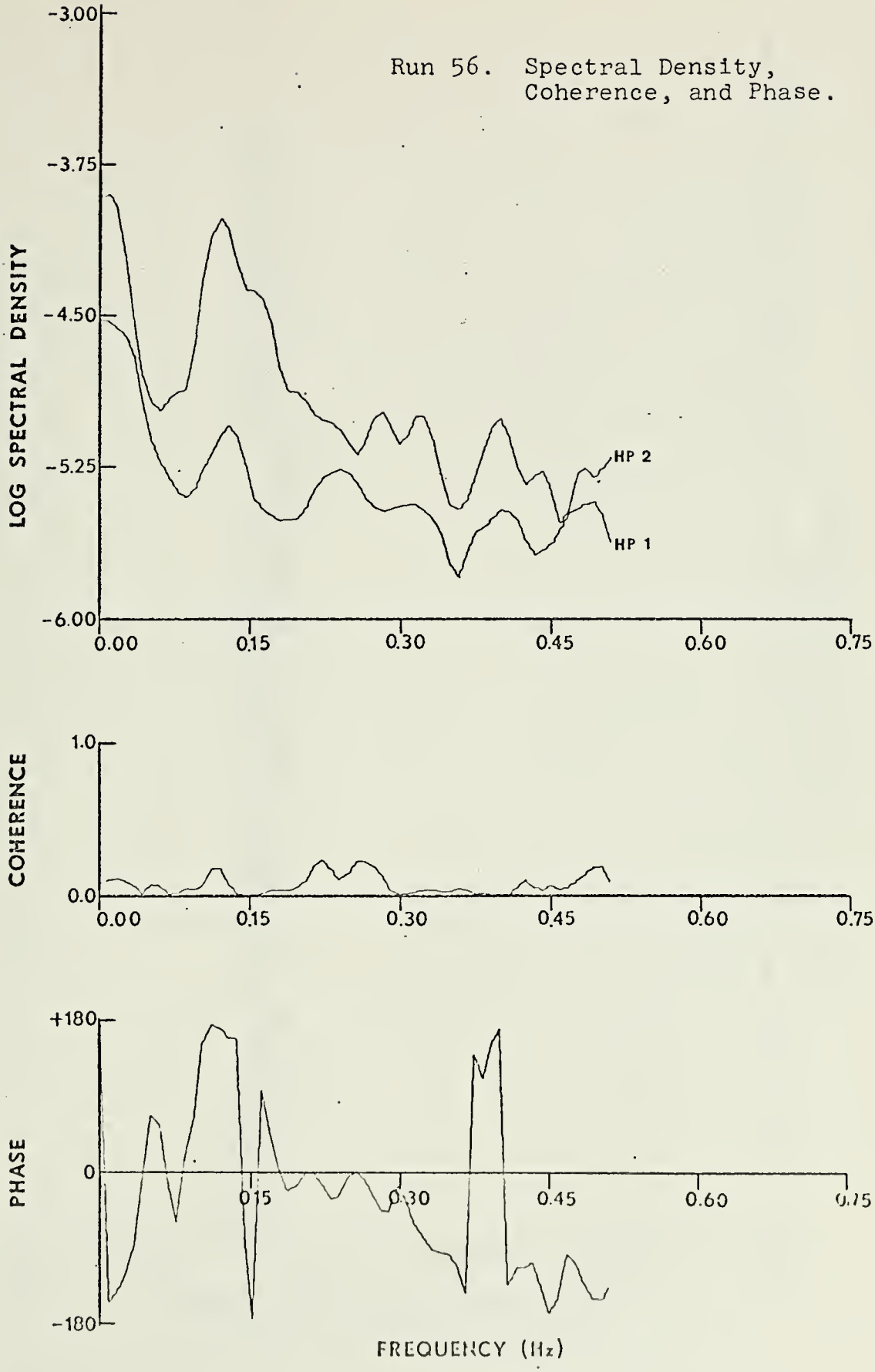

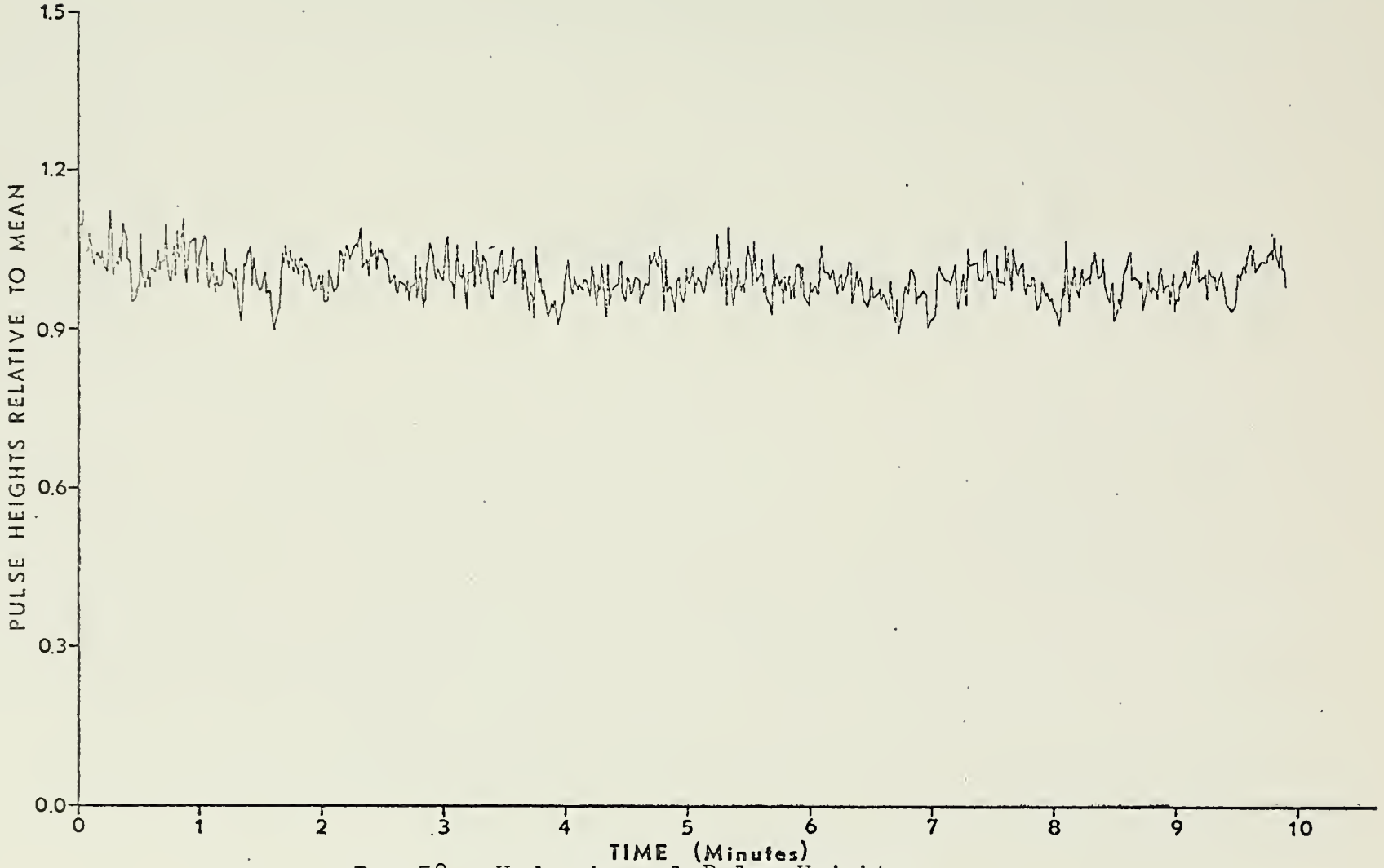

Run 58. Hydrophone 1 Pulse Heights.

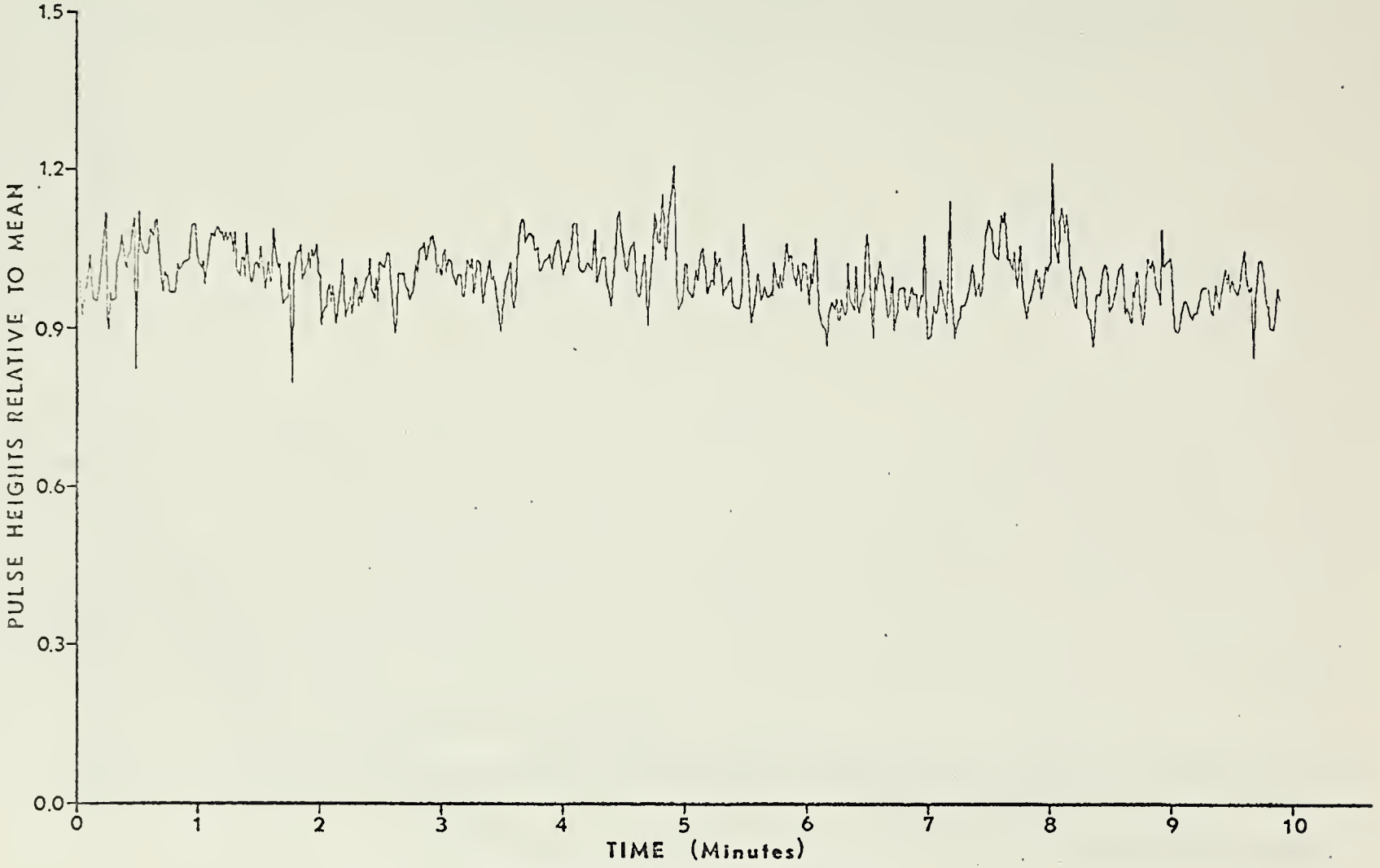

Run 58. Hydrophone 2 Pulse Heights.

Run 58. Autocorrelation Functions.

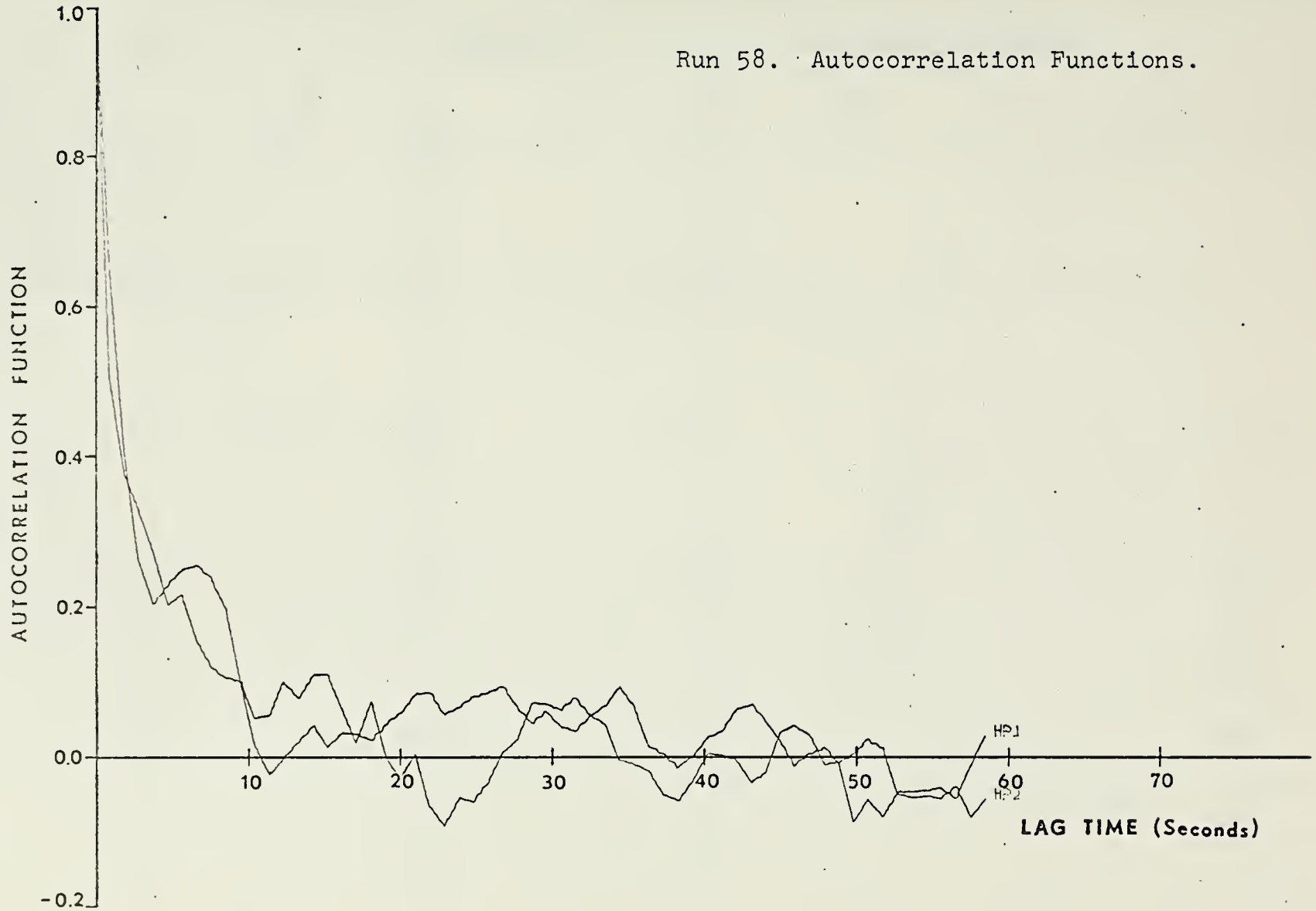

Run 58. Spectral Density, Coherence, and Phase.

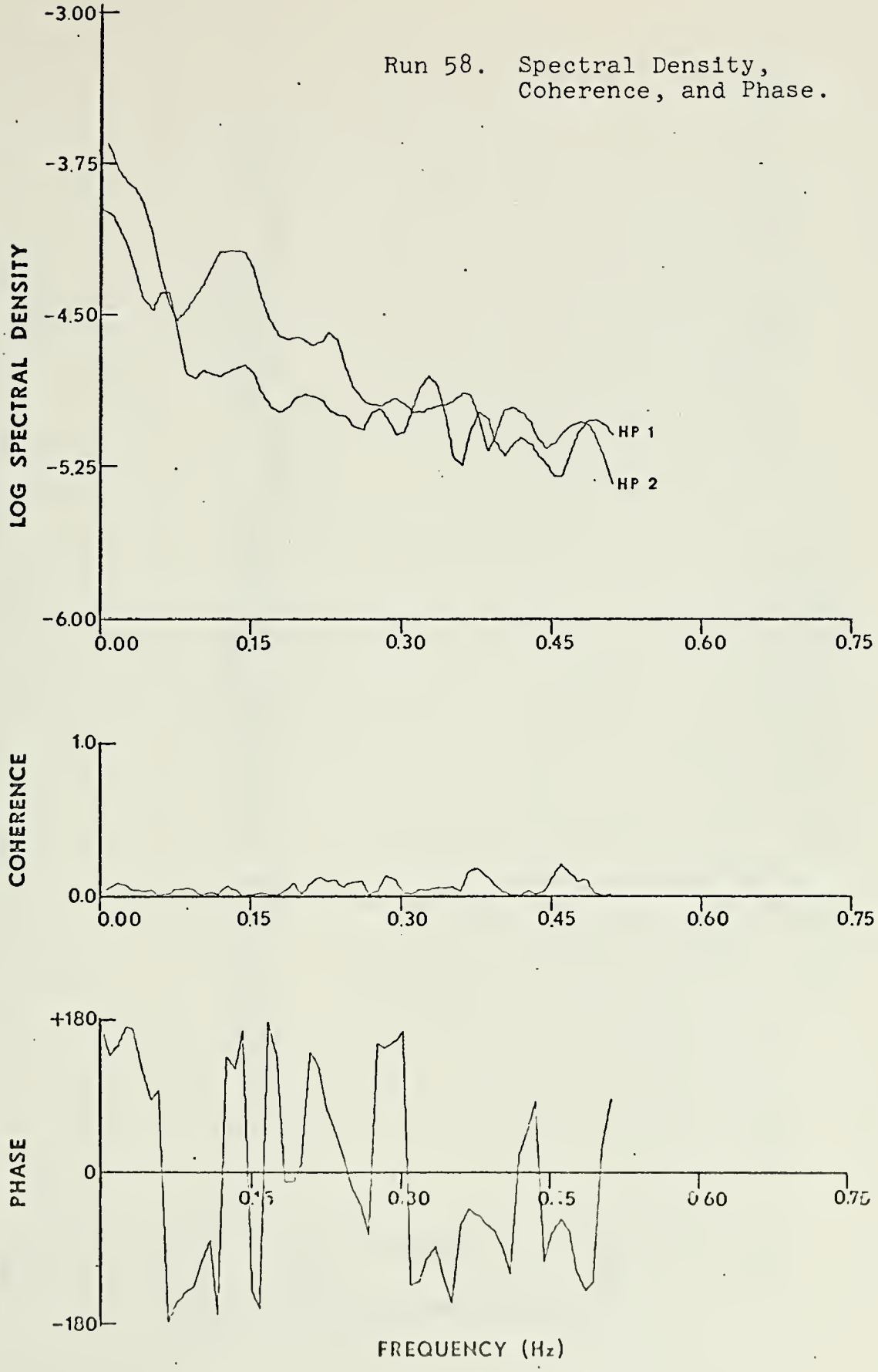

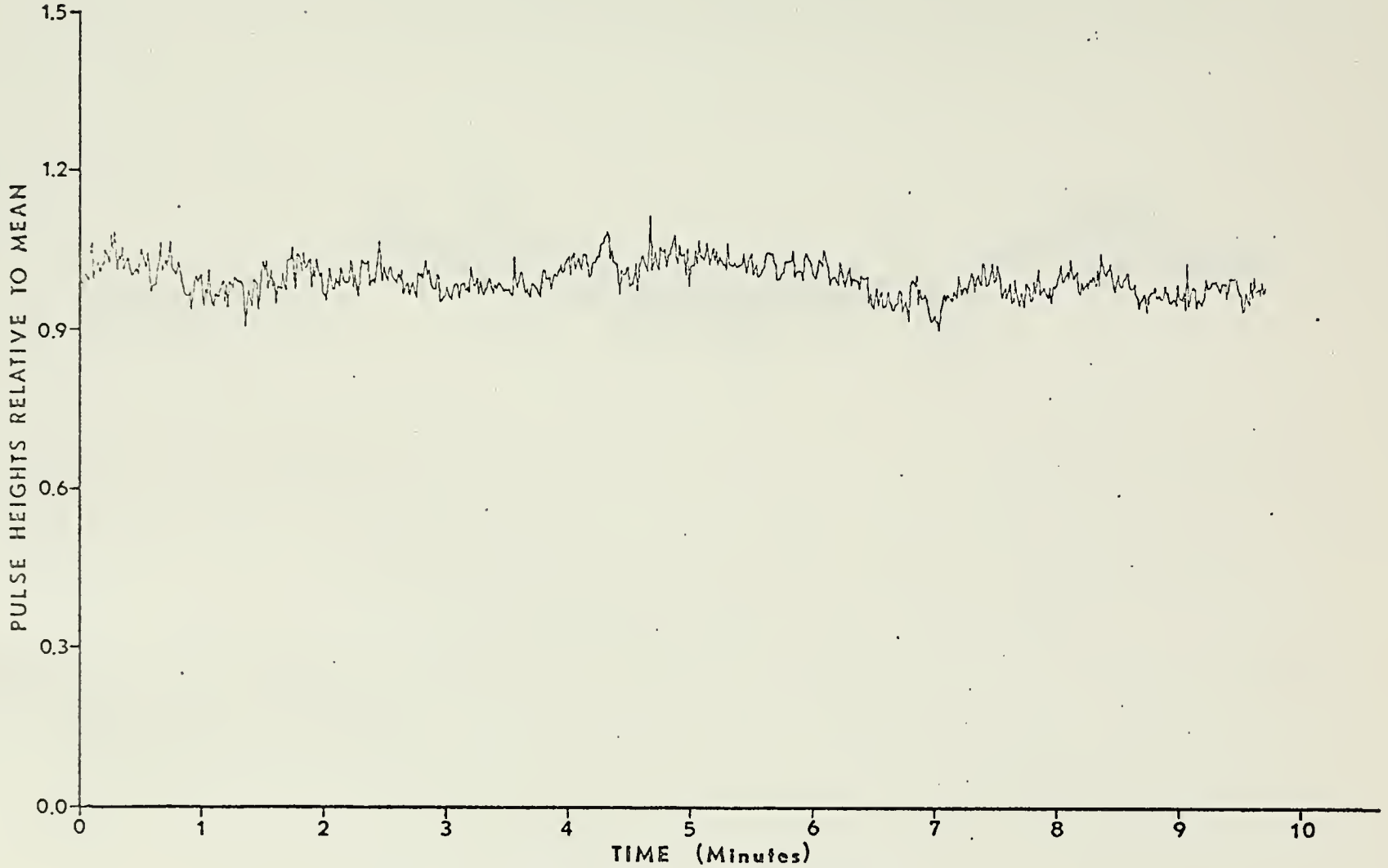

Run 60. Hydrophone 1 Pulse Heights.

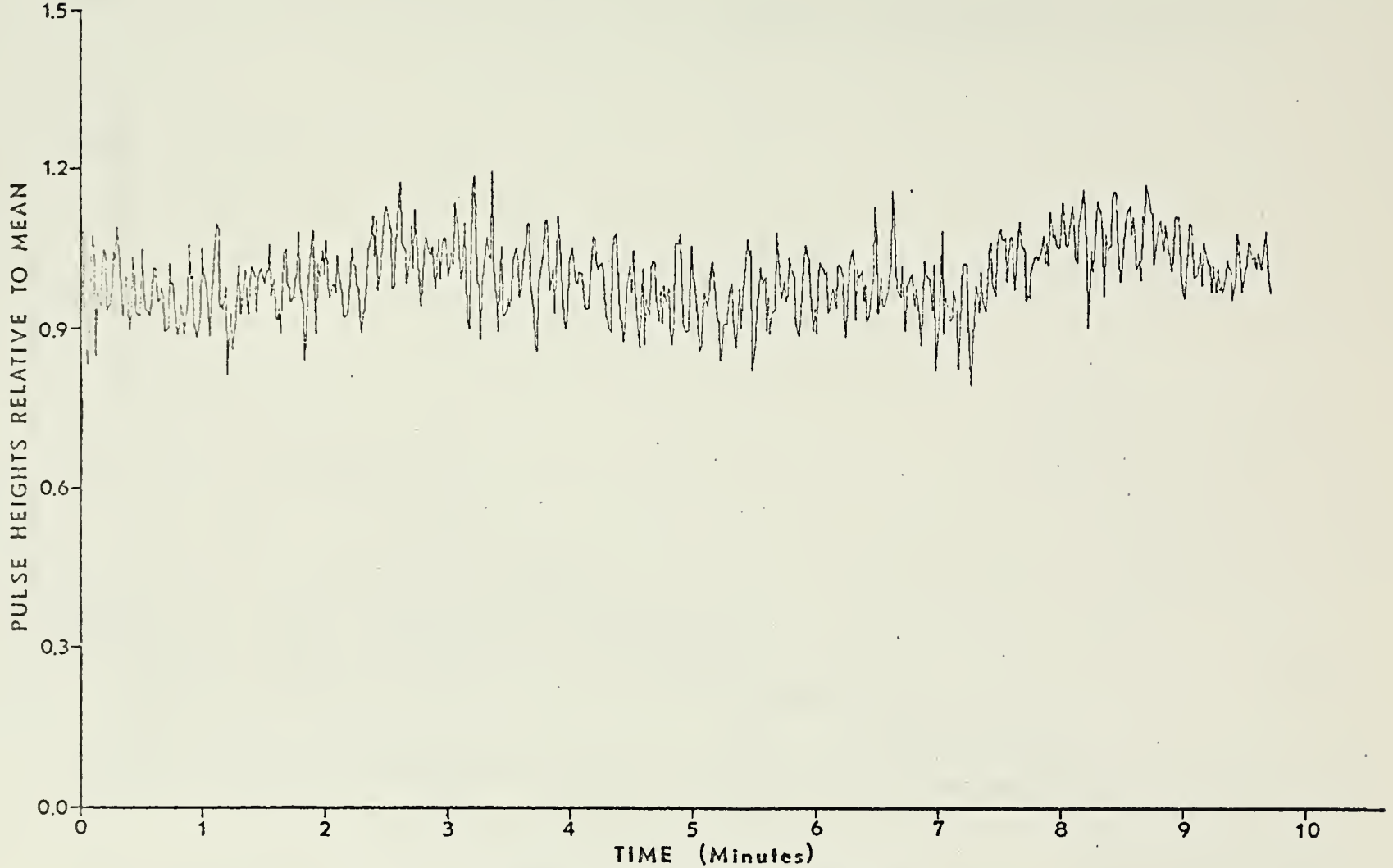

Run 60. Hydrophone 2 Pulse Heights.

Run 60. Autocorrelation Functions.

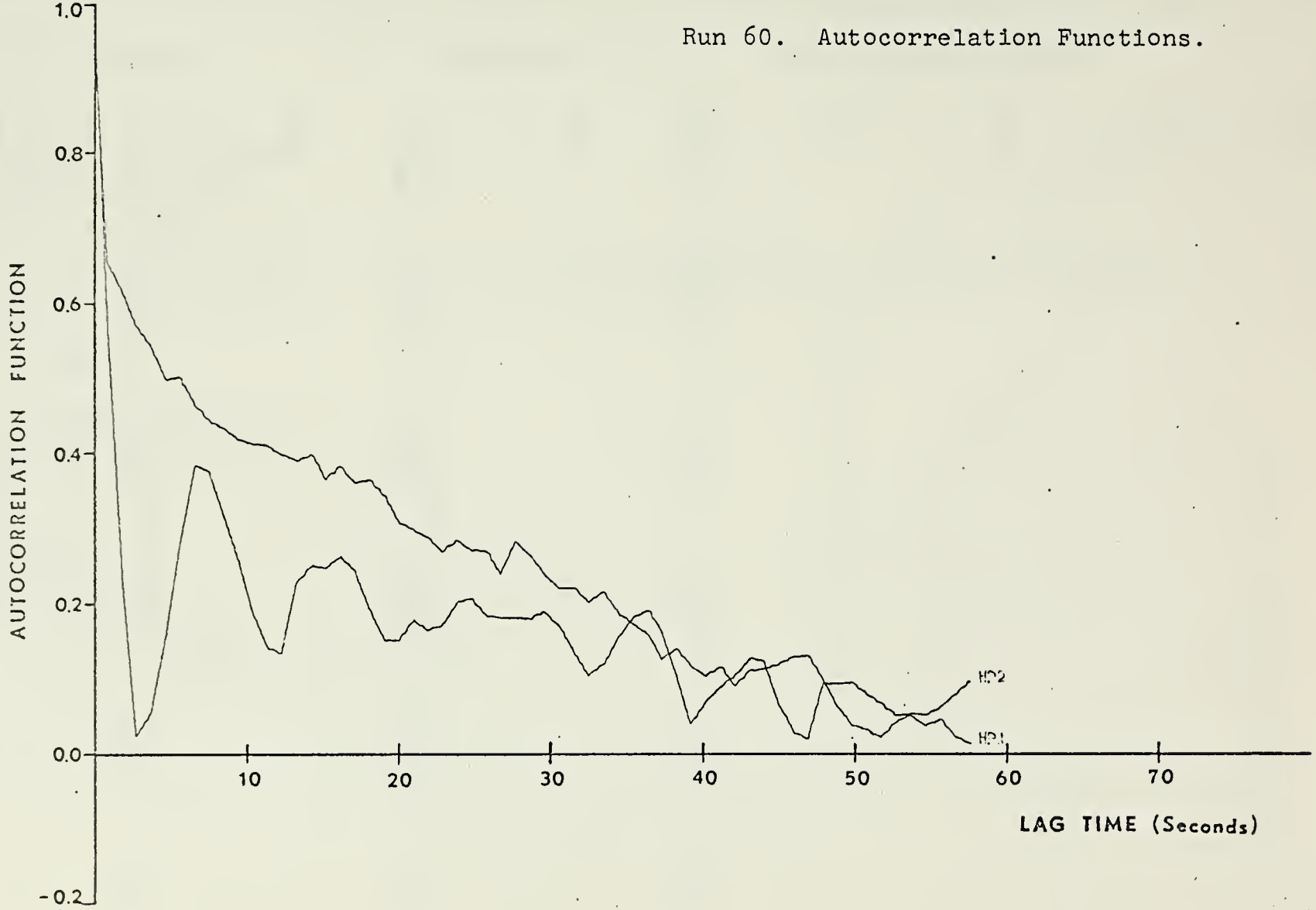

Run 60. Spectral Density, Coherence, and Phase.

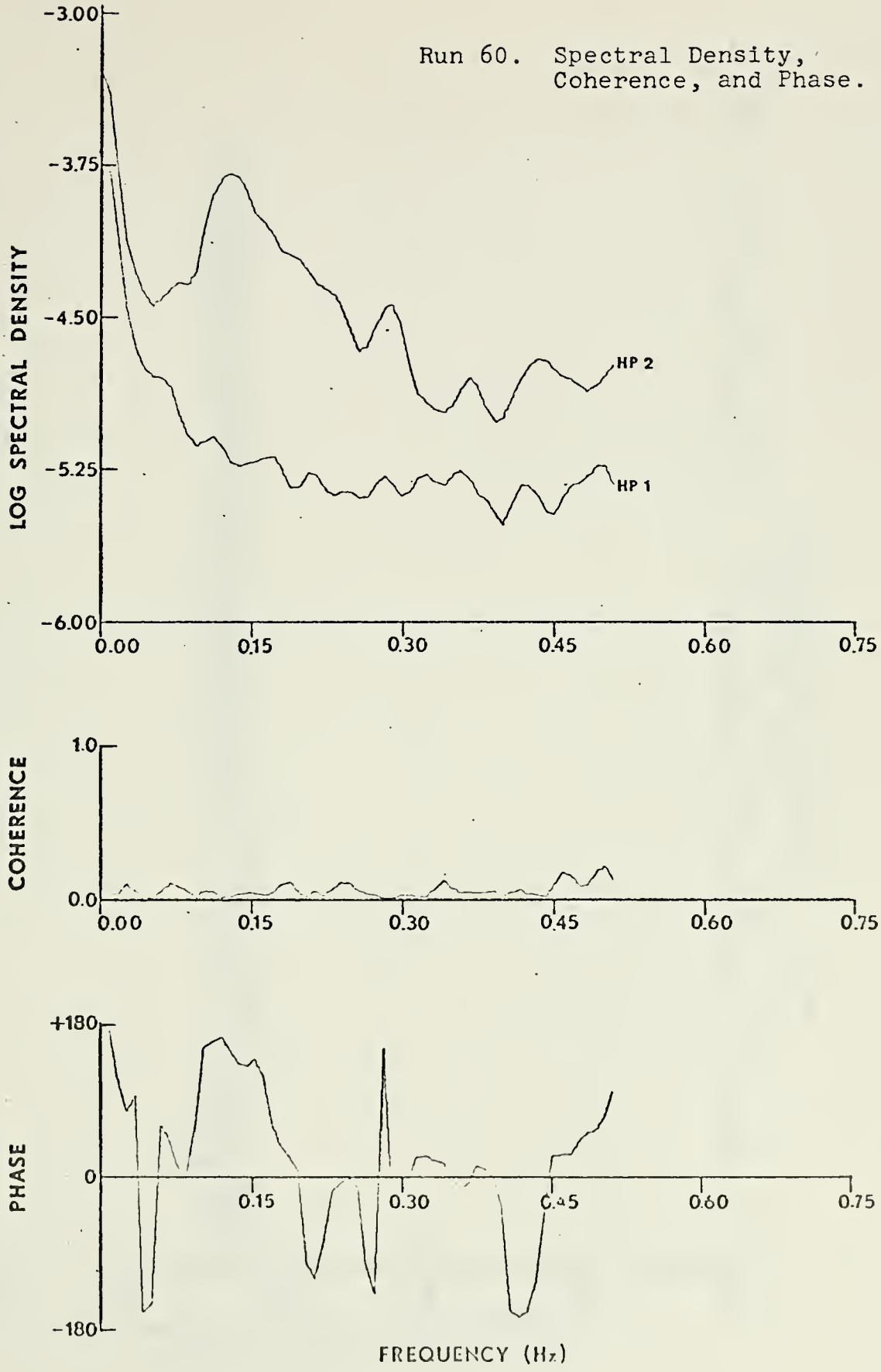

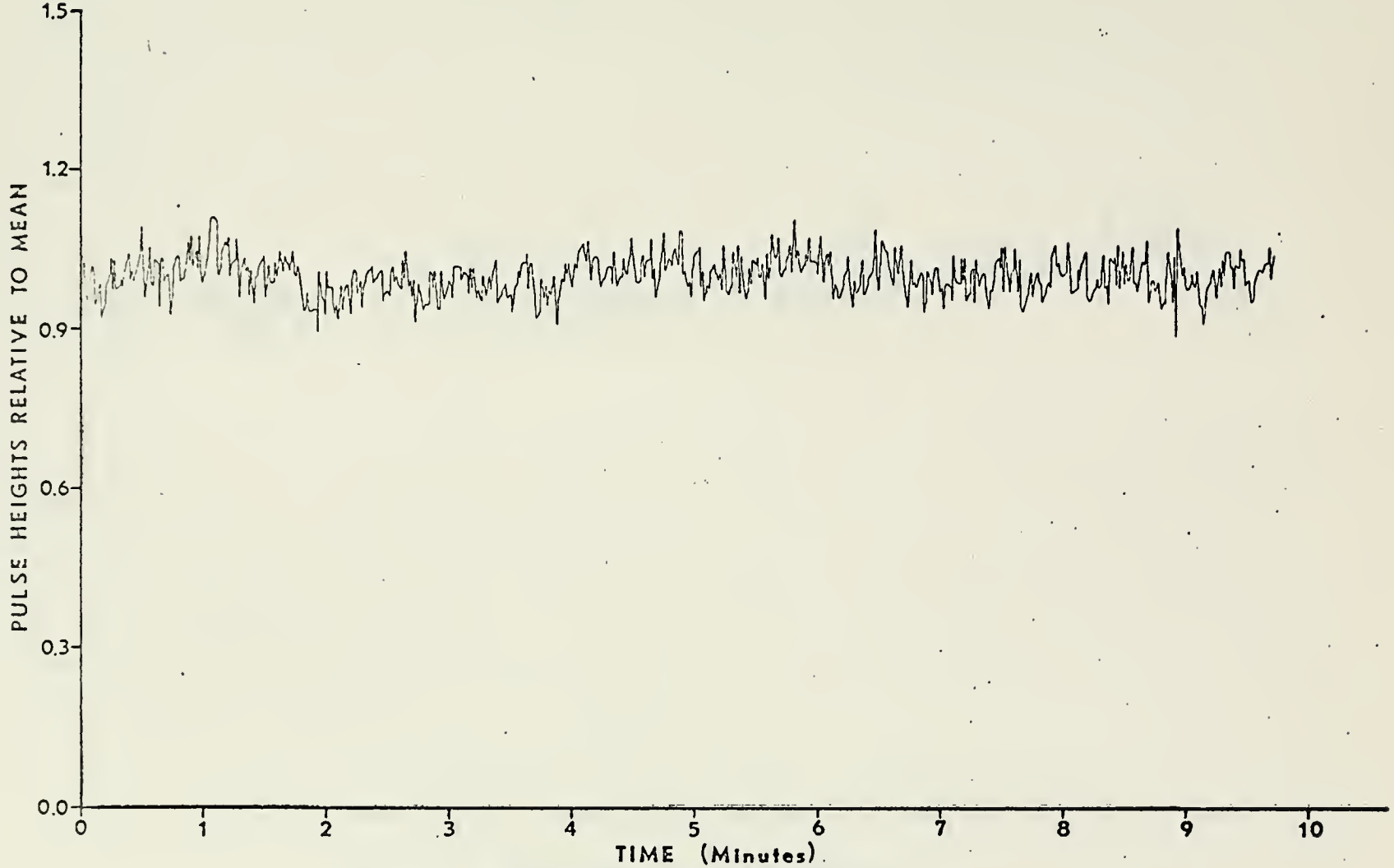

Run 61. Hydrophone 1 Pulse Heights.

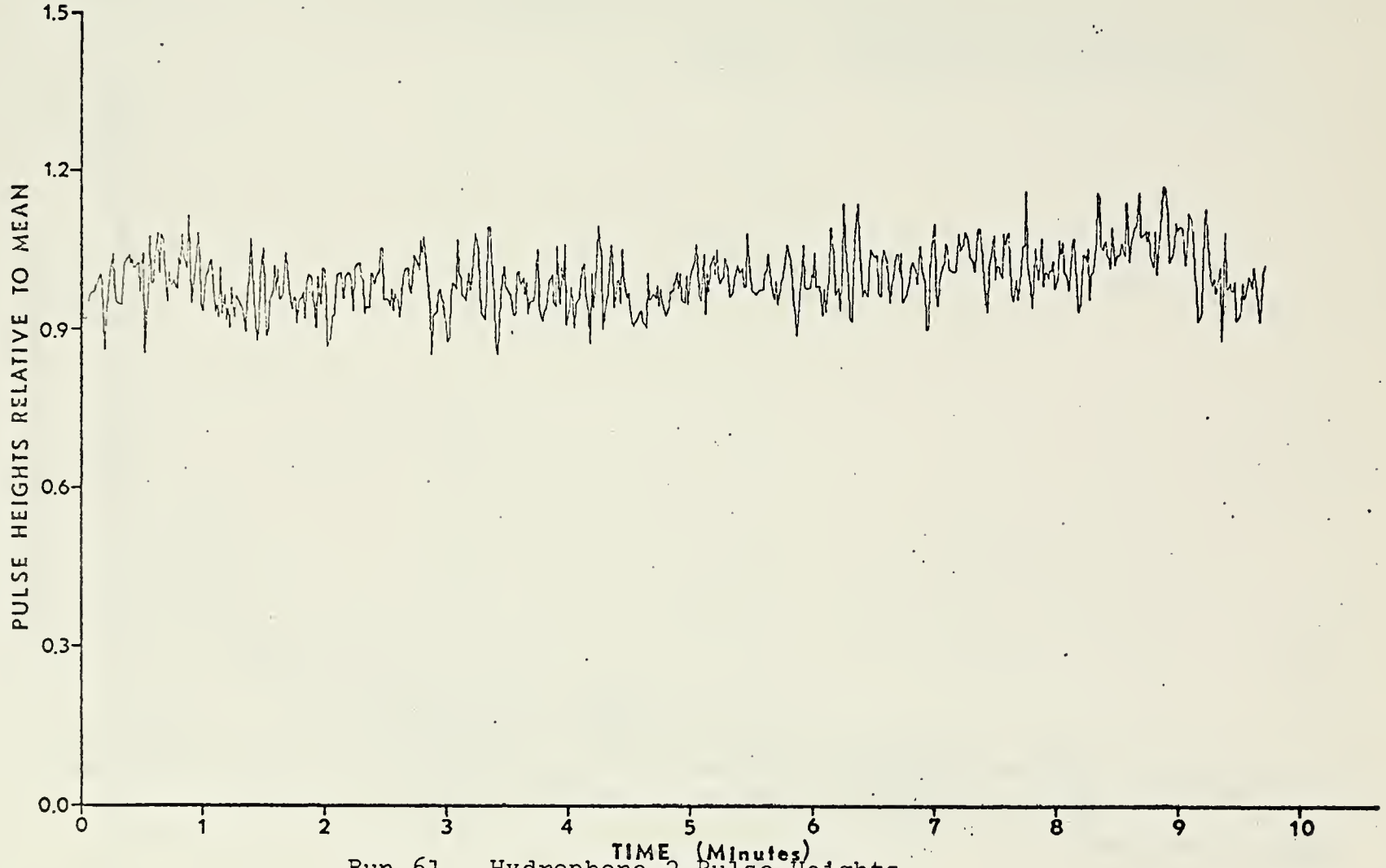

Run 61. Hydrophone 2 Pulse Heights.

Run 61. Autocorrelation Functions.

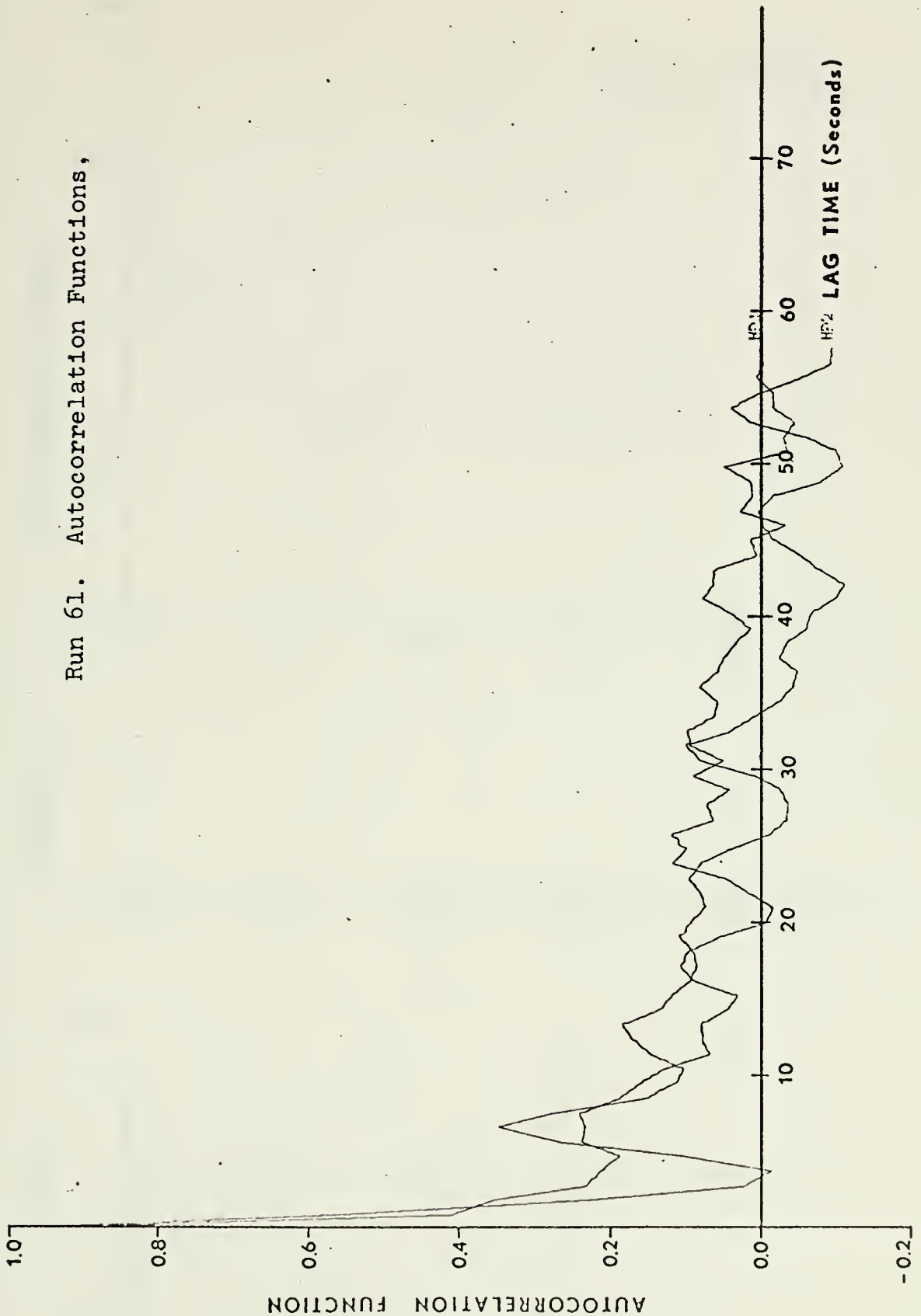

Run 61. Spectral Density, Coherence, and Phase.

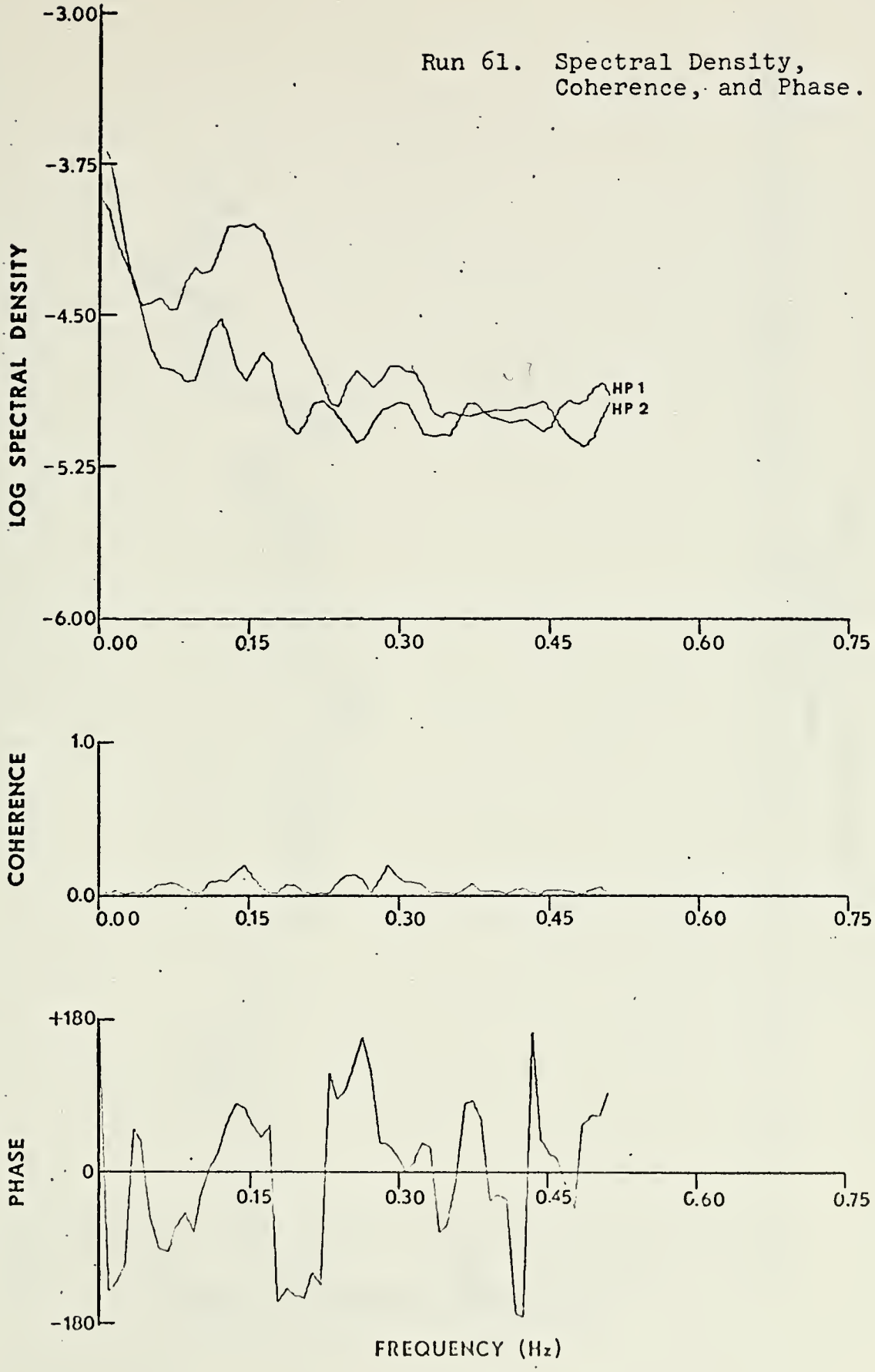

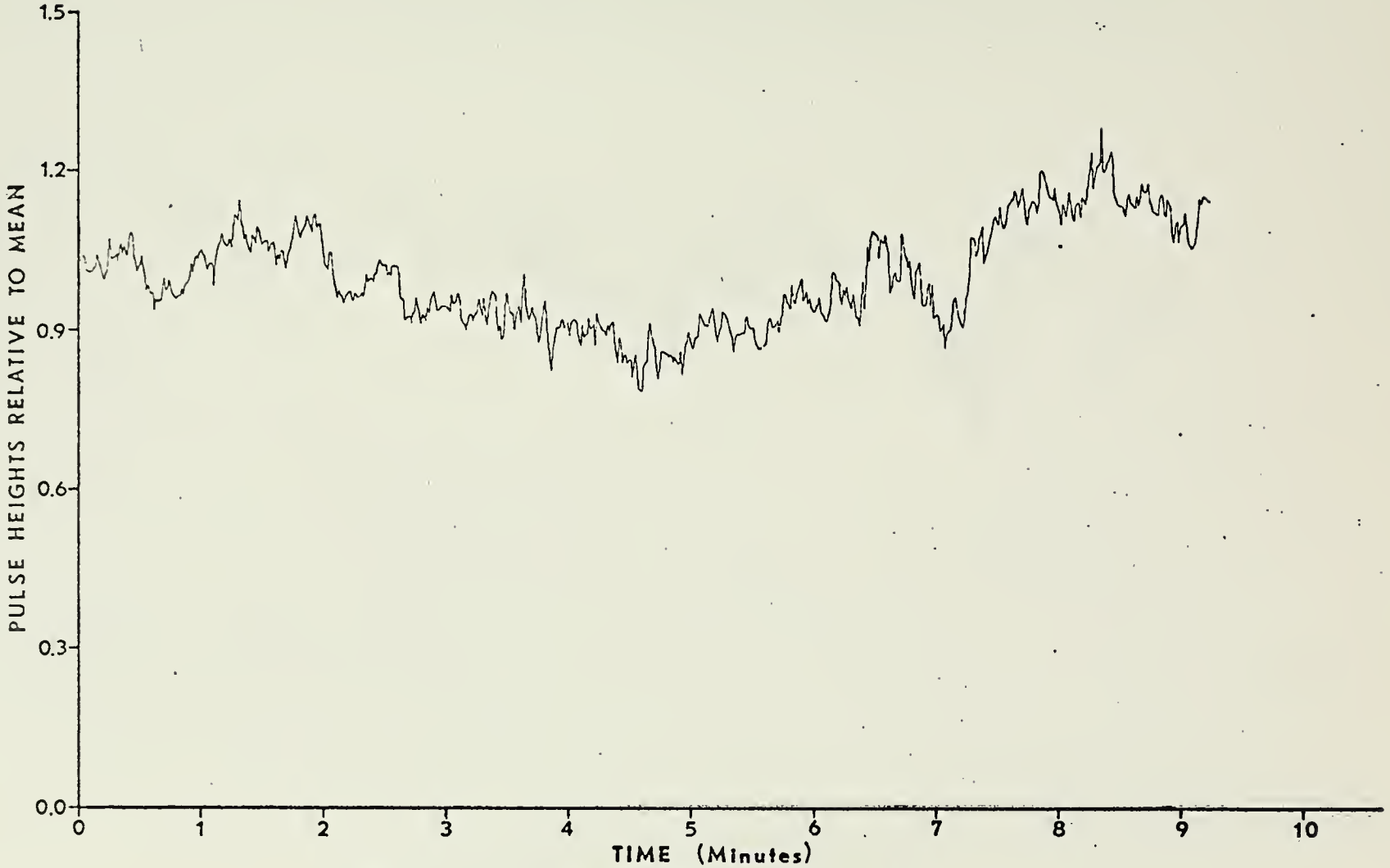

Run 72. Hydrophone 1 Pulse Heights.

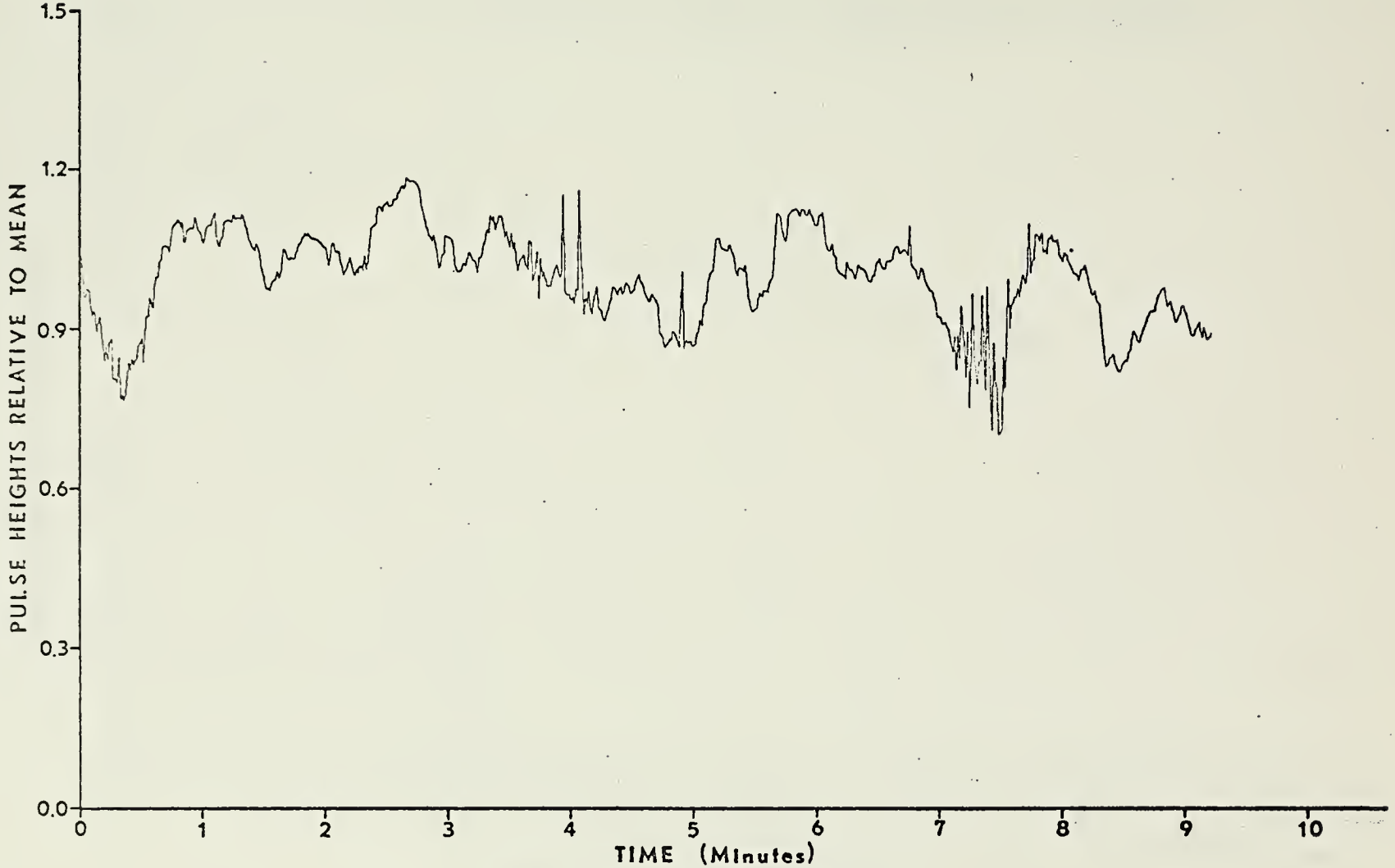

Run 72. Hydrophone 2 Pulse Heights.

Run 72. Autocorrelation Functions.

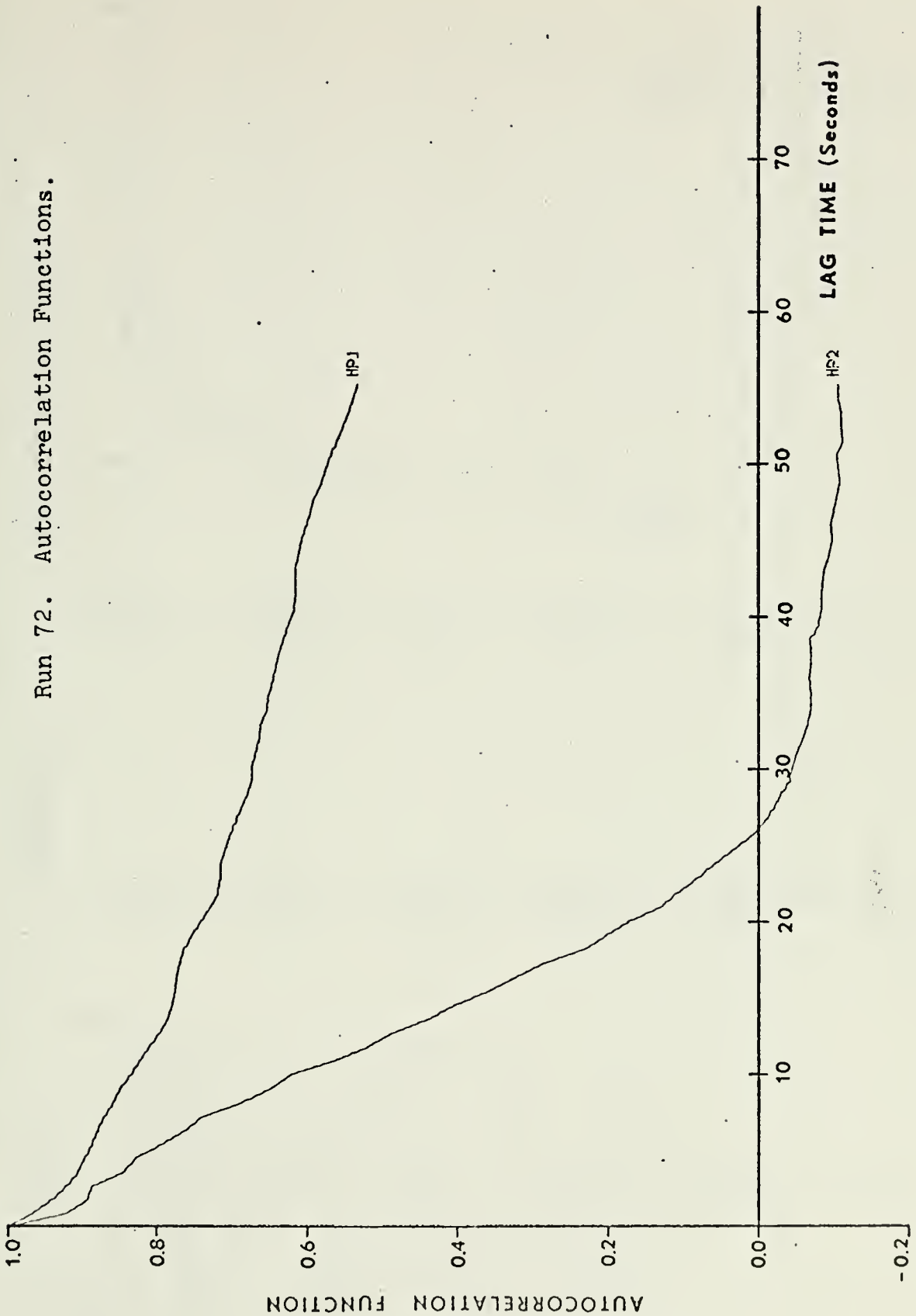

Run 72. Spectral Density, Coherence, and Phase.

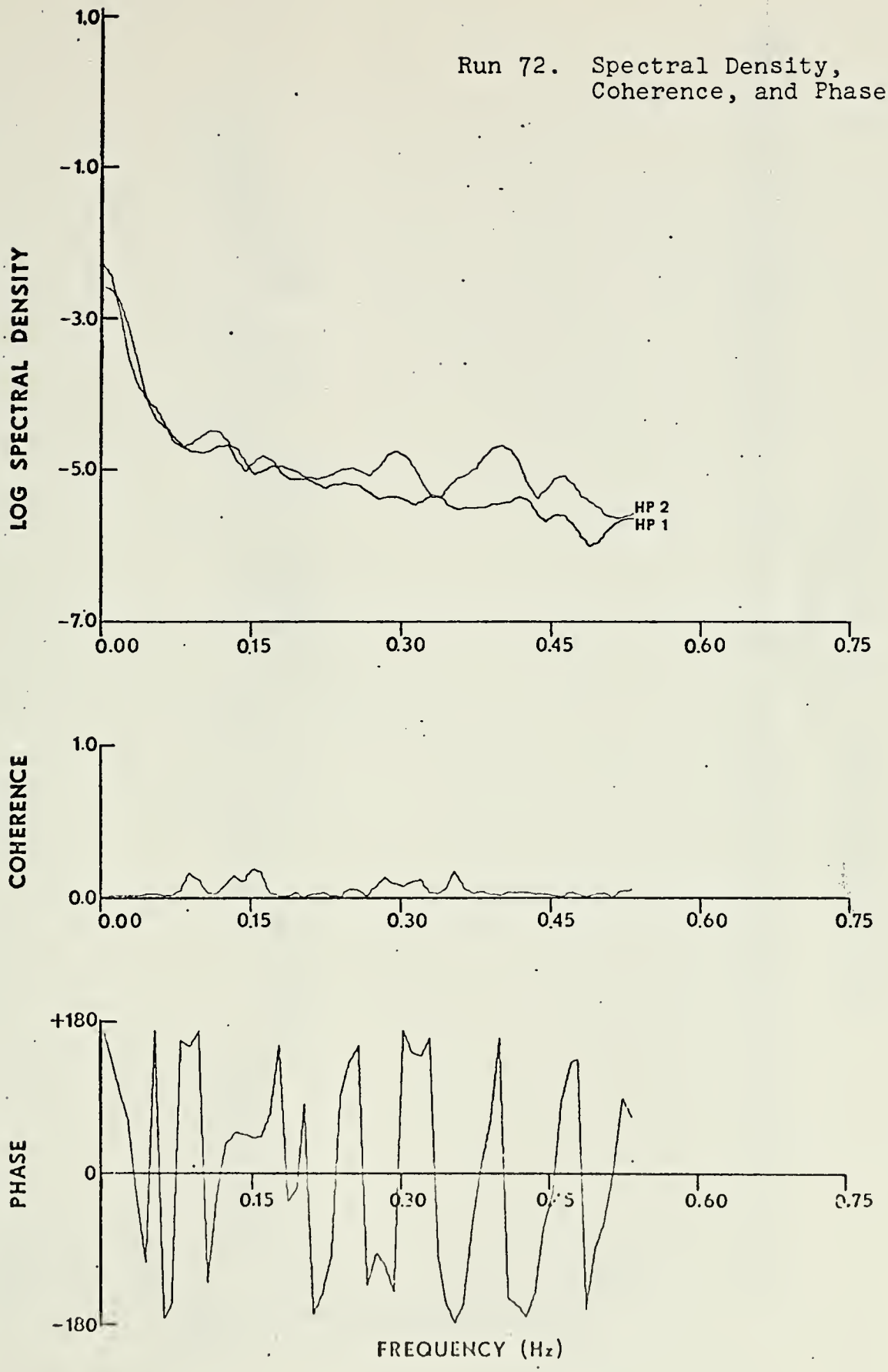

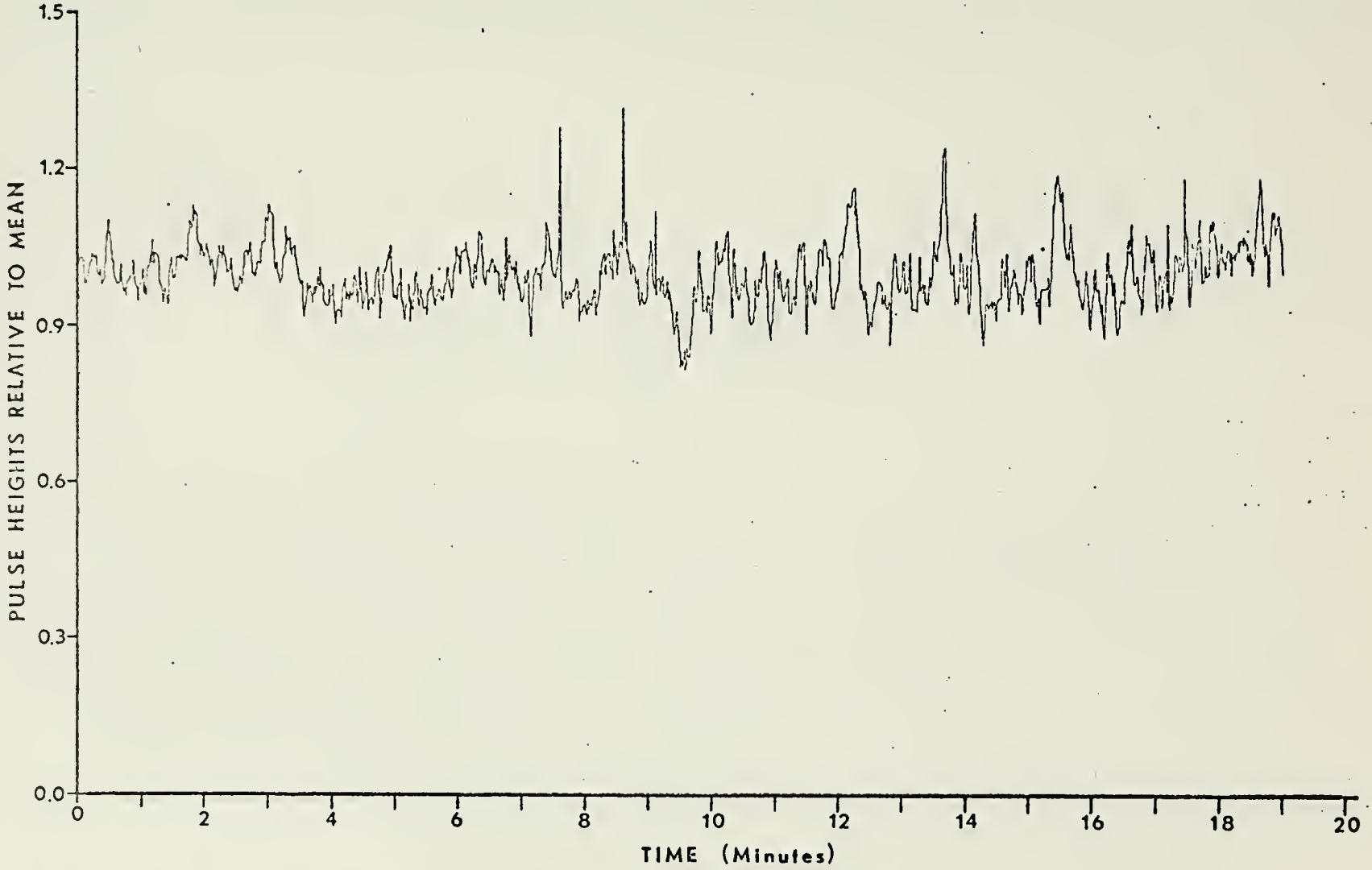

Run 73. Hydrophone 1 Pulse Heights.

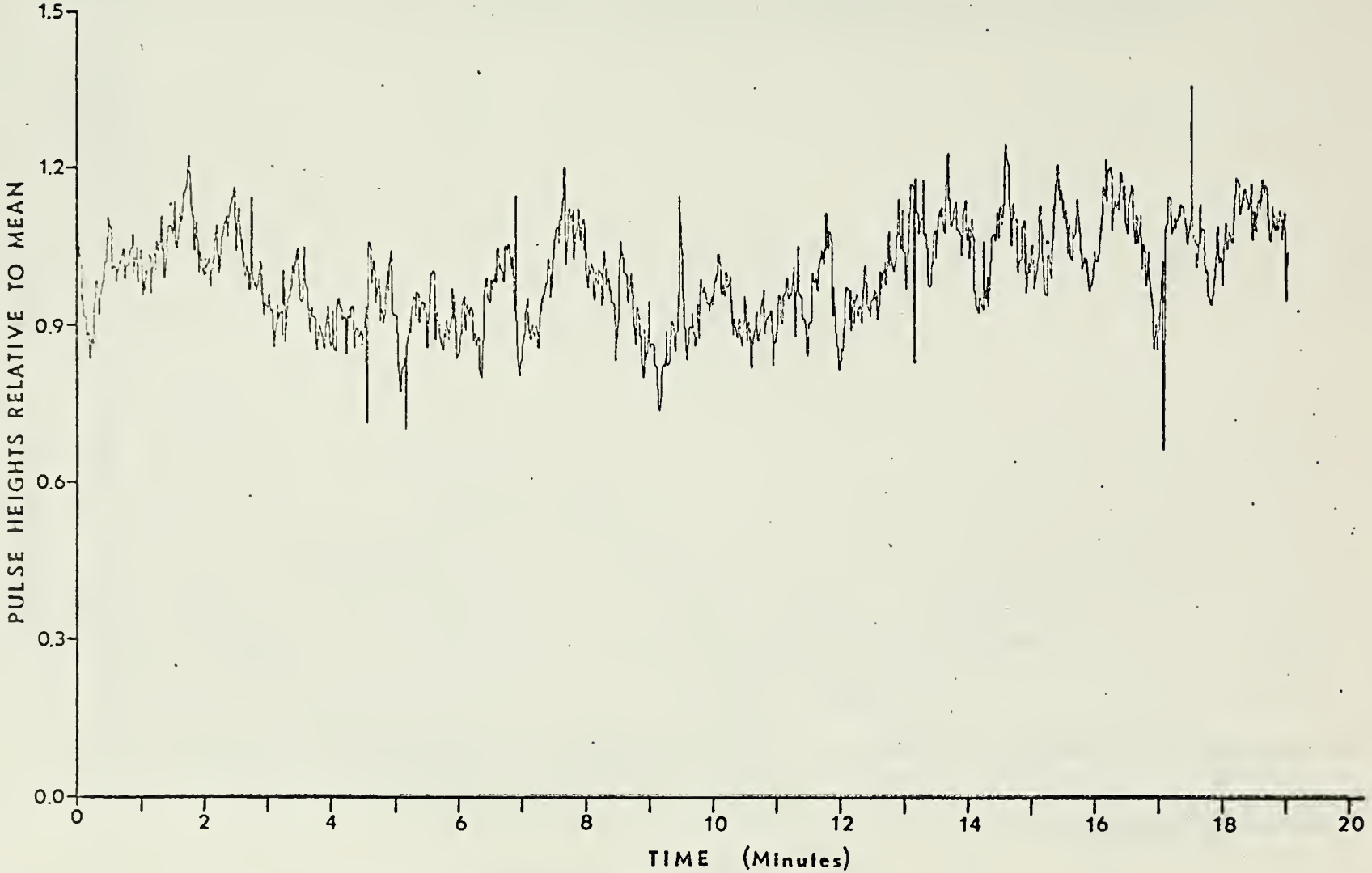

Run 73. Hydrophone 2 Pulse Heights.

Run 73. Autocorrelation Functions.

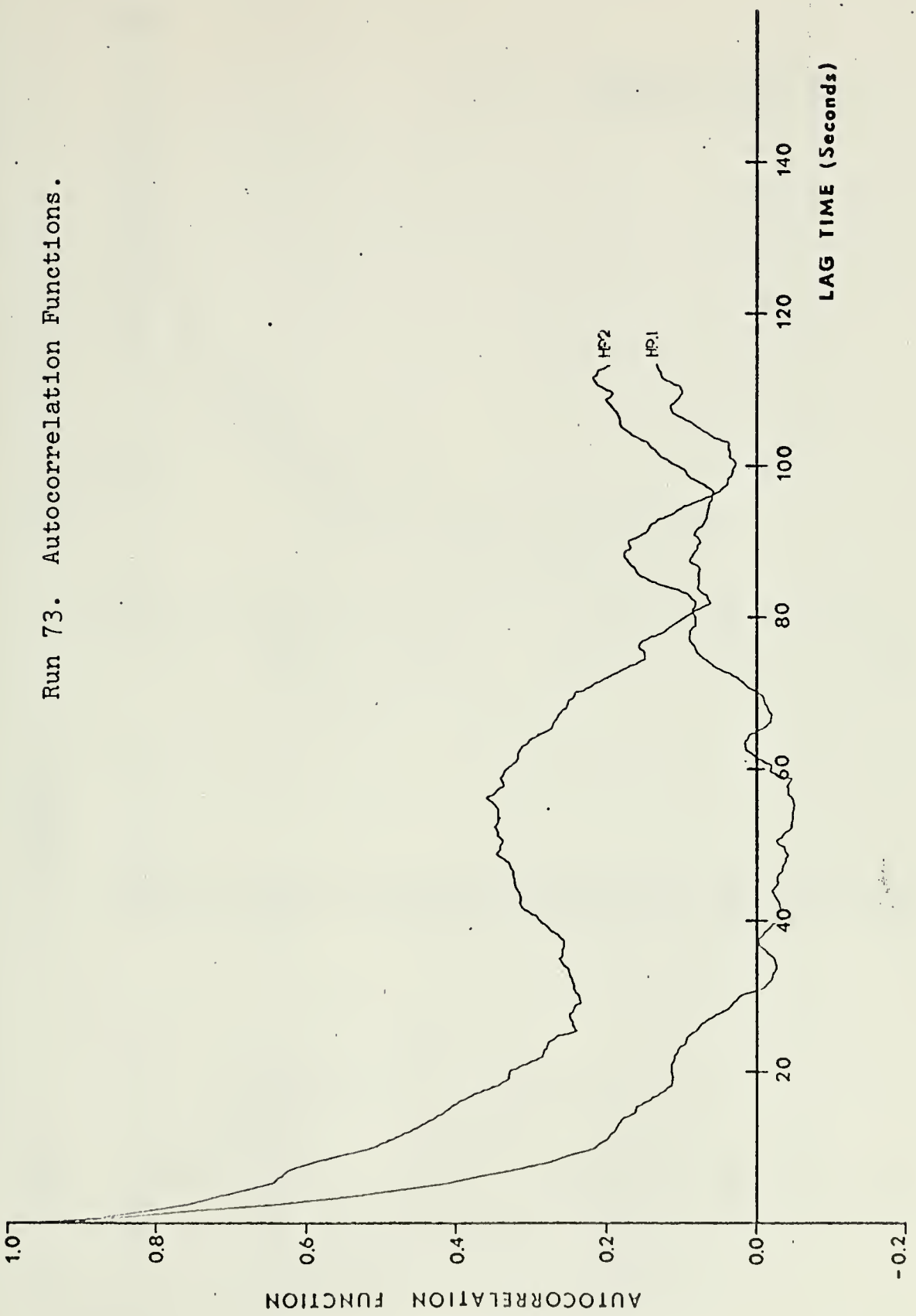

Run 73. Spectral Density, Coherence, and Phase.

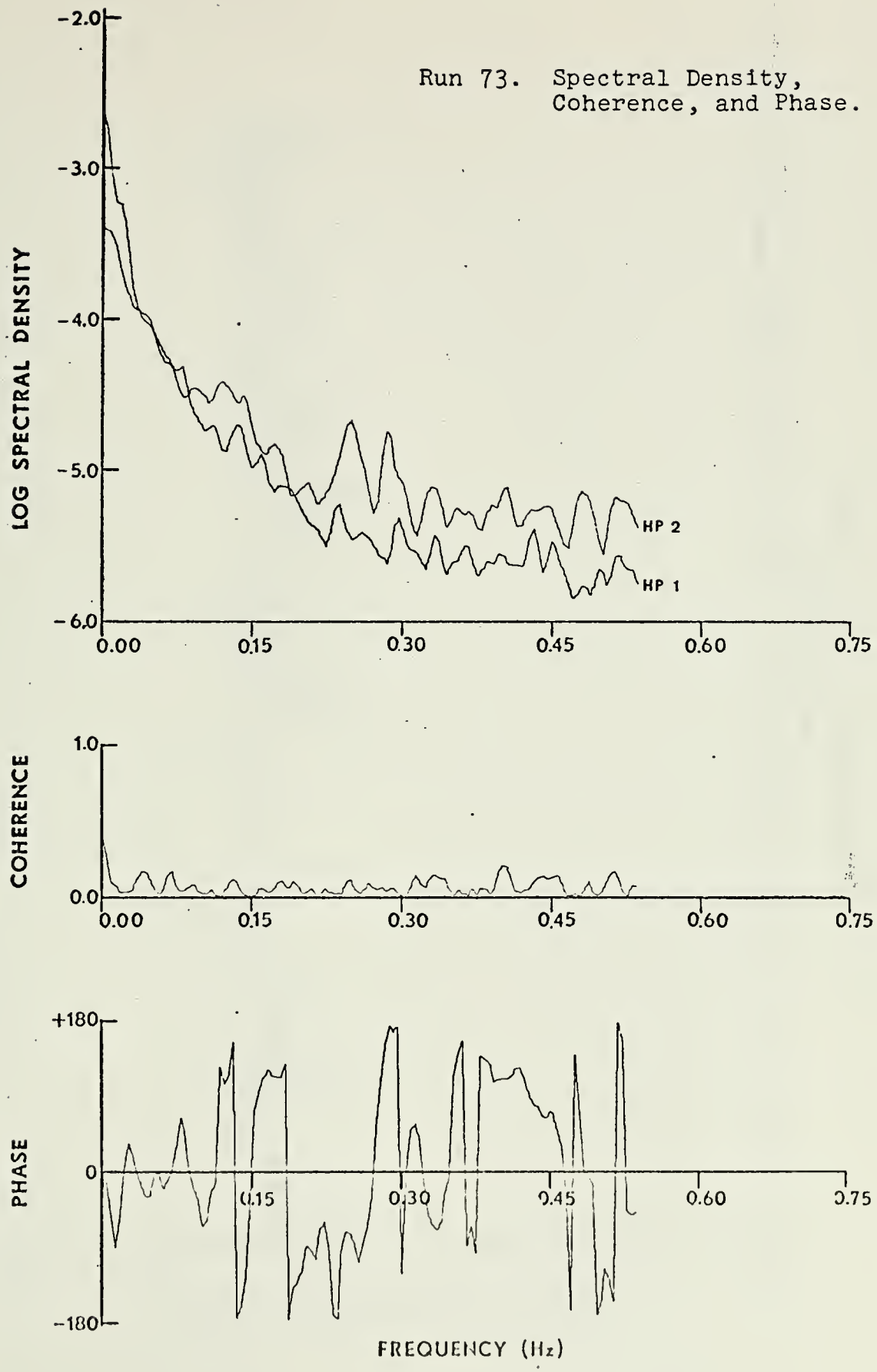

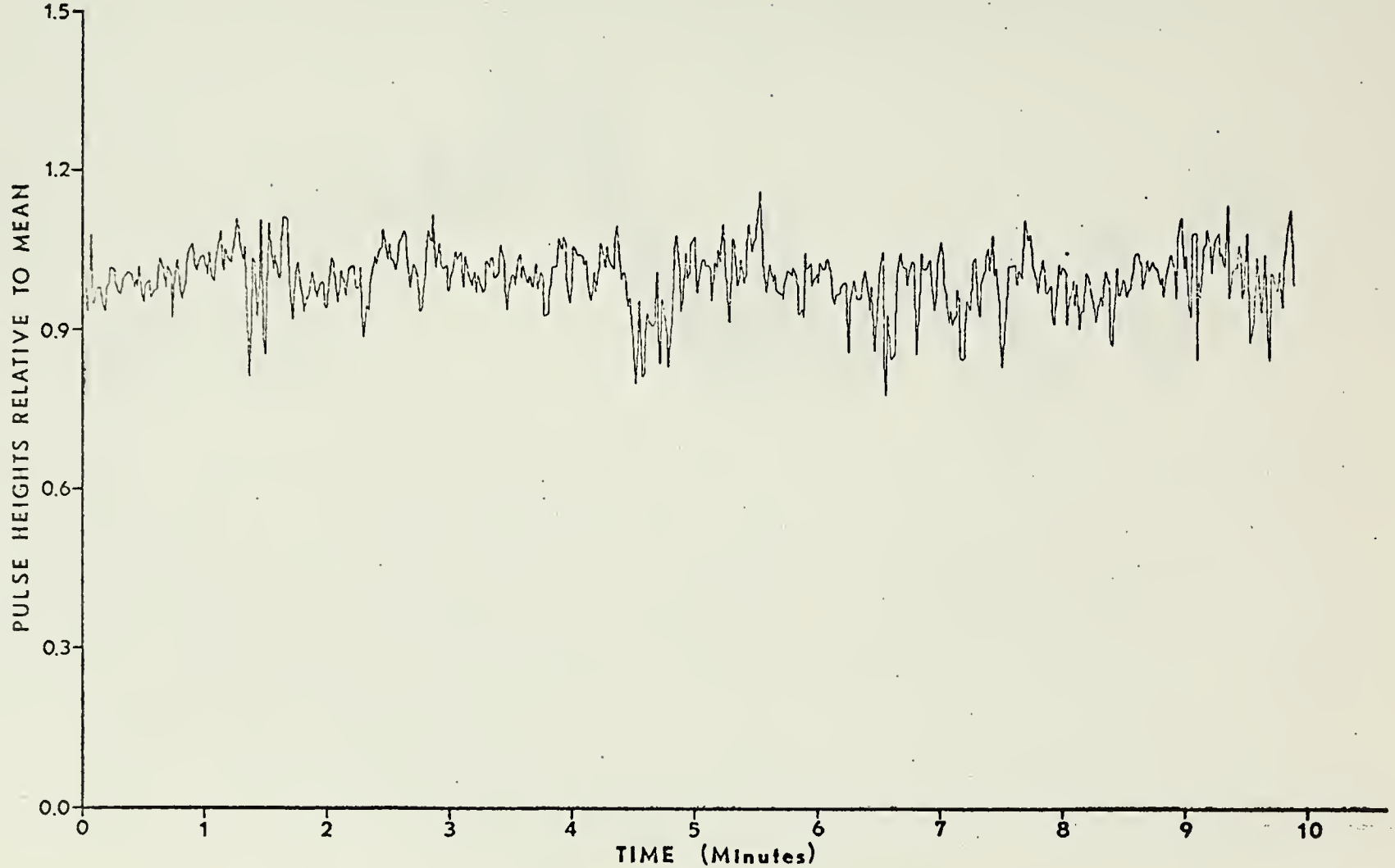

Run 116. Hydrophone 1 Pulse Heights.

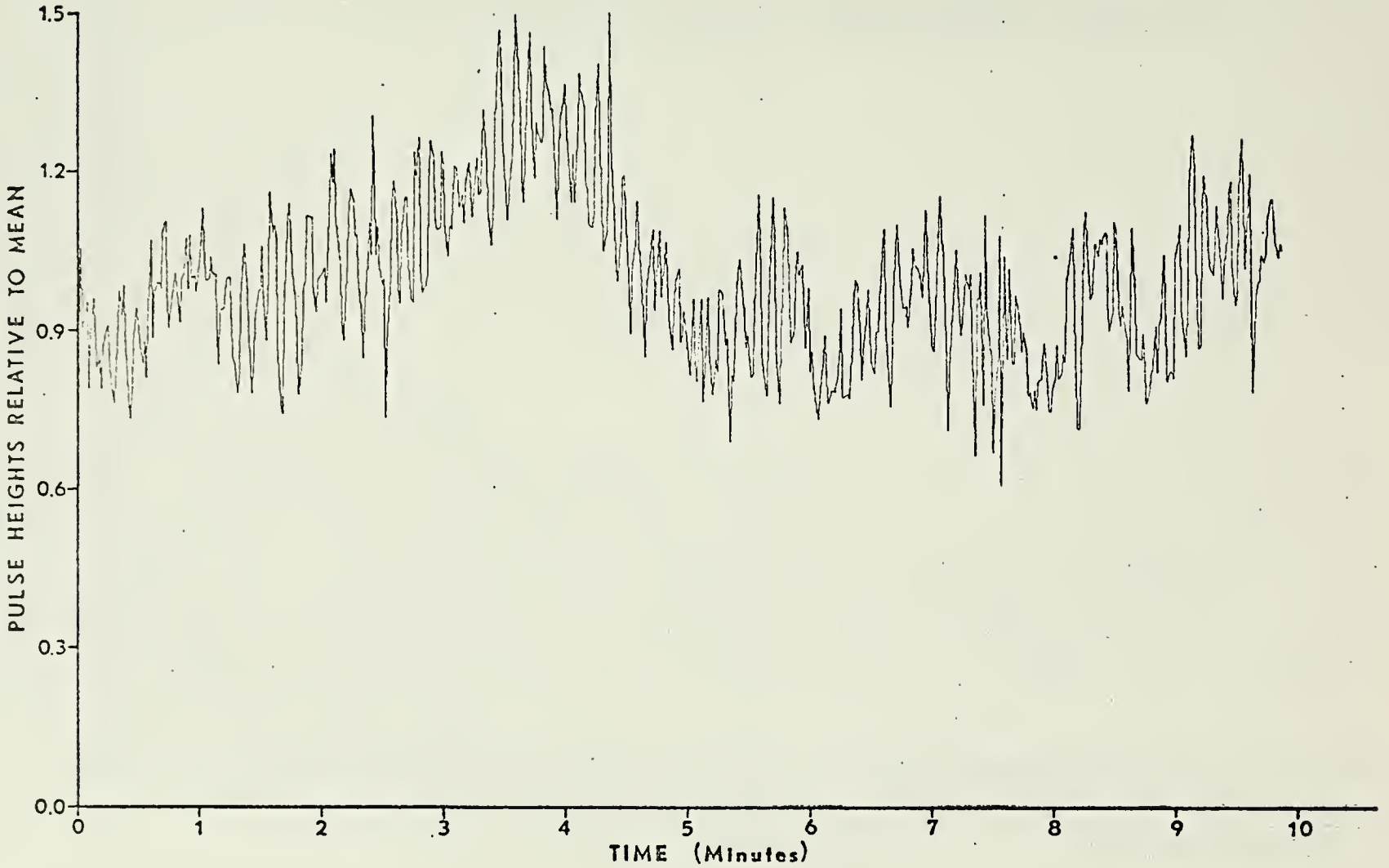

Run 116. Hydrophone 2 Pulse Heights.

Run 116. Autocorrelation Functions.

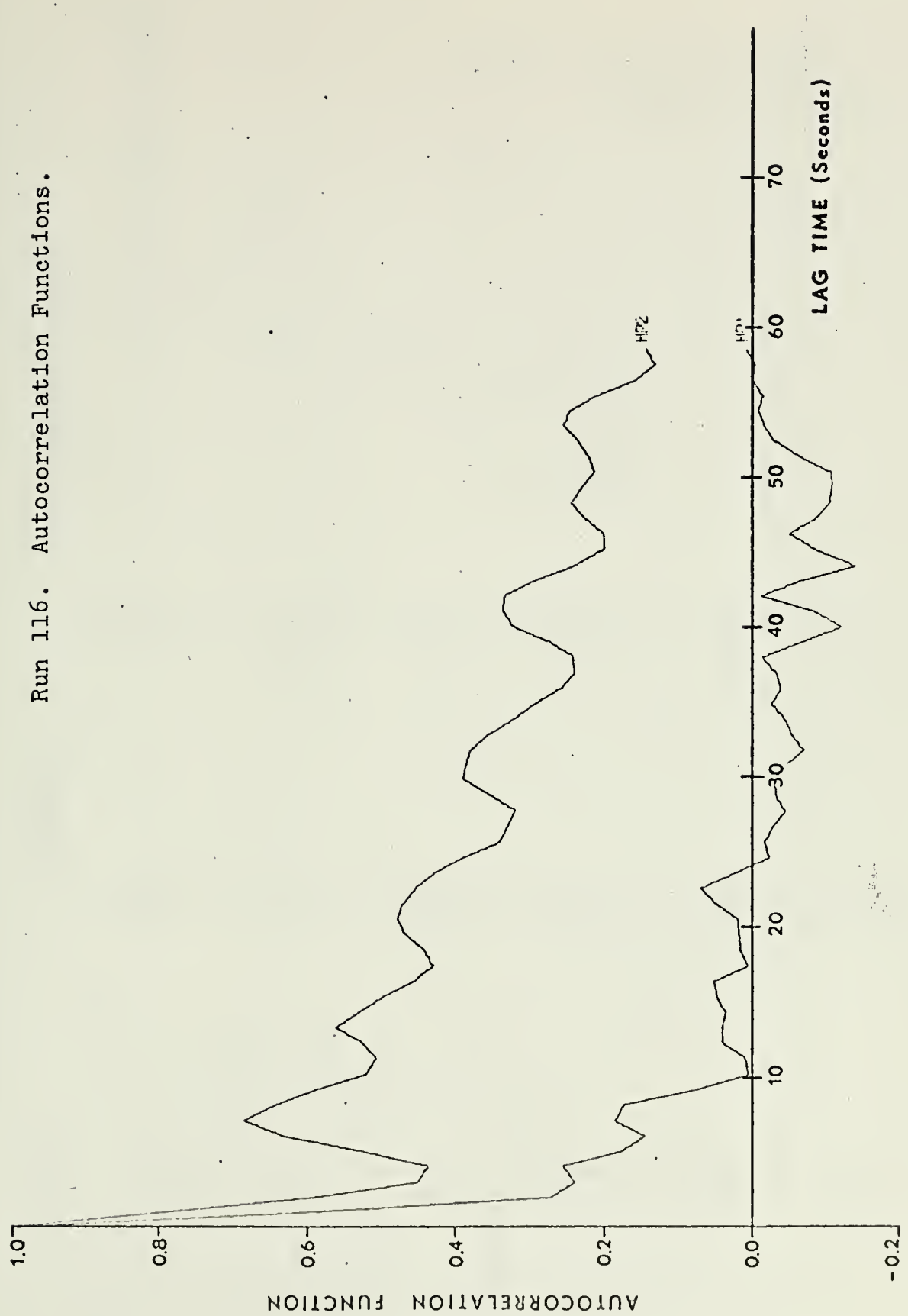

Run 116. Spectral Density, Coherence, and Phase.

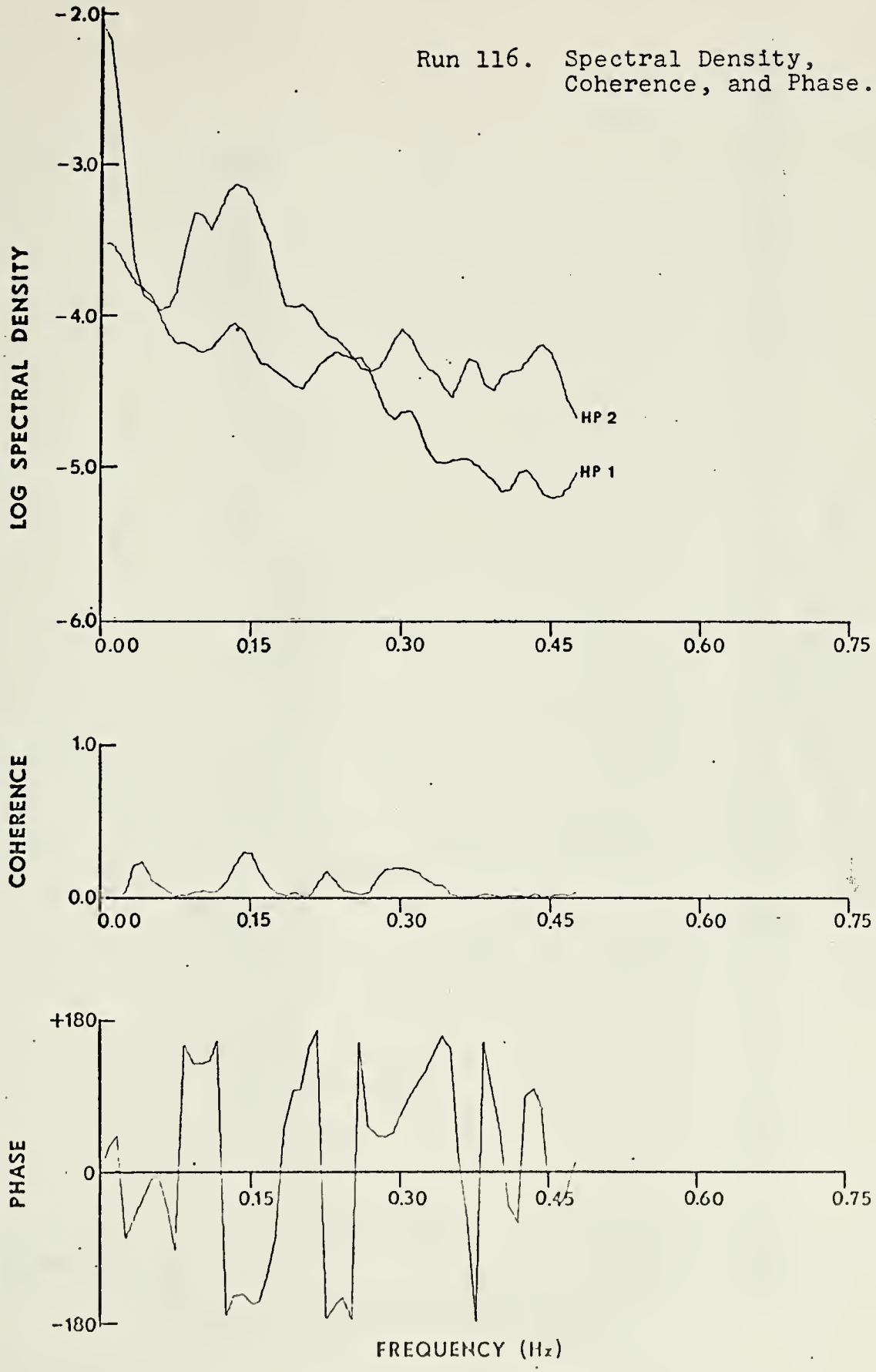

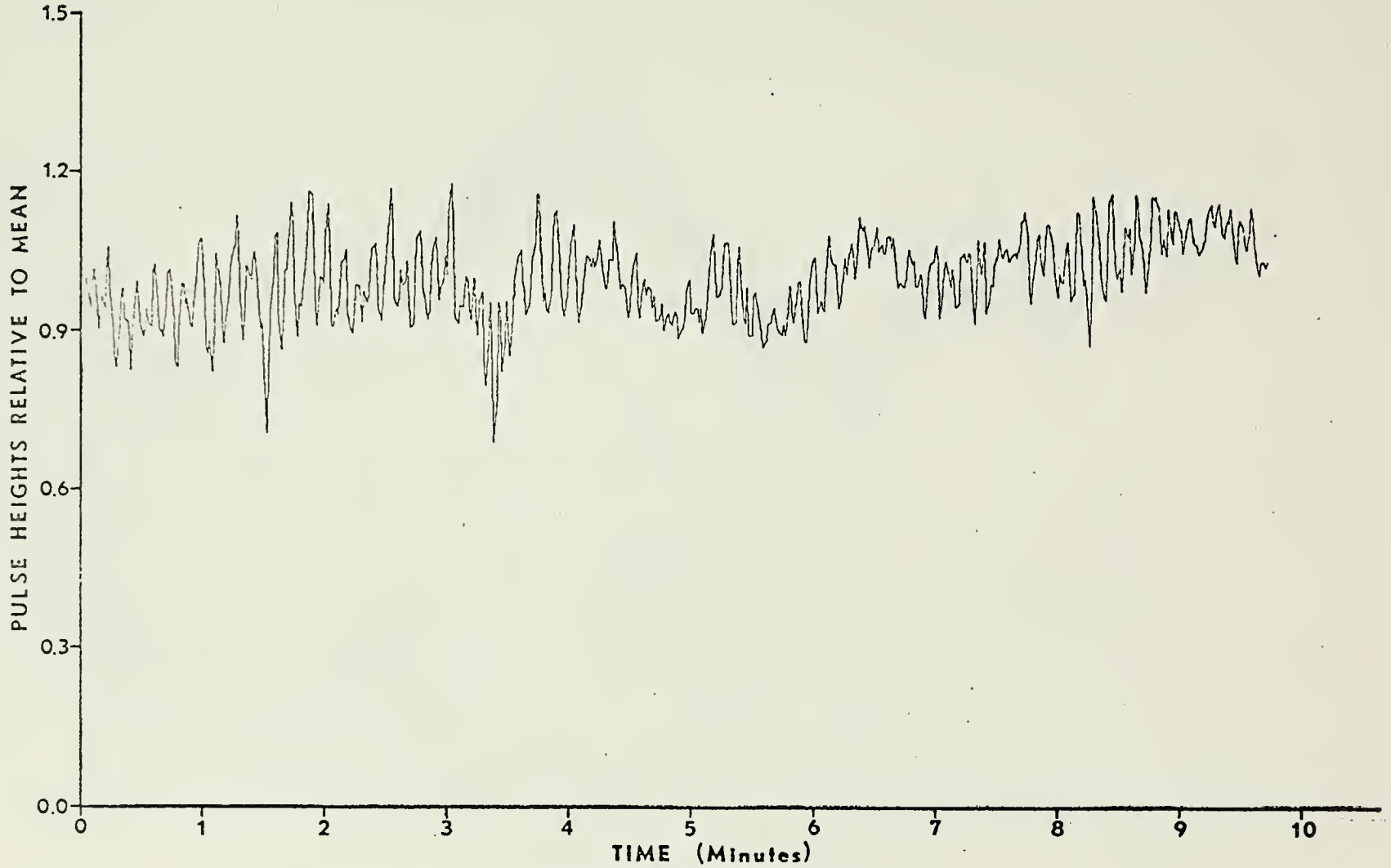

Run 117. Hydrophone 1 Pulse Heights.

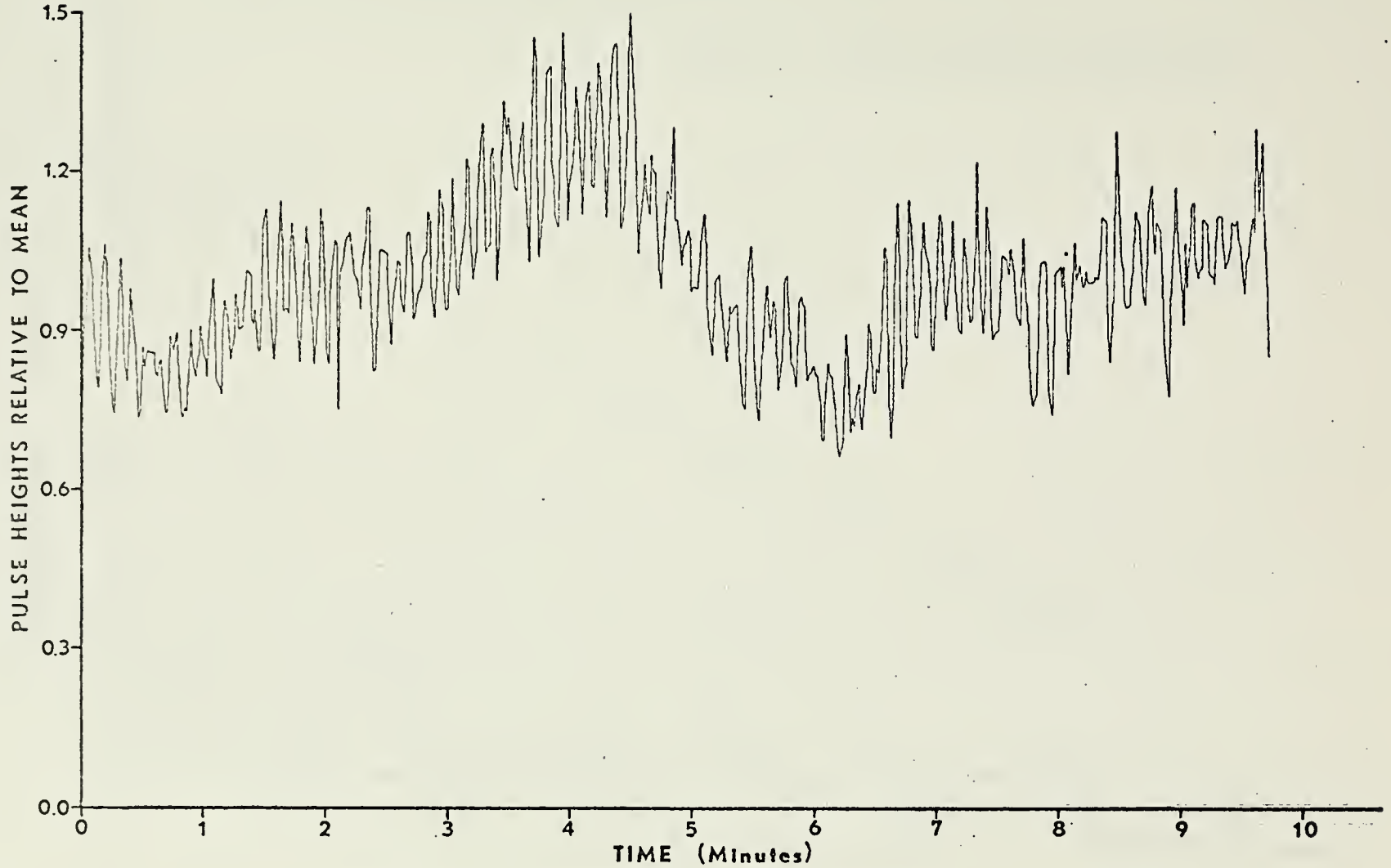

Run 117. Hydrophone 2 Pulse Heights.

Run 117. Autocorrelation Functions.

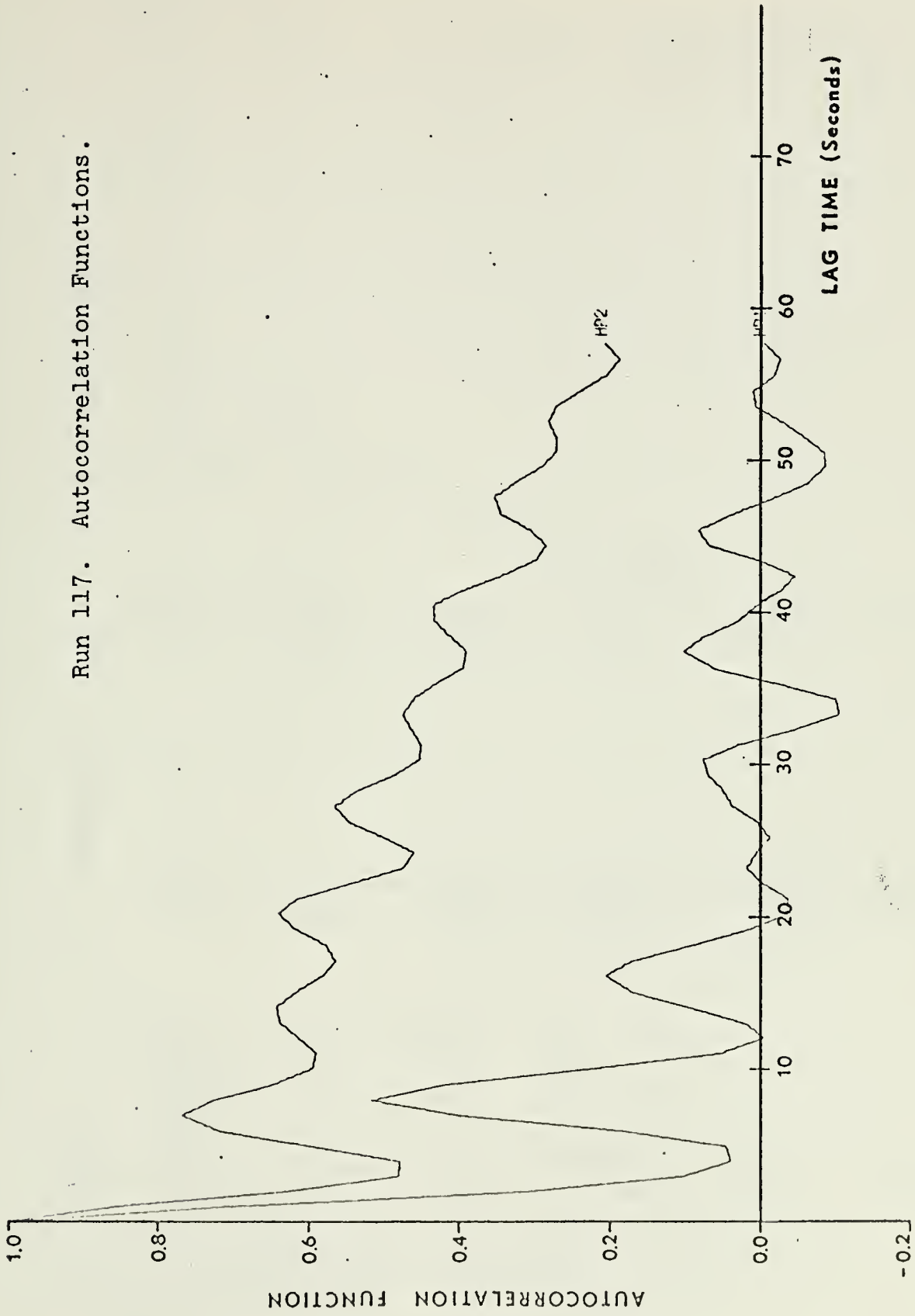

Run 117. Spectral Density, Coherence, and Phase.

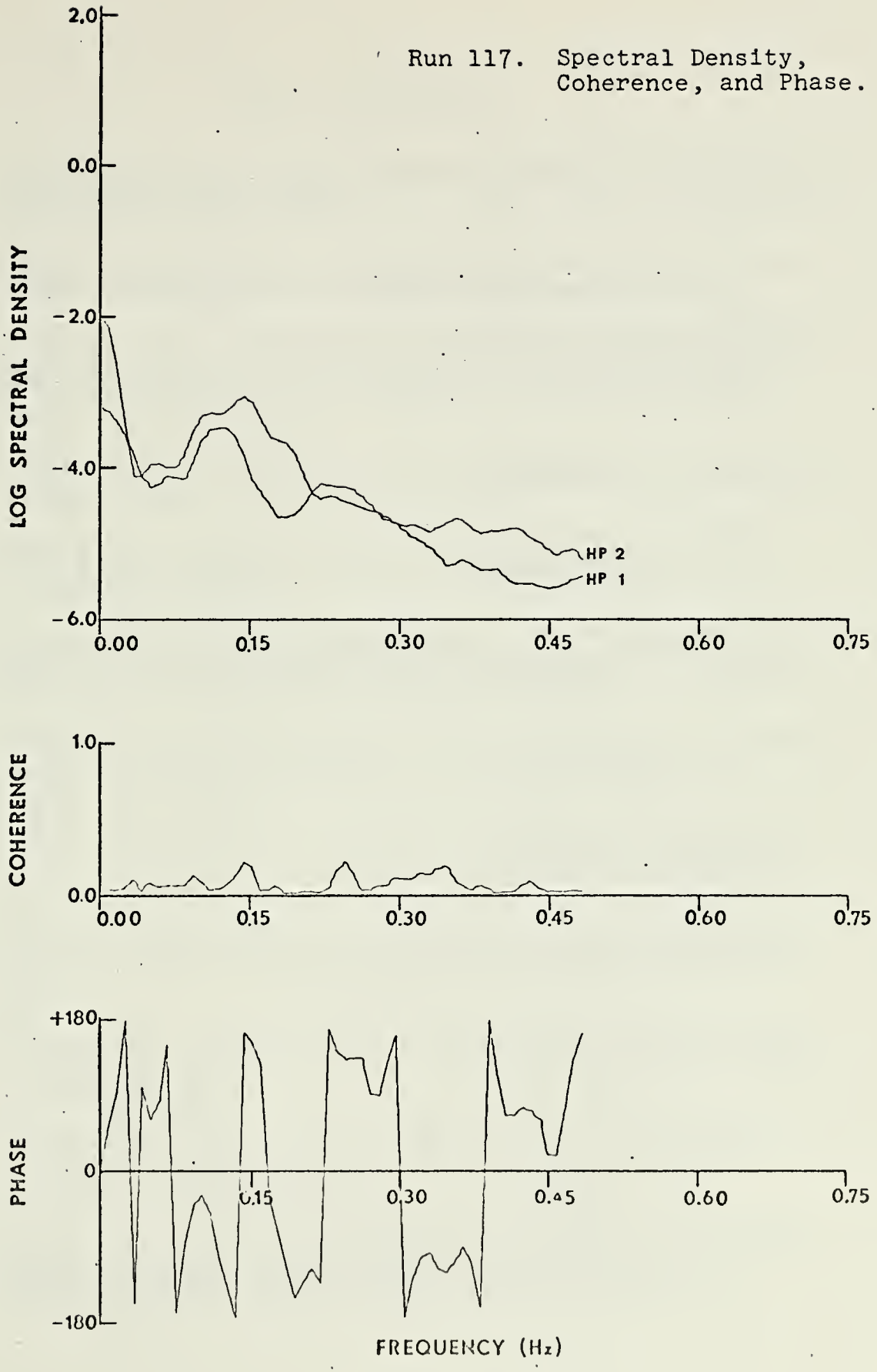

LIST OF REFERENCES

1. Alexander, C.H., Sound Phase and Amplitude Fluctuations in an Anisotropic Ocean, M.S. Thesis, Naval Postgraduate School, Monterey, 1972.

2. Ash, D.E., Description of Operation, unpublished manuscript, University of Auckland, New Zealand, 1972.

3. Barakos, P.A., The Effects of Internal Tides in Shallow Water Acoustics, paper presented at The Eighty-Fourth Meeting of the Acoustical Society of America, Miami Beach, Florida, November 1972.

4. Bendat, J.S. and Piersol, A.G., Measurement and Analysis of Random Data, Wiley, New York, 1966.

5. Bergmann, P.G., "Propagation of Radiation in a Medium with Random Inhomogeneities", Physical Review, v. 70, p. 486-492, 1946.

6. Brownlee, L.R., Sound Propagation in an Inhomogeneous Medium: The Sea - A Study and Measurement, M.S. Thesis, University of Auckland, New Zealand, 1969.

7. Campanella, S.J. and Favret, A.G., "Time Autocorrelation of Sonic Pulses Propagated in a Random Medium," J. Acoust. Soc. Amer., v. 46, p. 1234-1245, 1969.

8. Crease, J., "Internal Waves", in Underwater Acoustics, ed. V.M. Albers, p. 129-138, Plenum Press, New York, 1963.

9. Garrett, C. and Munk, W., "Oceanic Mixing by Breaking Internal Waves", Deep-Sea Research, v. 19, p. 823-832, 1972.

10. Gregg, M.C. and Cox, C.S., "The Vertical Microstructure of Temperature and Salinity", Deep-Sea Research, v. 19, p. 355-376, 1972.

11. Gregg, M.C., Cox, C.S., and Hacker, P.W., "Vertical Microstructure Measurements in the Central North Pacific", J. Phys. Ocean, v. 3, p. 458-469, 1973.

12. Medwin, H., Sound Speed Dispersion and Fluctuations in the Upper Ocean: Project BASS, Naval Postgraduate School, Monterey, Report NPS-61Md73101A, 1973.

13. Mintzer, D., "Wave Propagation in a Randomly Inhomogeneous Medium. I", J. Acoust. Soc. Amer., v. 25, p. 922-927, 1953a.

14. Mintzer, D., "Wave Propagation in a Randomly Inhomogeneous Medium. II", J. Acoust. Soc. Amer., v. 25, p. 1107-1111, 1953b.

15. Mintzer, D., "Wave Propagation in a Randomly Inhomogeneous Medium. III", J. Acoust. Soc. Amer., v. 26, p. 186-190, 1954.

16. Morton, J. and Chapman, V.J., Rocky Shore Ecology of the Leigh Area North Auckland, University of Auckland, New Zealand, 1968.

17. Neal, V.T. and Neshyba, S., "Microstructure Anomalies in the Arctic Ocean", J. Geophys. Research, v. 78, p. 2695-2701, 1973.

18. Neshyba, S., Neal, V.T., and Denner, W., "Temperature and Conductivity Measurements under Ice Island T-3", J. Geophys. Research, v. 76, p. 8107-8120, 1971.

19. Raney, S.D., Procedures for Converting 7-Track Magnetic Tapes to 9-Track Magnetic Tapes, informal report TN 0211-08 of W.R. Church Computer Center, Naval Postgraduate School, Monterey, February 1973.

20. Sagar, F.H., "Fluctuations in Intensity of Short Pulses of 14.5-kc Sound Received from a Source in the Sea", J. Acoust. Soc. Amer., v. 27, p. 1092-1106, 1955.

21. Sagar, F.H., "Comparison of Experimental Underwater Acoustic Intensities of Frequency 14.5 kc with Values Computed for Selected Thermal Conditions in the Sea", J. Acoust. Soc. Amer., v. 29, p. 948-965, 1957.

22. Sagar, F.H., "Acoustic Intensity Fluctuations and Temperature Microstructure in the Sea", J. Acoust. Soc. Amer., v. 32, p. 112-121, 1960.

23. Shoemaker, B.H., Interrelationship Between the Thermal Microstructure, Internal Waves and Acoustic Propagation in the Arctic Ocean, M.S. Thesis, Naval Postgraduate School, Monterey, 1971.

24. Skudryzk, E.J., "Thermal Microstructure in the Sea and Its Contribution to Sound Level Fluctuations", in Underwater Acoustics, ed. V.M. Albers, p. 199-233, Plenum Press, New York, 1963.

25. Stommel, H. and Federov, K.N., "Small Scale Structure in Temperature and Salinity near Timor and Mindanao", Tellus, v. 19, p. 306-325, 1967.

26. Taylor, F.J., Phytoplankton and Nutrients in the Hauraki Gulf Approaches, unpublished manuscript, University of Auckland, New Zealand, 1972.

27. Urick, R.J. and Searfoss, C.W., The Microthermal Structure of the Ocean near Key West, Florida: Part I - Description, Naval Research Laboratory, Washington, D.C., Report S-3392, 1948.

28. Urick, R.J. and Searfoss, C.W., The Microthermal Structure of the Ocean near Key West, Florida: Part II - Analysis, Naval Research Laboratory, Washington, D.C., Report S-3444, 1949.

29. Urick, R.J., Principles of Underwater Sound for Engineers, McGraw-Hill, New York, 1967.

30. Woods, J.D. and Wiley, R.L., "Billow Turbulence and Ocean Microstructure", Deep-Sea Research, v. 19, p. 87-121, 1972.

INITIAL DISTRIBUTION LIST

		No. Copies
1.	Defense Documentation Center Cameron Station Alexandria, Virginia 22314	2
2.	Library (Code 0212) Naval Postgraduate School Monterey, California 93940	2
3.	Department of Oceanography Naval Postgraduate School Monterey, California 93940	3
4.	Dr. Warren W. Denner Director Naval Arctic Research Laboratory Barrow, Alaska 99723	6
5.	Dr. Robert H. Bourke Code 58Bf Naval Postgraduate School Monterey, California 93940	1
6.	Dr. Edward B. Thornton Code 58Tm Naval Postgraduate School Monterey, California 93940	1
7.	Dr. Noel E.J. Boston Code 58 Bb Naval Postgraduate School Monterey, California 93940	1
8.	Oceanographer of the Navy Hoffman II 200 Stovall Street Alexandria, Virginia 22332	1
9.	Naval Oceanographic Office Library (Code 3330) Washington, D.C. 20373	1
10.	Dr. Ned A. Ostenso (Code 480D) Office of Naval Research Arlington, Virginia 22217	1

		No. Copies
11.	Mr. John F. Ropek (ORD 03C) Naval Ordnance Systems Command Navy Department Washington, D.C. 20360	1
12.	Dr. Robert E. Stevenson Scientific Liaison Office Scripps Institution of Oceanography La Jolla, California 92037	1
13.	Lt. Michael T. Korbet, USN c/o 1930 Pendennis Drive Annapolis, Maryland 21401	1
14.	SIO Library University of California, San Diego P. O. Box 2367 La Jolla, California 92037	1
15.	Department of Oceanography Library University of Washington Seattle, Washington 98105	1
16.	Department of Oceanography Library Oregon State University Corvallis, Oregon 97331	1

REPORT DOCUMENTATION PAGE

READ INSTRUCTIONS BEFORE COMPLETING FORM

1. REPORT NUMBER

2. GOVT ACCESSION NO.

3. RECIPIENT'S CATALOG NUMBER

4. TITLE (and Subtitle)
Shallow Water Acoustic Amplitude Fluctuations at 35 and 65 KHz

5. TYPE OF REPORT & PERIOD COVERED
Master's Thesis; March 1974

6. PERFORMING ORG. REPORT NUMBER

7. AUTHOR(s)
Michael Thomas Korbet

8. CONTRACT OR GRANT NUMBER(s)

9. PERFORMING ORGANIZATION NAME AND ADDRESS
Naval Postgraduate School
Monterey, California 93940

10. PROGRAM ELEMENT, PROJECT, TASK AREA & WORK UNIT NUMBERS

11. CONTROLLING OFFICE NAME AND ADDRESS
Naval Postgraduate School
Monterey, California 93940

12. REPORT DATE
March 1974

13. NUMBER OF PAGES
131

14. MONITORING AGENCY NAME & ADDRESS(if different from Controlling Office)
Naval Postgraduate School
Monterey, California 93940

15. SECURITY CLASS. (of this report)
Unclassified

15a. DECLASSIFICATION/DOWNGRADING SCHEDULE

16. DISTRIBUTION STATEMENT (of this Report)

Approved for public release; distribution unlimited.

17. DISTRIBUTION STATEMENT (of the abstract entered in Block 20, if different from Report)

18. SUPPLEMENTARY NOTES

Research supported through contracts from
Naval Ordnance Systems Command (Code 03C)

19. KEY WORDS (Continue on reverse side if necessary and identify by block number)

Underwater acoustics
Shallow water acoustics
Acoustic amplitude fluctuations
Temperature microstructure

20. ABSTRACT (Continue on reverse side if necessary and identify by block number)

An underwater acoustics experiment conducted in shallow water (70 feet) off the New Zealand east coast in 1972-1973 is described. Short acoustic pulses of 35 and 65 kHz sound were projected along near-orthogonal paths of approximately 300 yards. Environmental parameters were simultaneously observed.

Statistical and spectral analyses of pulse heights were performed on 12 selected runs using digital techniques.

(20. ABSTRACT continued)

Coefficients of variation ranged from 2.0% to 15.5%. In almost all cases, higher variability was observed along the acoustic path oriented perpendicular to the predominant swell direction. Along this same path, periods corresponding to common surface swell periods were frequently evident in the autocorrelation functions of the fluctuations. Coherence between the fluctuations along each path was low, averaging about 0.1. Long period oscillations suggestive of modulation by internal waves were apparent in several runs. No significant dependence of variability on acoustic frequency was detected.

Microscale temperature fluctuations measured simultaneously are discussed.